

Syracuse University

**SURFACE**

---

Dissertations - ALL

SURFACE

---

January 2015

## **MODULATION AND INTERACTIONS OF CHARGED BIOMIMETIC MEMBRANES WITH BIVALENT IONS**

Adolphe Kazadi Badiambile  
*Syracuse University*

Follow this and additional works at: <https://surface.syr.edu/etd>



Part of the [Physical Sciences and Mathematics Commons](#)

---

### **Recommended Citation**

Kazadi Badiambile, Adolphe, "MODULATION AND INTERACTIONS OF CHARGED BIOMIMETIC MEMBRANES WITH BIVALENT IONS" (2015). *Dissertations - ALL*. 336.

<https://surface.syr.edu/etd/336>

This Dissertation is brought to you for free and open access by the SURFACE at SURFACE. It has been accepted for inclusion in Dissertations - ALL by an authorized administrator of SURFACE. For more information, please contact [surface@syr.edu](mailto:surface@syr.edu).

## Abstract

The biological membrane of an eukaryotic cell is a two-dimensional structure of mostly phospholipids with embedded proteins. This two-dimensional structure plays many key roles in the life of a cell. Transmembrane proteins, for example, play the role of a gate for different ions (such as  $\text{Ca}^{2+}$ ). Also found are peripheral proteins that are used as enzymes for different purposes in the inner leaflet of the plasma membrane. Phospholipids, in particular play three key roles. Firstly, some members of this group are used to store energy. Secondly, the hydrophobic and hydrophilic properties inherent to phospholipids enable them to be used as building blocks of the cell membrane by forming an asymmetric bilayer. This provides a shielding protection against the outer environment while at the same time keeping the organelles and cytosol from leaking out of the cell. Finally lipids are involved in regulating the aggregation of proteins in the membrane. In addition, some subspecies such as phosphatidylinositol (PtdIns) are second messenger molecules in their own right, thus playing an important role in cellular signaling events. In my work presented in this thesis, I am focusing on the role of some phospholipids as signaling molecules and in particular the physicochemical underpinnings that could be used in their spatiotemporal organization in the cellular plasma membrane. I am specifically concerned with the important family of phosphatidylinositol lipids. PtdIns are very well known for their role as signaling molecules in numerous cell events. They are located in the inner leaflet of the plasma membrane as well as part of the membrane of other organelles. Studies of these signaling molecules in their *in vivo* environment present many challenges: Firstly, the complexity of interactions due to the numerous entities present in eukaryotic cell membranes makes it difficult to establish clear cause and effect relationships. Secondly, due to their size, our inability to probe these biomolecules in a dynamic environment and the lack of appropriate physical and biochemical tools. In contrast,

biomimetic membrane models that rely on the amphiphilic properties of phospholipids are powerful tools that enable the study of these molecules *in vitro*. By having control over the different experimental parameters such as temperature and pH, reliable and repeatable experimental conditions can be created.

One of the key questions I investigated in this thesis is related to the clustering mechanism of PtdIns(4, 5)P<sub>2</sub> into pools or aggregates that enable independent cellular control of this species by geometric separation. The lateral aggregation of PtdIns(4, 5)P<sub>2</sub> and its underlying physical causes is still a matter of debate. In the first part of this thesis I introduce the general information on lipid membranes with a special focus on the PtdIns family and their associated signaling events. In addition, I explain the Langmuir-Blodgett film balance (LB) system as tool to study lipid membranes and lipid interactions. In the second chapter, I describe my work on the lateral compressibility of PtdIns(4, 5)P<sub>2</sub>, PtdIns and DOPG monolayers and its modulation by bivalent ions using Langmuir monolayers. In addition, a theoretical framework of compressibility that depends on a surface potential induced by a planar layer of charged molecules and ions in the bulk was provided. In the third part, I present my work on the excess Gibbs free energy of the lipid systems PtdIns(4, 5)P<sub>2</sub> –POPC, PtdIns(4, 5)P<sub>2</sub>, and POPC as they are modulated by bivalent ions. In the fourth part, I report on my foray in engineering a light-based system that relies on different dye properties to simulate calcium induced calcium release (CICR) that occurs in many cell types. In the final chapter, I provide a general conclusion and present directions for future research that would build on my findings.

**MODULATION AND INTERACTIONS OF CHARGED BIOMIMETIC MEMBRANES  
WITH BIVALENT IONS**

by

Adolphe Kazadi Badiambile

*Doctoral Dissertation*

B.S. University of Kinshasa, 2006  
PGD African Institute for Mathematical Sciences, 2008  
M.S. Syracuse University, 2010

*Submitted in partial fulfillment of the requirements  
for the degree of Doctor of Philosophy,  
in the Graduate School of Syracuse University,*

Syracuse University  
August 2015

Copyright 2015 Adolphe Kazadi Badiambile

All rights reserved.

## Acknowledgements

*“Not to us, O Lord, not to us, but to your name give glory,  
for the sake of your steadfast love and your faithfulness!”*

*Psalm 115:1 (English Standard Version)*

To me, academic life is like a house: the taller the house, the deeper the foundation must be. A house is rarely built alone. As in all the stories built over many years of study and hard work that have brought me to this ultimate story, it would not be possible without many people’s guidance, teaching and help. I thank first and foremost my supervisor, Dr. Martin B. Forstner, for his active encouragement and enthusiastic help in all areas of scientific inquiry and his careful overseeing of my work. His training has helped make me the scientist I am today. His contributions are far greater than I can possibly detail, but I am grateful.

I also want to thank Professor Christina Marchetti, for giving me, and many others, the tremendous opportunity to build this top story of my life. She may not realize the far-reaching impact she has made by helping me in my endeavors as a scientist. Only the Most High knows.

I would like to express my appreciation for the members of my thesis defense committee: Kenneth Foster, Liviu Movileanu, Matthew LaHaye, Marina Artuso and Rebecca Bader for their willingness, time and interest in encouraging, correcting and giving insight into my work.

I would like also to thank my friends in the lab, Eleni Kinfe, Ian McCabe and Kathleen Kelly for many good times. I am also grateful for a small, faithful group in the Syracuse University community who warmly welcomed and cared for me in my time here. I especially want to thank Paul and Sandy Jewell for opening their home, treating me as a son and helping me in my adjustment to American life. And to friends, Kevin Smith, Ryan Felix and Sarah Jackson, who have helped in the final stages of editing and polishing of this thesis.

And to my loving parents, Joseph Badiambile Kalambayi and Adolphine Mujinga Kazadi Kupa, who have laid the foundation from which all the four stories have been lifted up, High school, college, postgraduate and Doctor of Philosophy (Ph.D.). To them, I dedicate this work, with deep gratitude for all the work they have done. I am also appreciative of all of my siblings for being a part of my life; their encouragement has been of great value.

In Africa, it is said, a child is raised by the whole village; I can say a scientist is a product of the world.

## Table of Contents

Acknowledgements.....	v
Table of Contents.....	vii
Table of Figures.....	viii
Chapter I : General Introduction and Background.....	1
1.1.    Motivation and Background.....	1
1.2.    Introduction to Cell Membranes : Structure and Organization.....	6
1.3.    Phosphatidylinositol Metabolism.....	11
1.4.    Membrane Rafts.....	14
1.5.    Phosphatidylinositol and Signal Transduction at the Cell Surface.....	16
1.6.    Imaging Techniques.....	22
1.7.    Interactions in Biological Systems of Phospholipids.....	24
1.7.1.    Van der Waals Interaction.....	25
1.7.2.    Monolayer technique and Langmuir Adsorption of phospholipids.....	26
1.7.3.    Langmuir-Blodgett Films Balance.....	26
1.7.4.    Hydrogen bonds in lipid monolayer and bilayer.....	32
1.7.5.    Electrostatic Interaction in a Biological membrane.....	32
Chapter II : Modulation of Phosphoinositide Monolayer Compressibility by Physiological Levels of $Ca^{+2}$ .....	35
2.1.    Abstract.....	35
2.2.    Introduction.....	36
2.3.    Materials and Methods.....	39
2.4.    Data Analysis and Discussion.....	41
2.5.    Conclusion.....	56
Chapter III : Calcium Induced Change in Excess Gibbs Energy of Charged Monolayer System.....	57
3.1.    Abstract.....	57
3.2.    Introduction.....	58
3.3.    Material and Methods.....	60
3.4.    Data Analysis and Results.....	61
3.5.    Conclusion.....	77
Chapter IV : Novel Technique for Calcium Oscillation.....	78
4.1.    Abstract.....	78
4.2.    Introduction.....	79
4.2.    Reagents and Procedures.....	86
4.2.    Preliminary Results.....	87
Chapter V: General Conclusion.....	91
Future Research.....	92
Reference.....	93
Vita.....	102



## Table of Figures

Figure I-1: Dynamics, Function and Structure of Biological Membranes .....	2
Figure I-2: Basic organization and composition of Eukaryotic cell membrane. ....	8
Figure I-3: Lipid structure .....	10
Figure I-4: Structure and configuration of the inositol ring (left panel), the phosphatidylinositol lipid (middle) and the clear marking of the whole head group (right hand panel) .....	12
Figure I-5: Phosphoinositide synthesis, Adopted from .....	13
Figure I-6 Pools of PIP <sub>2</sub> in the cytoplasm .....	16
Figure I-7 Examples of PtdIns (4,5)P <sub>2</sub> function in the Cytoplasm membrane .....	17
Figure I-8 Endosomal PTEN in PIP <sub>3</sub> and PIP <sub>2</sub> Control .....	18
Figure I-9 : PtdIns(4,5)P <sub>2</sub> -Fertilization.....	19
Figure I-10 PIP <sub>2</sub> mediates the budding process of human immunodeficiency virus type 1(HIV-1). ....	20
Figure I-11 Fluorescence microscope mains features. ....	23
Figure I-12 Langmuir Trough and Monolayer Formation.....	27
Figure I-13 Surface tension description .....	28
Figure I-14 DPPC Isotherm and Phases .....	29
Figure I-15 Force acting on the Wilhelmy Plate .....	30
Figure II-1. From left to right are highly charged PI(4,5)P <sub>2</sub> , PI and DOPG .....	40
Figure II-2. Isotherm of PIP <sub>2</sub> at different in the absence and presence of Ca <sup>+2</sup> .....	40
Figure II-3. Modulation of lateral isothermal compressibility of PIP <sub>2</sub> by Ca <sup>+2</sup> ions.....	43
Figure II-4 Modulation of lateral isothermal compressibility of PIP <sub>2</sub> by Mg <sup>+2</sup> ions.....	43
Figure II-5. Modulation of lateral isothermal compressibility of DOPG by Ca <sup>+2</sup> ions .....	45
Figure II-6. Modulation of lateral isothermal compressibility of DOPG by Mg <sup>+2</sup> ions .....	45

Figure II-7: Modulation of lateral isothermal compressibility of PI by $\text{Ca}^{+2}$ ions .....	48
Figure II-8: Modulation of lateral isothermal compressibility of PI by $\text{Mg}^{+2}$ ions .....	48
Figure II-9: Theoretical compressibility as a function of electrostatic surface potential for various mean area per molecule .....	54
Figure II-10: Theoretical compressibility as function of distance from membrane for various surface potential .....	54
Figure III-1. Isotherm of the mixture of PI(4,5)P <sub>2</sub> -POPC (25:75) at 37C and pH 7.4 .....	63
Figure III-2. Graph (a) shows surface pressure versus Gibbs free energy in the mixture of 10% PI (4, 5) P <sub>2</sub> and 90% POPC. Graph (b) shows the surface pressure versus Gibbs free energy in the mixture of 25% PI (4, 5) P <sub>2</sub> and 75% POPC. Both are regulated by $\text{Ca}^{2+}$ concentration at 37 °C and pH 7.4.....	66
Figure III-3. Graph (a) shows surface pressure versus Gibbs free energy in the mixture of 35% PI (4, 5) P <sub>2</sub> and 65% POPC. Graph (b) shows the surface pressure versus Gibbs free energy of pure POPC. Both are regulated by $\text{Ca}^{2+}$ concentration at 37 °C and pH 7.4 .....	67
Figure III-4: Excess Gibbs free energy ( $\Delta G^{\text{ex}}$ ) from the mixture of PI(4,5)P <sub>2</sub> and .....	70
Figure III-5. Excess Gibbs free energy ( $\Delta G_{\text{ex}}$ ) from PI(4,5)P <sub>2</sub> at 37 C and 25 °C .....	70
Figure III-6. Schematic of the monolayer of PI(4,5)P <sub>2</sub> in various conditions.....	71
Figure III-7. Modulation of surface pressure versus Gibbs free energy of PI(4,5) P <sub>2</sub> by $\text{Ca}^{+2}$ at 25°C and pH 7.4.....	72
Figure III-8. Modulation of surface pressure versus Gibbs free energy of PI(4,5) P <sub>2</sub> by $\text{Mg}^{+2}$ at 25°C and pH 7.4.....	72
Figure III-9. Modulation of surface pressure versus Gibbs free energy of PI(4,5) P <sub>2</sub> by $\text{Ca}^{+2}$ at 37 °C and pH 3.5.....	75
Figure III-10. Modulation of surface pressure versus Gibbs free energy of PI(4,5) P <sub>2</sub> by $\text{Mg}^{+2}$ 37 °C at pH 3.5.....	75
Figure III-11. Modulation of surface pressure versus Gibbs free energy of PI(4,5) P <sub>2</sub> by $\text{Ca}^{+2}$ 25 °C at pH 3.5.....	76
Figure III-12. Modulation of surface pressure versus Gibbs free energy of PI(4,5) P <sub>2</sub> by $\text{Mg}^{+2}$ 25 °C at pH 3.5.....	76
Figure IV-1 Calcium Microdomain .....	80
Figure IV-2 Calcium Puffs in Xenopus oocyte : .....	82

Figure IV-3 Calcium Sparks and the Global response of  $Ca^{2+}$  in Myocyte ..... 84

Figure IV-4 Calcium homeostasis mechanism ..... 85

Figure IV-5: Calcium oscillation induced changes in membrane organization. .... 87

Figure IV-6: Fluorescent images of Asante Calcium Red for different calcium concentrations (as shown from (a) to (f) and with the added effect of the scavenger (DIAZO) on the  $[Ca^{+2}]$  (f). ..... 88

Figure IV-7: Fluorescent Intensity of Asante Calcium Red for different calcium concentrations. .... 89

Figure IV-8: Fluorescent images of Asante Calcium Red for different calcium concentrations.. ..... 90

## **Chapter I : General Introduction and Background**

### **1.1. Motivation and Background**

A living, eukaryotic cell is a highly organized and compartmentalized biochemical system that is enclosed by a lipid bilayer that includes proteins. The plasma membrane (PM) is the largest membrane and is the site where numerous cell signaling events occur (Figure I-1). It is also a non-equilibrium, dynamic medium where hundreds of lipids' species and sterols interact in time and space with their associated proteins [1] to accomplish a large variety of cellular functions such as exocytosis, endocytosis, receptor mediated signaling, and transmembrane as well as lateral membrane transport [2]. It is also a primary target for viral entry [3-5], drug delivery[6] and is implicated in the progression of cancers [7, 8]. The PM is an active site and an impermeable structure that selectively allows certain molecules to pass across it by special, transmembrane proteins called channels [9]. In terms of mass composition, the major components of the PM are lipids and proteins, each of which contribute about half of the total weight [10]. The discovery of the lipid raft domain has dramatically revolutionized the perception that held that lipids act solely as passive fluid solvents, attributing all the functionalities to the proteins [11]. Lipid membranes play a key role in living cells as they organize molecules in time and space. For one, they are formidable barriers to random transport across membranes and thus help to compartmentalize eukaryotic cells [9]. In addition, they are also quasi-two-dimensional, highly-structured fluids [12] [9, 13]. As such, they provide the ideal environment for dynamic rearrangement of molecules within the plane of the membrane [14]. This feature is paramount for both time-dependent assembly of molecules into larger membrane structures [15], as well as the proper execution of membrane-associated biochemical reactions [16-18]. Ultimately, these two, intimately-linked aspects directly impact the membrane structures on lateral transport and vice versa [19]. It also

appears that this interplay has an important role in the proper execution of cellular processes [20]. Figure I-1 is a visual representation of this interconnection of all three aspects of the eukaryotic cell membranes.

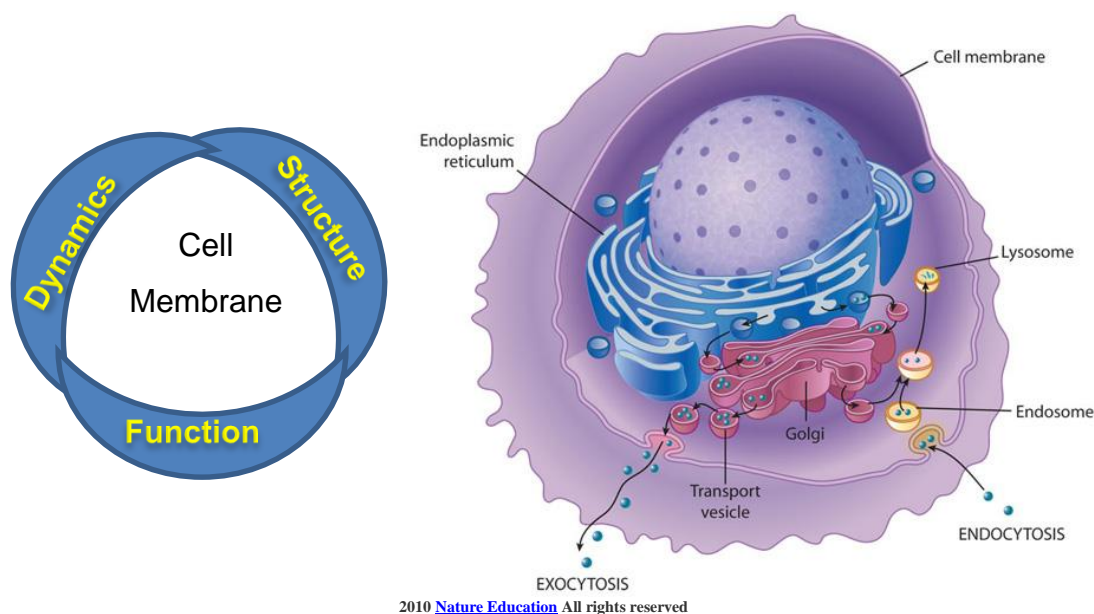


Figure I-1: Dynamics, Function and Structure of Biological Membranes

The schematic on the left represents the interconnection of the three principal aspects of biological, lipid-based membranes. On the right is a schematic showing the plasma (cell) membrane and other membrane enclosed organelles. Adopted from [21, 22])

Different approaches are being used to understand, both qualitatively and quantitatively, the different aspects of the plasma membrane at different length scales. Moreover, more techniques are currently being developed to probe the dynamics of the PMs in time and space. Among these more current techniques is super-resolution fluorescence microscopes which provide spatial resolutions down to a few nanometers and have revealed structures that had not been not observed with classic fluorescence microscopes [23, 24]. However, there is still not a single method that is capable of quantitatively accessing all three principle aspect of the plasma membrane. In addition,

the complexity of the PMs, arising from their rich, heterogeneous composition of interacting molecules, continues to present many challenges to a systematic study and a comprehensive understanding of this key biological system. Thus, despite recent technological advances, much is left to be desired in terms of our ability to conduct measurements on living cells that would permit the simultaneous, quantitative assessment of the main membrane aspects. This method would report on a molecules movement, how it is organized and what function it is executing.

It follows that attempting to understand the inter-connection of these three aspects of biological cell membranes (or any supra-molecular cellular assembly for that matter) will require a systematic bottom-up approach. First, PM components are isolated and studied individually and then progressively reassembled into reconstituted biomimetic structures of ever increasing complexity. Certainly, this approach cannot be used *in vivo* as a minimum degree of complexity of the PM is required for a cell to be viable. Moreover, our ability to probe molecular compositions of live cell membranes is all but limited to rather crude approaches, such as cholesterol depletion. Thus, the function(s) and properties of many important lipids as synthesized by cells is (are) still unknown [12]. The field of membrane biophysics is at a stage where experimentation in well-controlled artificial model systems are still very valuable and are often the only way to gain some basic understanding of lipidic molecules, their interactions and their physicochemical properties. In this thesis, I thus focus on one particular and very special family of glycopospholipids called Phosphatidylinositol (PtdIns) which are located at the PM and other organelles' membranes.

Phosphatidylinositol and its derivatives, such as PIP2 which is an exceptionally extraordinary lipid, play a crucial role in many aspects of cell physiology and cellular signaling [25, 26]. For example, PtdIns regulate the function of integral membrane proteins through their highly charged head groups or participate in the recruitment of proteins to the membrane [27-30].

PtdIns also play a key role in the processes of endocytosis and exocytosis [2, 27, 31]. In its most predominant function as a messenger, PIP<sub>2</sub> cleaved by phospholipase C (PLC) inside the cytoplasm, produces two messenger molecules, diacylglycerol (DAG) and inositol trisphosphate (IP<sub>3</sub>). IP<sub>3</sub> diffuses through the cytosolic fluid until it binds to the IP<sub>3</sub> receptor located in the membrane of the endoplasmic reticulum (ER). Since the IP<sub>3</sub> receptor is part of the a ligand-gated Ca<sup>2+</sup> channel assembly, IP<sub>3</sub> binding causes the release of Ca<sup>2+</sup> [29]. In fertilization, for example, PLC $\gamma$  is released by the sperm once inside the cytoplasm of the ovule. There it cleaves PIP<sub>2</sub> and the resulting calcium release from the ER triggers mitosis and puts growth in the cell into motion [32]. In order to avoid cross-talk, despite the multiple implications of PIP<sub>2</sub> in different biological functions, it is likely that PtdIns are segregated into ‘pools’ along the plasma membrane that can be individually controlled. However, the mechanisms underlying the formation of such pools of PtdIns (and in particular its most common representative, PIP<sub>2</sub>) are not yet really understood. In addition, the associated mechanical properties of such pools during Ca<sup>2+</sup> signaling have not been yet studied.

As mentioned above, understanding the proposed pool formation of PtdIns *in vivo* presents a huge challenge due to the complexity of plasma membrane compositions and the possible interactions of its constituents. The numbers of entities that are present in a biological cell such as lipids, proteins, ions and other biomolecules and their interactions render such systems extremely difficult to model mathematically.

To our knowledge, there are no adequate tools to study this lipid in its cellular environment. Not only are lipids highly complex, they are unlike proteins that allow the utilization of fluorescence fusion proteins, the toolbox for studying the dynamics of lipids *in vivo* is much more limited. This is for two reasons: the much smaller size of lipid molecules and the much more

complex pathway of lipid synthesis. As well, there is a general lack of a “lipid code” analogous to the DNA-amino acid sequence correspondence in protein synthesis. Thus, lipid studies in particular benefit from the use of biomimetic systems, rely on self-assembly properties inherent in the amphiphilic nature of these phospholipids and offer the advantages that come with full control over parameters such as pH, temperature, and buffer composition.

One of the ways that PtdIns interact with other molecules, and with those in the cytoplasm in particular, is through their head group. Based on an inositol ring, it allows for several degrees of phosphorylation which gives rise to a highly negatively charged lipid. Different models have been developed to describe the electrostatic potential generated by these charged lipids. To the best of my knowledge, there is no model as yet describing the mechanical properties associated with their lateral organization and their interactions with each other in these systems. I have developed a model that enables the probing of the mechanical properties of a monolayer of any charged lipids or molecules. By building on an electrostatic potential model, I am able to compute the compressibility as well as to deduce an approximate potential of the monolayer: the multiple-charged PtdIns and the singly-charged lipid 1,2-dioleoyl-sn-glycero-3-phospho-(1'-rac-glycerol) (DOPG). In addition, I also investigated the energetics of these systems from a thermodynamic point of view and studied the excess Gibbs free energy associated with charged lipids in the presence of varying amounts of  $\text{Ca}^{2+}$  ions. Lastly, I demonstrated the possibility of constructing a system that can be used to mimic the oscillation of calcium waves in the cytosol *in vitro*, thus enabling the study of the dynamic of biomimetic systems' response to calcium fluctuations *in vitro*.



## 1.2. Introduction to Cell Membranes : Structure and Organization

A living, eukaryotic cell is highly compartmentalized and contains functionalized blocks called organelles, most of which are surrounded by membranes. These membranes –thin, almost quasi-2-dimensional sheets, are made of proteins, lipids and cholesterol. The particular compositions, however, are specific to each particular organelle, so that the lipidic and proteinous content differ for the membranes enclosing the endoplasmic reticulum, the Golgi apparatus or the cell as a whole. What is the same though, is that these cellular biomembranes consist of two layers of lipids ( as shown in Figure I-1) that embed the other molecules such as proteins.

It has been now more than four decades since S. J. Singer and Garth L. Nicolson [11] have proposed the mosaic fluid membrane model that describes the basic structure and function of cellular lipid membranes. It is based on thermodynamic considerations and proposes a liquid disordered phase for all the phospholipids due to low melting temperature of their hydrophobic tails [33]. The discovery of distinct membrane domains by the end of the 1990s has modified this model due to the liquid ordered phase found in these so-called “lipid raft domains [33-35].The basic model is still in use as it provides a basic consensus of membrane organization, but has been increasingly modified over the years to reflect the experimental data and resulting insights. For example, the original model did not predict the constraints on rotational and lateral mobility of proteins as well as the dynamic lateral organization of lipids and lipid domains through diffusion of both the normal and anomalous types. Typical diffusion coefficients of domains are 10 to 100 times larger than those of membrane proteins and they can occupy area of  $0.1-1\mu\text{m}^2$  [36] while eukaryotic cells of multicellular species have typical surface areas in the order of  $\sim 2000\mu\text{m}^2$ [37]. At this point the complexity of cellular signaling at membranes as well as the detailed nature of all the different interactions have not been included in the mosaic model. This includes, the local

mechanical properties and the electrostatic interaction of charged lipids and their contribution to membrane organization.

A current illustration of the Fluid—Mosaic Membrane Model (F-MMM) of biological membrane that includes several updates to the original model is as shown in Figure I-2[38]. The figure shows a basic biological membrane with its constituents. These constituents can be roughly divided into two groups: proteins and lipids. Proteins have different shapes and structures which are directly linked to their different functions. Depending on their location and position, proteins are subdivided further into peripheral proteins and integral proteins. The second main component of biomembranes are lipids that represent about 50% of the total mass of the plasma membrane. Besides acting as the main building block of membranes, lipids play a crucial role in the life of cells as they associate with proteins and are often involved in their functional regulation and in recruiting or anchoring proteins to the plasma membrane. Lipids themselves can be grouped into three classes: sphingolipids, glycolipids and sterols (see Figure I-3). Sphingolipids and glycerophospholipids are amphiphilic biomolecules due to their hydrophobic hydrocarbon tail and hydrophilic head group. Thus, they combine different solvation preferences with respect to aqueous solutions on geometrically different parts of the same molecule. This property is central for the formation, structure and organization of biological cell membranes. The hydrophobic part of a lipid is made of two acyl chains of generally different lengths that can be either saturated or unsaturated. Specifically, the chain length can be varied in the number of carbon atom from 12:0 to 22:6 (sn-1) for one chain and 12:0 to 22:6 (sn-2) for the other chain (the number behind the column indicates the number of unsaturated bonds) [36]. The glycerol group in glycerophospholipids itself can be modified by the substitution of ester, alkyl ether or alkenyl ether at the position 1, 2 or 3 as shown in Figure I-3. Another distinguishing property between different

lipids is the head group, i.e. the hydrophilic part of the lipid. In the case of glycerophospholipids, it can be modified to yield six classes of lipid. The most common head group is phosphatidylcholine (PC) which makes up approximately 50% of all lipids [39]. The others are phosphatidyl glycerol (PG), phosphatidyl-serine (PS), phosphatidyl-ethanolamine (PE), phosphatidic-acid (PA) and phosphatidyl-inositol (PI). In terms of abundance, the majority of membrane lipids belong to the glycerophospholipids, with sphingolipids being the second largest group. Due to possible permutations with respect to the length and degree of saturation of the acyl chains and the head group, there are up to 10,000 different lipids species [40] that are used.

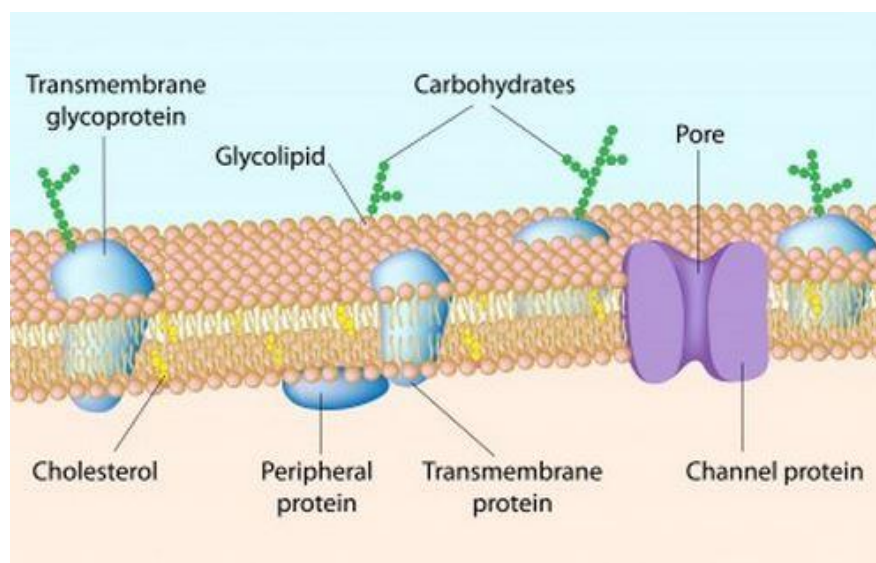


Figure I-2: Basic organization and composition of eukaryotic cell membrane. Adopted from [41]

Sphingolipids differ from glycerophospholipids by the substitution of the ester, alkyl ether and alkenyl groups by an amide group to form a ceramide (Cer). This modification together with different possible head groups (capital R in Figure I-3) yields seven classes of sphingolipid. These include sphingomyelin (SM), ethanolaminephosphoryl ceramide (EPC) and inositol phosphoryl ceramide (IPC) where the head group is respectively replaced by phosphocholine, ethanolamine

and phosphoinositol. In addition to these are glucosylceramide (GlcCer) for glucosphingolipids, galactosylceramide (GalCer) in the case of galactose. GalCer includes a wide variety of glycosphingolipids created by substituting the phosphate (orange oval in Figure I-3) and the head group with monosaccharides (represented as a G Figure I-3) [36].

In addition to the structural differences between the lipidic components of biomembranes, there are also distinct differences in their localization. The outer leaflet or extracellular leaflet is enriched with sphingolipids while the inner leaflet, or cytoplasmic leaflet is enriched with glycerophospholipids. The sterol cholesterol is found in both leaflets of the cell membranes but can spontaneously flip from one leaflet of plasma membrane to the other [42]. However, it is believed that it prefers to interact with sphingolipids.

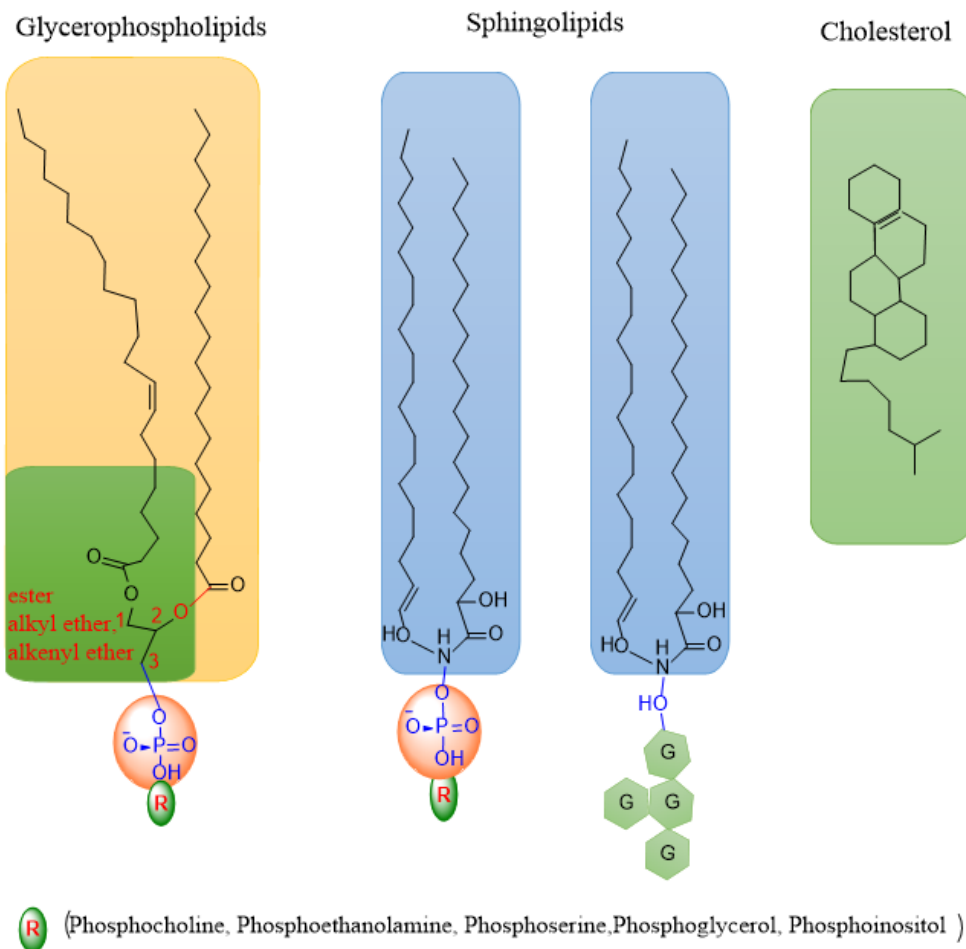


Figure I-3: Structure of phospholipid family: glycerophospholipids, (on left), sphingolipids (middle) and sterol (on right)

Functionally, cholesterol is important as it facilitates membrane fluidity and permeability. The differences in membrane composition give rise to the asymmetric double layer of lipids membranes. In addition, sphingolipids are packed more tightly due to their long saturated acyl chain when compared to glycerophospholipid that are richer in unsaturated acyl chain [13, 43].

A direct outcome of asymmetrical double layer membranes and the packing differences of its components is the potential to separate into two phases: a liquid-order phase ( $l_o$ ) and a liquid-disordered ( $l_d$ ) phase. In general, cell membranes and their mimics can take up the different behaviors of fluid and solid phases. Sphingolipids and cholesterol are tightly packed in the plasma

membrane. The interactions between sphingolipids and cholesterol are mediated through hydrogen bonds involving their hydrophilic head group and Van der Waal interactions between the ceramide moiety of sphingolipid and the sterol ring system [33]. As a result the Sphingolipid-cholesterol clusters can support more mechanical stress than glycerophospholipids [12]

### **1.3. Phosphatidylinositol Metabolism**

Since its incidental discovery in the 1970s and 1980s when scientists were investigating the pathway of G protein-coupled receptors (GPCRs) that lead to the activation of the enzyme phospholipase C by the receptor tyrosine kinases (RTKs) [44] phosphatidylinositol has fascinated scientists because of its numerous functions at the plasma membrane and other subcellular compartments and due to its unique ability to phosphorylate in seven species. This uniqueness of PtdIns makes this particular phospholipid the most important lipid in any cell membrane. Polyphosphoinositides are synthesized in different locations inside the cell by different Kinases and Phosphatases. The head group of all polyphosphoinositides is called the myo inositol ring and its spatial representation was introduced by Bernard William Agranoff in 1978 [45]. Bernard used the turtle as a representation for the inositol ring and the position of the phosphate groups are given by the head, legs and tail of the turtle. The parts are numbered counterclockwise starting from the right front leg as shown in Figure I-4. But not all the positions (hydroxyl group OH) can carry a phosphate group. In addition, position one is connected to the diacylglycerol ( DAG) through a phosphate group to form PtdIns. PtdIns is synthesized inside the endoplasmic reticulum (ER) and can be transported into the cytoplasm or other subcellular compartments by either cytosolic PtdIns transfer proteins or vesicles[1].

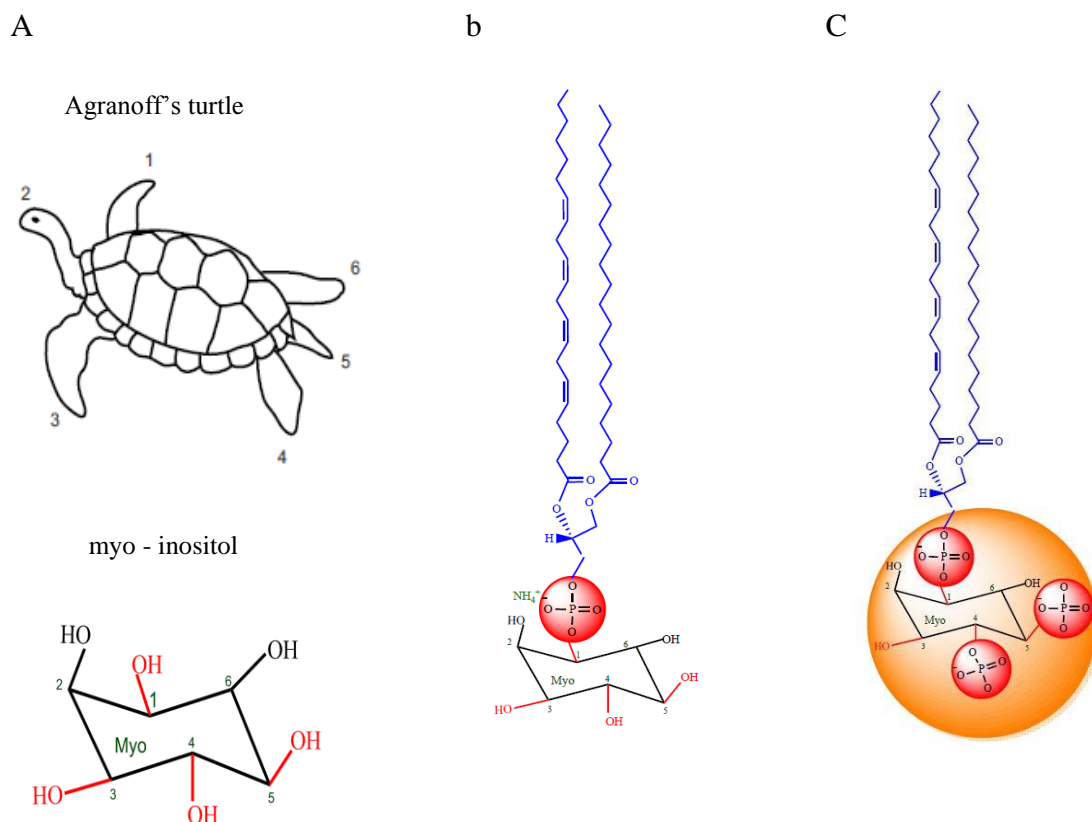


Figure I-4: Structure and configuration of the inositol ring (left panel), the phosphatidylinositol lipid (middle) and the clear marking of the whole head group (right hand panel)

Moreover PtdIns can phosphorylate only at the position 3,4 and 5 inositol rings to yield seven phosphoinositides as shown in Figure I-5 and Figure I-4 . The seven phosphoinositides are : PtdIns, PtdIns(3)P, PtdIns(4)P, PtdIns(5)P, PtdIns(3,4)P<sub>2</sub>, PtdIns(4,5)P<sub>2</sub>, PtdIns(3,4,5)P<sub>3</sub>. PtdIns range between ten to fifteen percent of the total amount of phospholipids depending on cell type whereas PtdIns(4)P and PtdIns(4,5)P<sub>2</sub> represent only 0.2- 1% of all the phospholipids. PtdIns(4,5)P<sub>2</sub> are now estimated to be around 5,000-20,000 molecules/ $\mu\text{m}^2$ [46].

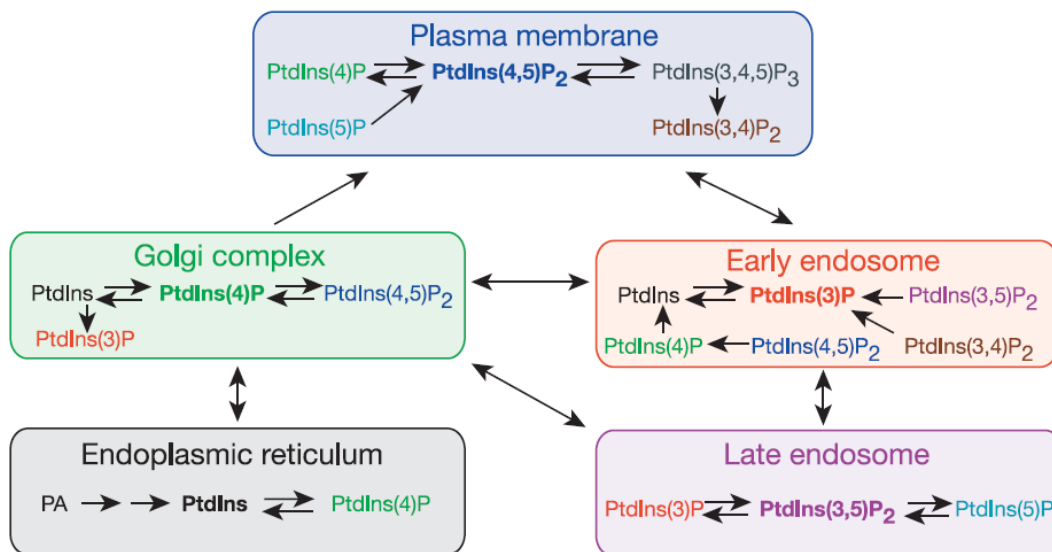


Figure I-5: Phosphoinositide synthesis. Many isoforms of Kinases and Phosphatases are located on membranes that are involved in the synthesis of PtdIns and one phosphoinositide which can be converted to the other and vice versa. Adopted from [14]

The manufacturing of Polyphosphoinositides involves hundreds of isoforms of kinases and phosphatases distributed in different subcellular compartments and the plasma membrane of the cell as shown in Figure I-5 and Table I-1[1] [14].

Kinases	Phosphatases
PI4KA, PI4KB, PI4K2A, PI4K2B (Stt4, Pik1, Lsb6)	SAC1M1L, (Sac1), SYNJ1/2 ??
PIP5K3/PIKfyve ??	SYNJ1, SYNJ2, OCRL, INPP5B, INPP5E,
PI3KC3, (Vps34), PI3KC2A	INPP5F, (Inp51, Inp52, Inp53)
PIP5K1A, PIP5K1B, PIP5K1C (Mss4)	TMEM55 ??
PIP5K2A*, PIP5K2B*, PIP5K2C*	MTMs, MTMRs
PIP5K3/PIKfyve (Fab1)	INPP4A, INPP4B
PI3KCA, PI3KCB, PI3KCG, PI3KCD	SAC3
	PTEN
	SHIP1, SHIP2, INPP5E, INPP5J, INPP5K

Table I-1 Phosphoinositol Kinases and Phosphatases



#### 1.4. Membrane Rafts

Eukaryotic cells utilize 5% of their genes to synthesize all lipids and only the function of a very small amount of these are well known, such as Phosphatidylinositol (PtdIns or PI). There is not a clear answer regarding a variety and numerous lipids produced by cells and their functions are still ambiguous[12]. Phospholipids, in particular play three key roles. Firstly, some members of this group are used to store energy. Secondly, the hydrophobic and hydrophilic properties inherent to phospholipids enable them to be used as building blocks of the cell membrane by forming an asymmetric bilayer. This provides a shielding protection against the outer environment while at the same time keeping the organelles and cytosol from leaking out of the cell. Finally lipids are involved in regulating the aggregation of proteins in the membrane. In addition, some subspecies such as phosphatidylinositol (PtdIns) are second messenger molecules in their own right, thus play an important role in cellular signaling events. All lipids are manufactured or synthesized in the inner leaflet of the endoplasmic reticulum or in the Golgi complex (sphingolipids or glycosphingolipids are manufactured in the Golgi complex) [40, 47]. Their synthesis depends on their functions which is directly connected to their local lateral segregation in either leaflet of the plasma membrane (PM) or other organelles. The outer leaflet or extracellular leaflet (sometimes called exoplasmic) is enriched with unsaturated Phosphatidylcholine (PC), saturated sphingomyelin (SM) and cholesterol. The inner leaflet or cytoplasmic leaflet is populated by phosphatidylinositol (PI), Phosphatidylethanolamine (PE), Phosphatidylserine (PS), PC and cholesterol. The distribution of PC and cholesterol are equal in both leaflets[48]. The uneven lipid composition in both leaflets of the PM yields to an asymmetrical structure of the PM[13]. Cholesterol interacts more with sphingolipids to make it a fluid like membrane therefore its concentration is controlled or determined by that of the sphingolipids in the plasma membrane.

Lipids move from the ER to the plasma membrane either by free diffusion or by specialized proteins carrier or vesicles [14].

The development of light based techniques has enhanced our understanding of biological cell membranes tremendously. These techniques have allow us to probe the dynamics of biological membranes to a few hundred nanometers and to discover the existence of lipid domains called rafts. They also help to obtain quantitative data [49]. The concept of lipid rafts found its root in the heterogeneity of cell membrane composition and function. It was proposed by Kai Simons & Elina Ikonen in 1997 from a study conducted on the interaction of sphingolipids and cholesterol[50]. They observed a formation of clusters that were dynamic in the bilayer and their role in the functionality of protein in the fluid bilayer. These observations have dramatically changed the perception that viewed lipids as passive fluid solvents and attributed all the functionalities to protein [11].

The transportation of glucosylceramide to the exoplasmic leaflet ( apical) of epithelial MDCK cells was also explained by taking into consideration the clustering of glycosphingolipid in the exoplasmic leaflet of the Golgi membrane[51]. Another argument that supports the above propositions comes from the role played by glycol-lipid anchors as a factor determinant in the regulation of glycosylphosphatidylinositol(GPI)-anchored proteins[52]. Membrane rafts are divided into three groups depending on their size ( rafts are lipid domains of 250nm in size [49]): rafts, cluster rafts and a subset of cluster rafts called caveolae. The constituents of a membrane raft can be lipid-lipid, cholesterol-lipid , proteins-lipids and proteins-proteins. Membrane rafts are dynamic, nanoscale and they can cluster to form micro domain raft membrane. Lipid rafts have received more focus in the scientific community as more cellular events that occur at the plasma

membrane require membrane rafts. Lipid rafts are used by many viruses, toxins and microbial pathogens as a gate for the entry into and exit from the host cell [4, 53, 54].

Viruses exploit membrane rafts for their intrusion or evasion(budding) in the host cell. One of the influenza virus family called the fowl plague virus (FPV) for example uses membrane rafts containing more detergent-insoluble complexes(glycoproteins) compared to other viruses such as vesicular stomatitis(VSV) and Smliki Forest virus(SFV). The depletion of cholesterol by methyl-beta-cyclodextrin in the envelope of the FPV virus has shown an increased solubility of glycoproteins and sphingomyelin in the envelope of the FPV virus[5]. The use of membrane rafts formed with protein-lipid interaction is seen in the budding of the FPV virus.

### 1.5. Phosphatidylinositol and Signal Transduction at the Cell Surface

The most well known phosphoinositides involved in the regulation of a plethora of events or processes occurring at the plasma membrane of a eukaryotic cell is the PtdIns(4,5)P<sub>2</sub> [55, 56] [2].Figure I-6 show the basic functionality of PtdIns(4,5)P<sub>2</sub> in its regulatory function, enzyme interactions and pools formation. The cellular events associated with either one of the three aspects of PtdIns(4,5)P<sub>2</sub> are represented in Figure I-7.

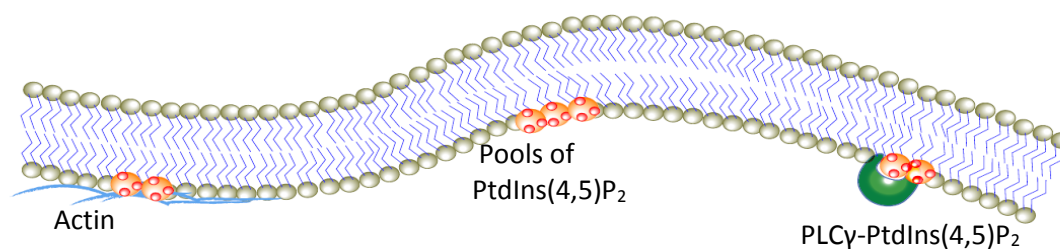


Figure I-6: Pools of PIP<sub>2</sub> in cytoplasm: Pools of PIP<sub>2</sub> in interaction with actin protein (left), aggregation of PIP<sub>2</sub>(middle) and hydrolyzation of PIP<sub>2</sub> by phospholipase C (PLCγ) (right)

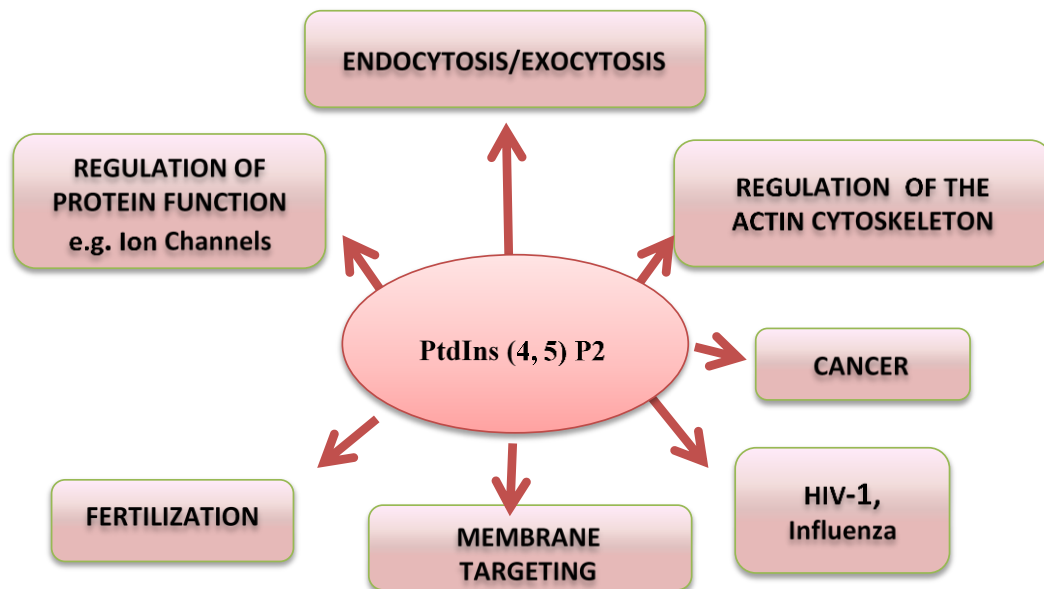


Figure I-7: Examples of signaling and processes regulated by PtdIns (4,5)P<sub>2</sub> in the cytoplasm membrane

#### ✚ PtdIns(4,5)P<sub>2</sub>-Actin

Polyphosphoinositides (PPI) regulate many cytoskeletal proteins and PPI recruits actin proteins to form a subcellular domain or restrain their function [57-59]. PtdIns (4, 5)P<sub>2</sub> in particular has been found to regulate the polymerization of the actin proteins. In vitro experiments conducted on many non-muscle cells have shown the dissociation of the profilin/actin complex and the induction of actin polymerization by PtdIns (4, 5)P<sub>2</sub> [57, 58]

✚ **PtdIns(4,5)P<sub>2</sub>-Cancer.** The tumor-suppressor protein (PTEN) is at the center of many types of cancer such as prostate, kidney, breast tumors, leukemia or Lymphoma, Lung, liver, bladder and others [7, 8] [60]. PTEN contains a phosphate domain and Lipid membrane-binding domain that fulfill the role of a tumor suppressor. In addition, PTEN is mostly found at the plasma

membrane where it acts as an enzyme to dephosphorylate phosphatidylinositol (3,4,5)-triphosphate (PIP<sub>3</sub>) to phosphatidylinositol (4,5)-biphosphate (PIP<sub>2</sub>). The dephosphorylation of PIP<sub>3</sub> induces a negative response in inhibiting the activity of class I phosphatidylinositol-3-OH kinase (PI3K) enzymes involved in cancer pathway signaling.

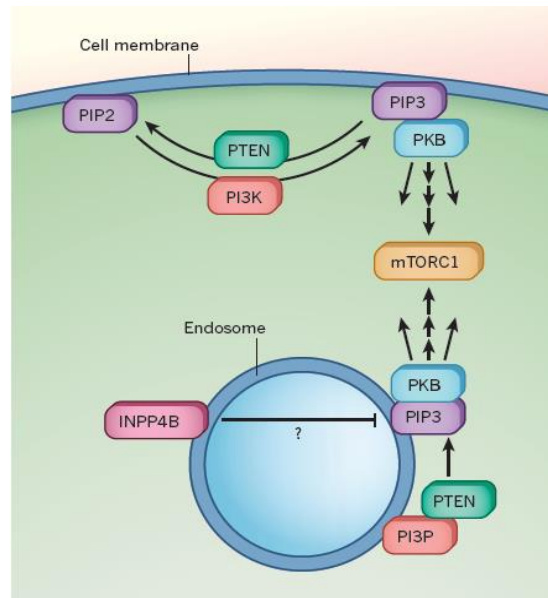


Figure I-8: Endosomal PTEN inhibiting the phosphorylation of PIP<sub>2</sub> by the Kinase PI3K and triggering the mechanisms that lead to cancer [7]

This activity of PTEN on PIP<sub>3</sub> has a negative regulatory function on the enzyme protein kinase B (PKB) and the mammalian target of rapamycin complex 1 (mTORC1). The membrane PTEN can also bind to the endosome via PI3P and interact in a similar way with PIP<sub>3</sub> phosphorylate by another lipid phosphate INPP4P (Figure I-8).

#### ✚ PtdIns(4,5)P<sub>2</sub>-Fertilization

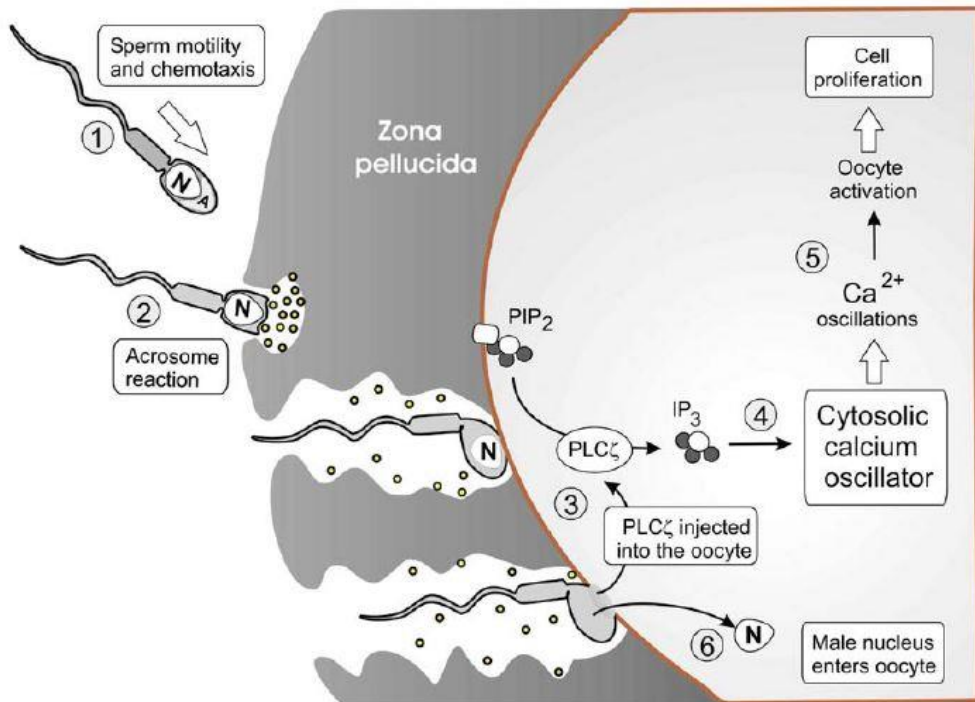


Figure I-9: PIP<sub>2</sub> signaling molecule in fertilization. The activation of Oocyte after the PtdIns(4,5)P<sub>2</sub> is cleaved by PLCξ from sperm which triggers the release of Ca<sup>2+</sup> from ER. [32]

The mechanism of calcium-induced calcium release elaborated upon (see Chapter IV) in connection with PI(4,5)P<sub>2</sub> is actively involved in oocyte activation and cell proliferation [19], calcium control chemotaxi (1), hyperactivation(2) and acrosomal exocytosis(3) of sperm[61] as shown in Figure I-9

**Virus Cycle:** Most budding of viruses from the host cell requires a formation of lipid raft-fluid. raft lipid membrane, HIV-1[4] and the influenza virus [5]

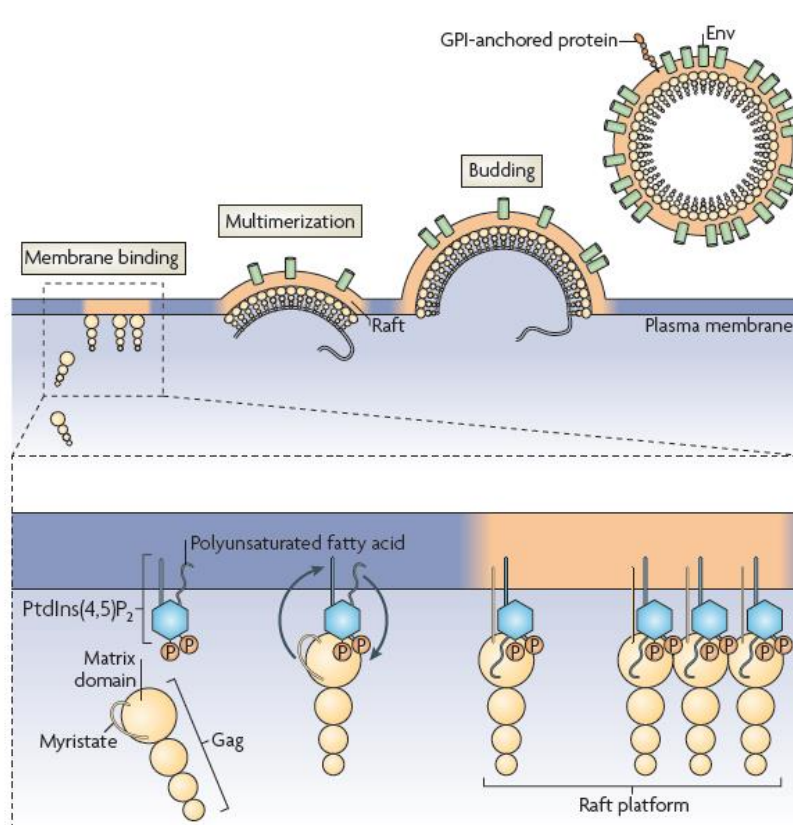


Figure I-10: PIP<sub>2</sub> mediates the budding process of human immunodeficiency virus type 1(HIV-1). [3]

The microdomains are enriched in cholesterol, phosphatidylinositol-4,5-bisphosphate [PI(4,5)P<sub>2</sub>] and play an important place in the budding process of human immunodeficiency virus type 1 as shown in Figure I-10 above[3]. In the process of budding, the HHV-1 assembly glycoprotein and lipids form a membrane raft around its nucleocapsid that will constitute the viral envelope. The formation of the HIV-1 envelope is driven by the Gag protein of HIV and constitutes the platform that interacts with the glycoprotein in the cytoplasm. In addition, the process depends on cholesterol and sphingolipids but the viral envelope is highly enriched in cholesterol, ceramide[62], phosphatidylinositol-4,5-bisphosphate PI (4, 5) P<sub>2</sub> ganglioside GM3[63].

Figure I-10 above shows how phosphoinositides phosphatidylinositol phosphate (PtdInsP) and [PI (4, 5) P<sub>2</sub>] are clustered as a matrix that interacts with Gag-HIV. During the interaction, scientists believe that there is a swapping of myristate fatty acids located at the N-terminus of Gag with the polyunsaturated fatty acid from [PI (4, 5) P<sub>2</sub>]. The clustering of [PI (4, 5) P<sub>2</sub>] in raft membranes has been proposed to be facilitated by Protein myristoylated Ala-rich C-kinase substrate (MARCKS) and growth-associated protein 43 (GAP43) [2]. Moreover the two phosphate groups from PI (4, 5) P<sub>2</sub> interact with an aggregation of amino acids that form the matrix domain. The later interaction has been proposed to be the one that mediates the clustering formation of PI (4, 5) P<sub>2</sub> domain by Gag-HIV. During the budding process, Gag will multimerize at the N-terminus and bind to PI (4, 5) P<sub>2</sub>, the myristate fatty acid will move into the hydrophobic cleft and be buried while the polyunsaturated fatty acid chain from PI (4, 5) P<sub>2</sub> will move into the pocket of the matrix domain of Gag due to its poor packing with cholesterol and its high flexibility and disordered structure.

#### **PtdIns(4,5)P<sub>2</sub>-Membrane Targeting**

The growing interest in the study of this minor family of glycopospholipid are strongly linked with its multiple implication in cellular event that occur at the membrane and the role of PIP<sub>2</sub> as a precursor of two messenger IP<sub>3</sub> and DAP. PIP<sub>2</sub> played a role of a recruiter of many different protein during specific cellular event such inflammation,

The distribution and formation of PIP in plasma membrane is still an active debate[ref3][64]



## 1.6. Imaging Techniques

### **Fluorescent Microscope Descriptions**

Imaging techniques have advanced the area of biophysics tremendously in terms of our understanding of cell biology, composition, structure and function. In the last few decades, however, the classic fluorescence microscope has experienced an important breakthrough with the development of super resolution fluorescence techniques. This fluorescent technique has overcome the limitations set by the law of diffraction due to the wavelength of light [24]. Hence achieving a high spatial resolution in the visualization of cell biology, composition and interaction. In addition, the dynamic of different biomolecules can be probed with good accuracy in time and space up to a few nanometers.

#### **Conventional Classic Fluorescence Microscope**

A conventional fluorescence microscope can be defined as a set of optical lenses that guides light to the sample and collects the emitted light from the fluorophore probe.

The goal of all fluorescence microscopes is to magnify biological cell constituents by relying on the properties of light and optics. The basic functionalities of all fluorescence microscopes are presented in Figure I-11a. Light travels from the source (e.g., lasers) through a divergent lens and is redirected by a mirror to a dichroic mirror that selects a specific wavelength. The selected wavelength will go through another set of lenses into an objective to be focused on a small region of the specimen or sample. Three events can happen when the incident light comes into contact with the sample: reflection, absorption and transmission (emission). Based on these events, due to the behavior of light, different modes of operation of fluorescence microscopes have been developed. Among the modes that can be cited are total internal reflection (TIRF), force resonance microscopy (FRET) and fluorescence recovery after photobleaching (FRAP).

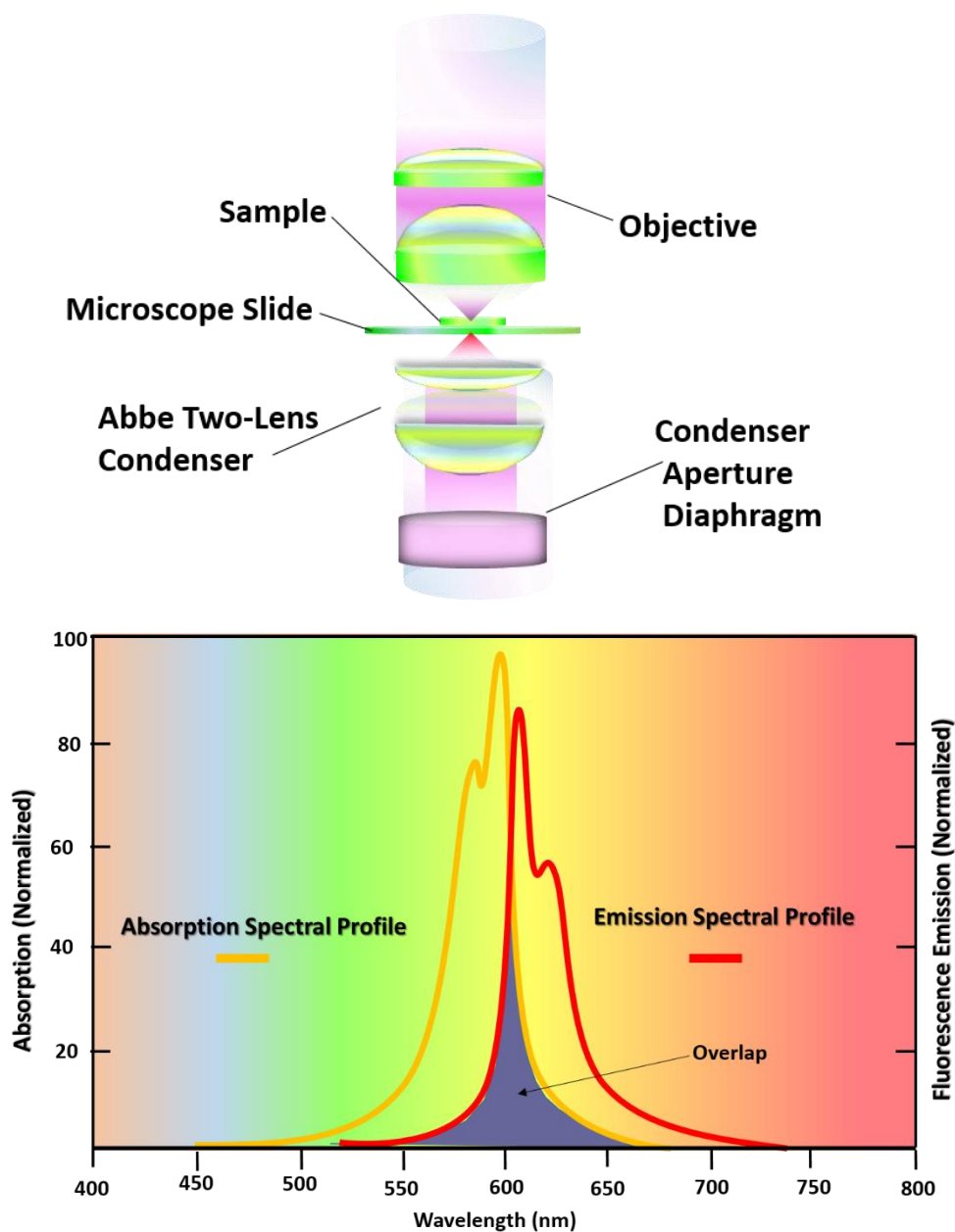


Figure I-11: Main features of Fluorescence microscopes: Abbe condenser optical pathway (top) and fluorophore absorption and emission profiles of Alexa Fluor 555(bottom).

The emitted light and the transmitted light from the specimen are characterized by a spectrum. When the incident light spectrum (or absorption spectra) intercepts the emitted light spectrum (emission spectrum), the intersection or the overlapping region it called Stroke (Figure I-11c). This overlap causes a disturbance in the image captured by the observer.

## 1.7. Interactions in Biological Systems of Phospholipids

Whenever there are at least two entities in contact (electrons, atoms, molecules, planets or stars) there is some sort of interaction that is involved. There are varieties of interactions (described by either a force or energy) that depend on the nature, distance and environment in which two or more entities interact. Based on these parameters, interactions are divided into four fundamental categories: strong, weak, gravitational, and electromagnetic interactions. Biological systems fall into the last category of interaction; almost all interactions in cell biology can be traced back to the electromagnetic interaction [65].

Physical systems are divided into three groups based on the strength of the interactions that govern their constituents. A physical system (matter) in which the strength of the interaction between its constituents (atoms, molecule etc.) has an order of magnitude close to  $K_B T$  is called the gas state (with  $K_B$  the Boltzmann constant(J/K) and T: temperature(K)). There are two types of gas state: ideal gas and parfait gas. As the strength between atoms or molecules increases above  $K_B T$  matter can change into two more states called liquid (sometimes called fluid depending on the viscosity) and solid. Many times in sciences such as condensed matter, researchers are more interested about the intermediate state or phase transition. Interactions that occur inside a cell biology can be classified in to three categories: Van der Waal, Hydrogen bonds and Electrostatic forces. These interactions regulate lipid organization in the plasma membrane, hence membrane structure, protein folding and cell signaling events [66]. Interactions in a biological system can be grouped in two categories: long-range and short-range interactions [67]. In contrast with short-range interaction or forces (interatomic, intermolecular), long range interactions in solids or liquids are those that appear at a distance greater than  $5\text{\AA}$  [68]

### 1.7.1. Van der Waals Interaction

Van de Waals interactions are interactions that result from fluctuating charges (electrodynamic ) and are classified as long-range interactions[67-70]. They play an important role in the organization of lipids or other biomolecules. These forces can appear between biological molecules (acyl chain of lipids) that are neutral (electrostatic). There are five types of Van der Waals interactions associated with fives isotherms [71]. A general formulation that includes all types has been proposed in the equation (I-1).

$$v = \frac{v_m c x}{1 - x} \frac{1 - (n + 1)x^n + nx^{n+1}}{1 + (c - 1)x + cx^{n+1}} \quad (\text{I-1})$$

with  $x = p/p_0$   $v$  and  $p$  respectively the volume and pressure adsorbed,  $v_m$  the volume of the monolayer of gas that covers the full surface,  $p_0$  the gas vapor pressure,  $c = e^{(E_1 - E_L)/RT}$  with  $E_1$  and  $E_L$  respectively the adsorbed and liquefaction heat of the gas;  $n$  is the maximum number of layers of the adsorbed gas on the planes of the capillaries. For  $n = 1$  we recover type I or the Langmuir isotherm:  $\frac{p}{v} = \frac{p_0}{cv_m} + \frac{p}{v_m}$ .

All others are obtained by imposing different conditions on parameters  $n$  and  $c$  (e.g. type II  $n = \infty$  and  $c \gg 1$ ). The values of  $v_m$  and  $c$  are given by the slope and intercept of the plot of  $\frac{p}{v}$  versus  $p$ .

### **1.7.2. Monolayer technique and Langmuir Adsorption of phospholipids**

The impetus for constructing biomimetic membrane systems has been imposed first by our inability to study cell membrane constituents *in vivo* due to the complexity of their interactions. From the structure and composition of cell membranes, interactions can be classified in three groups: interactions within phospholipids, interactions between phospholipids and proteins [72], and interactions with ions and other biomolecules across the two dimensional structure of the cell membrane. The second reason is our limited ability to probe these biomolecules at nano scale as they interact in their environment. The intrinsic amphiphilic properties inherent to biomolecules in particular phospholipids to self-assemble into a bilayer that mimics a cell membrane have led to the development of many techniques that aim to answer different key questions about cell biology. In addition, these techniques are extensively used in nanobiotechnology for various applications. This section will discuss a few of them with a primary focus on Langmuir-Blodgett Films balance. LB offers many advantages that are not provided by other technologies or techniques such as full control over the packing density and easy manipulation of the buffer solution.

### **1.7.3. Langmuir-Blodgett Films Balance**

The LB technique was introduced in 1917 by Irving Langmuir and his research assistant Katharine Blodgett[73]. In 1932 Langmuir received the Nobel Prize in chemistry for his work on intermolecular forces in the film monolayer. This section underlines the fundamental concepts of Langmuir-Blodgett films balance (LB). Organic molecules like lipids with their dual properties of hydrophobic tail and hydrophilic head groups self-assemble at an air/water interface by minimizing their free energy. Moreover they form a thin insoluble monolayer called a Langmuir film of one molecule thick (Figure I-12). The instrument used to produce the monolayer is called

a Langmuir trough. It is made with a Teflon trough which holds an aqueous subphase (water) and two movable barriers as shown in Figure I-12 below. In addition, the instrument is equipped with The Wilhelmy Plate (a grey rectangle), a sensor that measures the force, and another detector attached to the barrier to measure the area per lipid as the monolayer is compressed.

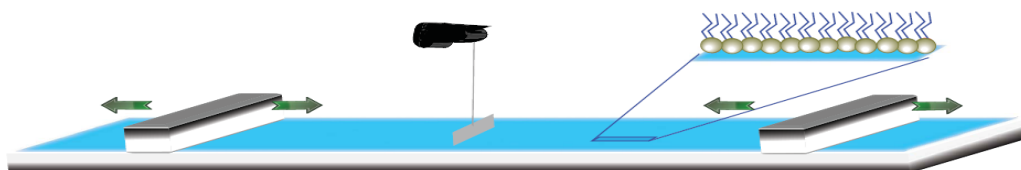


Figure I-12: Langmuir Trough and Monolayer Formation. The packing density of the monolayer is controlled by the moveable and symmetrical barriers (gray rectangles) as the surface pressure is recorded through a force transducer (black).

**Surface Tension.** The study of the Langmuir-Film or monolayer is based on the notion of thermodynamics. According to the thermodynamic properties of the air/liquid interface, the molecule in the bulk solution experiences a balance in interaction with all the neighboring molecules. However, the molecule at the interface experiences excess free energy due to the variation in the environment. The molecule at the interface experiences more inward attractive force than the gas phase; the result of unbalanced forces will spontaneously minimize its area and contact. A direct response to these changes is an increase in free energy due to the work done to extend the surface against the attractive force. Because of the attractive force, there will be more diffusion of molecules from the surface to the bulk and the equilibrium is attained when an equal amount of molecules leave the bulk to the surface [74]

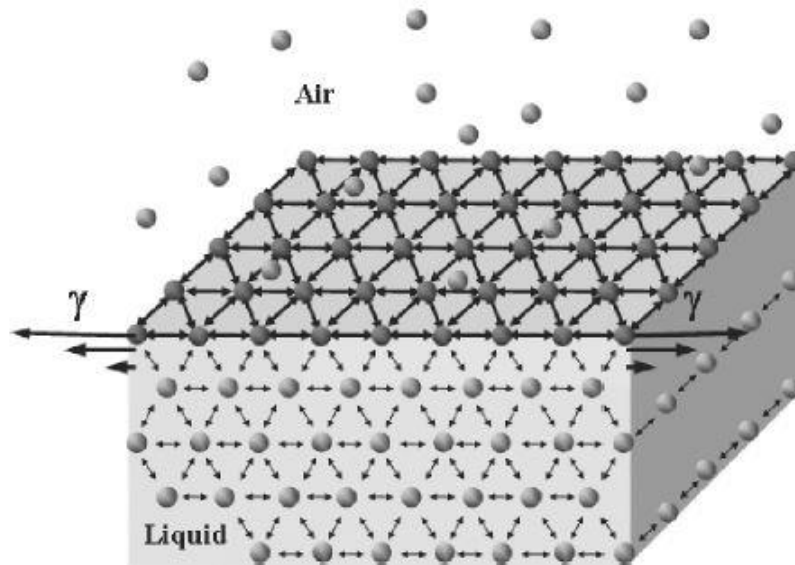


Figure I-13: Surface tension description [74]

The surface tension ( $\gamma$ ) is defined as the linear force acting on the molecule and it is given by the partial derivative of the free energy with respect to the area per molecule ( $S$ ) (I-2).

$$\gamma = \left( \frac{\delta F}{\delta S} \right)_{T,V,n_i} = \left( \frac{\delta G}{\delta S} \right)_{T,P,n_i} \quad (\text{I-2})$$

The

Helmholtz and Gibbs free energy are respectively represented by the letter  $F$  and  $G$  and the temperature ( $T$ ), volume ( $V$ ), pressure ( $P$ ) and the number of components ( $n_i$ ) are kept constant. For a pure liquid in equilibrium with the saturated vapor, the surface tension is only given by the excess Helmholtz free energy per unit area as in equation (I-3)

$$\gamma = F^s / A \quad (\text{I-3})$$

The

unit of the surface tension is  $\text{J}/\text{m}^2$  or  $\text{N}\cdot\text{m}/\text{m}^2$   $\text{mN}/\text{m}$ . For water, the surface tension is  $72.8 \text{ mN}/\text{m}$ . This high value is due to the fact that water is a polar liquid and the intermolecular interactions are strong.

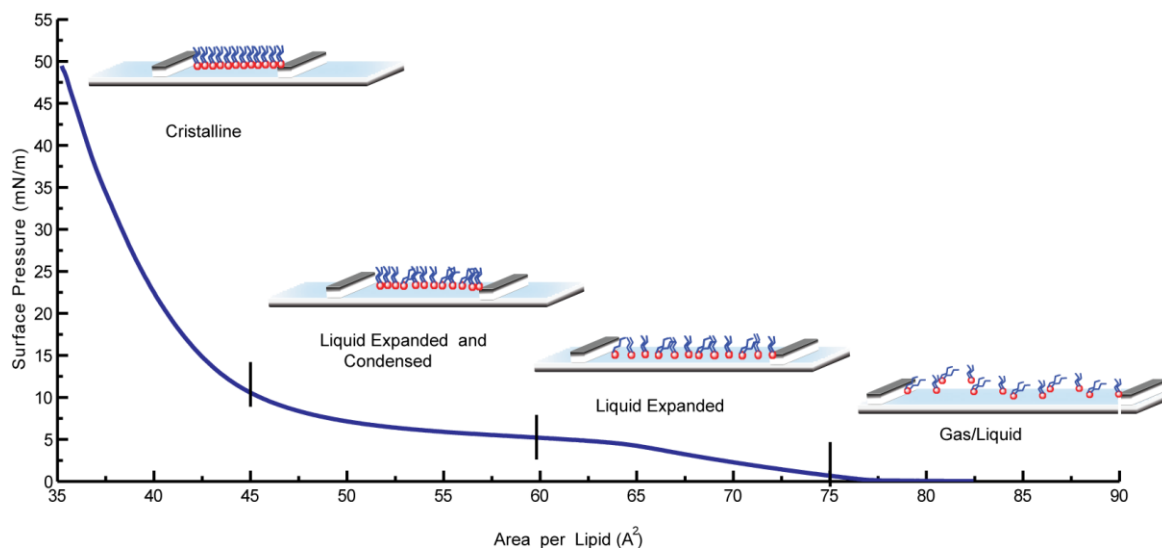


Figure I-14: DPPC Isotherm and Phases. Different phases are observed in the monolayer of DPPC as the area occupied by the monolayer decreases.

**Surface Pressure.** The free interface of air/water has a negative pressure due to the attraction of molecules (water or oil) in the bulk as described above. When adding or spreading an amphiphilic molecule at the interface of water/air, a spontaneous monolayer will form. The hydrophilic polar group will interact with the polar molecule (water) that causes the reduction of surface tension and free energy. Different phases are distinguished based on the area covered by surfactants (amphiphilic molecules or lipids) to the area available. When the amount of lipids is not sufficient and the area is larger, the effect is negligible on surface tension and this phase is referred to as the gas phase. Moreover, when the area is being reduced by moving barriers, the hydrophobic regions start to interact repulsively on each other and the surface tension starts lowering more. The monolayer will go from the liquid expanded phase to the liquid expanded and condensed phase,



then end in the crystalline phase (Figure I-14). The difference between the surface tension of a pure liquid or water ( $\gamma_0$ ) and the surface tension of the monolayer ( $\gamma$ ) is called surface pressure ( $\pi$ ).

$$\pi = \gamma_0 - \gamma \quad (\text{I-4})$$

The

surface tension of pure water at 20 C is known to be 72.8 mN/m. This value sets the upper limit of the surface pressure of any monolayer formed on the water surface.

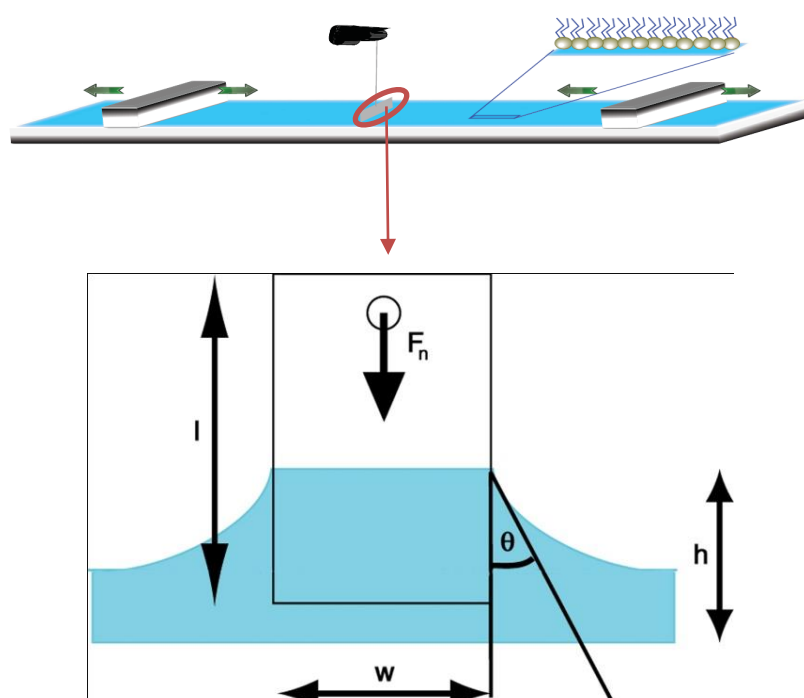


Figure I-15 Force acting on the Wilhelmy Plate

**The Wilhelmy Plate.** A Langmuir-Blodgett system is mounted by a force sensor that records the surface pressure as a function of an area per lipid on the aqueous subphase surface. A plot record is called an isotherm. A Wilhelmy plate is a force transducer that measures the force exerted by the monolayer due to variations in surface tension. For a rectangular Wilhelmy plate, downward force is a function of the rectangular dimensions ( $l$ =length,  $w$ =width,  $t$ =thickness,  $h$ =depth) and plate density  $\rho_p$ .

For a pure surface (without any surfactant), the downward force  $F_0$  is given by:

$$F_0 = \rho_p g l w t + 2\gamma_0(t + w)\cos\theta_0 - \rho_L g t w h \quad (\text{I-5})$$

For a surface cover with a monolayer, the downward force  $F_m$  is given by

$$F_m = \rho_p g l w t + 2\gamma(t + w)\cos\theta_m - \rho_L g t w h \quad (\text{I-6})$$

with  $\theta_0$  and  $\theta_m$  respectively the contact angle of the pure water and the monolayer at the interface,  $g$  and  $\rho_L$  are respectively the gravitational constant and the liquid density.

The difference between (I-6) and (I-5) yields to the change in surface tension which is the variation of the surface tension of pure water with the surface pressure of the film monolayer.

$$\Delta F = 2(t + w)(\gamma\cos\theta_m - \gamma_0\cos\theta_0) \quad (\text{I-7})$$

For a wet plate by the liquid, the contact angle can be approximated to zero and thickness can also be negligible compared to the width ( $t \ll w$ ). In these conditions the relation (I-7) is reduced to:

$$\Delta F = 2w(\gamma - \gamma_0) \quad (\text{I-8})$$

By

using the relations (I-4) and (I-8) the surface pressure is directly connected to the change in the force  $\Delta F$  as in the relation (I-9)

$$\pi = -\Delta\gamma = -\Delta F/2w \quad (\text{I-9})$$

The Langmuir-Blodgett film balance used in our laboratory is equipped with a microstepping motor that drives barriers during the compressions and has a sensitive

electrobalance directly coupled to the Wilhelmet plate as shown in Figure I-12 and Figure I-15. The ability of phospholipids to self-assemble has opened doors to other technologies, as mentioned above. In vivo study presents many challenges due the complexity of the biological membrane. These challenges have been the driving force behind all the technology developed and each has its own advantages. The LB studied above offer not only offer possibility of working with a monolayer system, but it also provides a way of forming a multilayer [75, 76]. In addition, other types of artificial membrane can be made, such as vesicles[77]

#### **1.7.4. Hydrogen bonds in lipid monolayer and bilayer**

An anomalous property of water that presents great advantages in many biological molecules is its dipolar property that results from the hydrogen-oxygen-hydrogen interaction. The hydrogen bond is the underlying explanation of these anomalous behaviors observed in water molecules. The interaction of a hydrogen atom with an electro-negative atom leads to a polar molecule in which the hydrogen atom represent the positive pole. The resultant dipole can interact with another dipole that leads to what is called dipole induced dipole. Dipole- dipole interactions are classified as short-range interactions because the distances at which interactions occur are less than the Van der Waals interaction. The space that separates two dipole is 0.26 nm or 0.31 nm and the hydrogen atom that bridges the two dipoles belong to both dipoles. The energy related to a hydrogen bond varies between 13 and 25kJ/mol and this makes the hydrogen bond interaction weak and as such it can easily break under thermal variation in the environment (e.g. temperature in cellular biology).

#### **1.7.5. Electrostatic Interaction in a Biological membrane**

The inner leaflet of the cell membrane is populated with charged (ionized or polar) molecules (proteins and lipids) that regulate the function, organization and structure of the

cytoplasmic membrane due to the electrostatic interaction. The Coulomb interaction as a result of these charged biomolecules and bivalent ions gives rise to surface electrostatic potential  $\varphi_0$  that plays a crucial role in cell transport functions[78]. Since lipids and proteins that form the cytoplasmic membrane are negatively charged, the potential associated with these lipids and proteins is below the neutral point. This potential is cell type dependent. The potential is about -60mV in erythrocytes [79] and -120 to -170mV in freshwater algae. For eukaryotic cells the resting potential varies between -60 to -75mV for tumor and neuron cells. These potentials are very sensitive to the environment, a change in ions, outer membrane or pH will dramatically affect the potential[78]. One can ask about the calculations or method used to determine these potentials and the accuracy of the models or techniques used.

### **The Gouy-Chapman Model**

The Gouy-Chapmann theory on electrostatic surface potential is a good model that is still being used today. It was developed more than a century ago independently by Gouy and Chapmann. There are assumptions made about the theory in relation to the inner leaflet layer of the cell membrane and ions in bulk solutions. The theory treats the charged lipids of the cytoplasmic membrane as fixed and forming a smear plane of semi-infinite monolayer and the counter ions or co-ions as a point charged massless particles and equally distributed  $g_1 = g_2$  [80]. The interactions between the negatively charged lipids in the cytoplasmic surface and the ions(counter-ions or counter-ions) give rise to two layers. This creation of a double layer of charged molecules has been a focus of much scientific research for more than a century. Many formulations have been proposed base on Poisson and Boltzmann equations (PB) for different systems and conditions. The Gouy-Chapman model, formulated in 1910 by Gouy and 1937 by Chapman, is based on PB theory

and Langmuir adsorption isotherm theory[81]. Gouy-Chapman used two major concepts in physics and bridged them to form an elegant theory that describes the surface potential generated by charged molecules as a function of the charged density. The first concept comes from the Poisson equation that states that the Laplacian of the electrostatic potential is proportional to the charge density in a given system.

$$\nabla^2 \varphi = \frac{\sigma}{\epsilon_0} \quad (\text{I-10})$$

For a system of two different ions in bulk solution the work required to move an ion  $i$  from  $|r| = \infty \Leftrightarrow \varphi(r) = 0$  to the position where  $\varphi(r) \neq 0$  is given by  $z_i e \varphi(r)$  with  $z_1 = -1$  or  $z_2 = +1$  the valence, with  $z_i \in \mathbb{R}$ . The Boltzmann distribution law relates the concentration of ion  $i$  close to the membrane to its concentration in the bulk  $C_i = C e^{z_i e \varphi(r) / K_B T}$ . The total charge density is therefore given by:

$$\sigma(r) = C_+ e - C_- e = -2C e \sinh\left(\frac{e\varphi(r)}{K_B T}\right) \quad (\text{I-11})$$

After substituting (I-11) into (I-10) we obtain:

$$\nabla^2 \varphi(r) = \kappa^2 \left(\frac{K_B T}{e}\right) \sinh\left(\frac{e\varphi(r)}{K_B T}\right) \quad (\text{I-12})$$

where  $\kappa = \left(\frac{8\pi N_A e^2}{1000\epsilon K_B T}\right)^{1/2} J^{1/2}$  Debye-Huckel length and  $J = \frac{1}{2} \sum_{i=1}^2 g_i z_i^2 = \frac{1000C}{N_A}$  the ionic strength. Stern deduced a more general formulation of the equation (I-12) which is explained in section 2.4

## Chapter II : Modulation of Phosphoinositide Monolayer Compressibility by Physiological Levels of $\text{Ca}^{+2}$

### 2.1. Abstract

In the cytoplasmic membrane, charged lipids play many key roles in the life of a cell, signaling and regulating the cytoskeleton proteins. Polyphosphoinositides (PIPs) are involved in most cells' many complex signaling events that happen at the inner cytoplasmic leaflet of the cell membrane and other organelles' membranes. These glycerophospholipids feature an inositol ring at their head group which provides potentially five locations for phosphorylation. The possible permutations that give rise to seven different PI subspecies with PI(4,5) P<sub>2</sub> apparently omnipresent in many cellular events that occur at the plasma membrane. PI(4,5) P<sub>2</sub> is a prevalent form representing the version with phosphate groups on carbon 4 and 5 (properly known as phosphatidylinositol (4,5)-bisphosphate). It only occupies 1% of all lipids. This class of lipids has attracted the attention of many researchers. Two main routes have been taken in an attempt to understand these complex lipids. One route examines the nature of the interaction of this lipid in the presence of bivalent ions (monolayer or bilayer system or vesicle containing PI(4,5) P<sub>2</sub>). The other route looks into the surface potential induced by charged lipids in general and PIPs in particular, in the presence of bivalent ions. Different models about the form of the surface potential have been proposed. In experimental results, the Gouy-Chapman-Stern model is most commonly used and its predictions match in most cases. There has been no study yet done about the elasticity properties of the monolayer and bilayer systems of ionic lipids in the presence of bivalent ions. We address this problem by studying the lateral isotherm compressibility in a monolayer system. We also developed a theoretical framework for the compressibility that depends on the electrostatic surface potential. Our experimental results for the compressibility of the monolayer are in

agreement with our theoretical framework for compressibility. We used the Gouy-Chapman-Stern (GCS) model.

## 2.2. Introduction

Lipid membranes play a key role in living cells as they organize molecules in time and space. For one, they are formidable barriers to random transport across membranes and thus help to compartmentalize eukaryotic cells [13, 33]. In addition, they are also quasi-two-dimensional, highly-structured fluids [9, 12]. As such, they provide the ideal environment for dynamic rearrangement of molecules within the plane of the membrane. This feature is paramount for both time-dependent assembly of molecules into larger membrane structures [15], as well as the proper execution of membrane-associated biochemical reactions [16-18]. Ultimately, these two aspects are intimately linked through the impact of membrane structures on lateral transport and *vice versa* [19]. It also appears that this interplay has an important role in the proper execution of cellular processes [20]. Underpinning these exceptional properties of biomembranes are the peculiar physicochemical characteristics of lipids, in particular their amphiphatic character.

Although the structural importance of lipids and lipidic molecules for membranes is well established, it should be remembered that there are also many members of these species that are important because of their biological functions. Great examples of the roles that lipids play in cellular processes are exocytosis, fertilization, and gene transcription [16, 32, 82]. It is indisputable now that phosphoinositides (PIs) reign supreme in the realm of lipids with distinct biological functionality [2, 55]. These glycerophospholipids feature an inositol ring at their head group which provides potentially five locations for phosphorylation. The possible permutations that give rise to seven different PI subspecies with PI(4,5) P<sub>2</sub> apparently omnipresent. PI (4,5) P<sub>2</sub> is a prevalent form representing the version with phosphate groups on carbon 4 and 5 (properly known as

phosphatidylinositol (4,5)-bisphosphate). Given the multitude and diversity of processes in which even a single sub-species such as (4,5) PIP<sub>2</sub> is involved [83, 84], one central question is inevitable: “How does the cell funnel these diverse functionalities through one particular molecule species while avoiding unwanted crosstalk between the different cellular processes involved?” One possible and arguably the most likely answer is: “Via spatial-temporal regulation”. In other words, spatially separated pools of, for example PIP<sub>2</sub>, that are, for the most part, regulated and controlled independently [85]. This would allow for specific PIP<sub>2</sub>-related functionality to be executed at one end of the cell, while at a different location, a separate pool of PIP<sub>2</sub> is involved in another set of biochemical reactions.

Experimental observations of distinct areas of (PtdIns(4,5)P<sub>2</sub>) enrichment in living cells support this idea [14, 86]. Yet, given the typical lateral fluidity of the lipid membranes such as the cellular plasma membrane, the question then becomes: “What physicochemical mechanisms might a cell exploit to form, maintain and regulate these ‘pools’ or domains of high PIP<sub>2</sub> concentration?” Currently, a few different possibilities have been proposed. For one, phase separation mechanisms that rely on cholesterol dependent fluid–fluid de-mixing of lipids could play a role [87-89]. Others, however, might employ at least in part the fact that at physiological conditions, each phosphate group contributes about one negative charge, thus making highly phosphorylated PIs such as PIP<sub>2</sub> strongly anionic. For example, it has been shown that myristoylated alanine-rich C kinase substrate (MARCKS) does not rely on specific PIP<sub>2</sub> binding sites but is able to organize the highly negative PIP<sub>2</sub>s by exploiting highly positively charged regions of the peptide [28][2].

Another intriguing avenue is the aggregation of phosphoinositides due to the action of bivalent ions [89-91]. This is in particular appealing as it directly couples biological functions such as calcium signaling to the spatial organization of membranes. Recent investigations have provided



some basic insight into the interactions of highly acidic lipids in the presence of bivalent ions such as calcium and magnesium. However, the range of ion concentrations in these studies lies mostly between 1  $\mu\text{M}$  and 1  $\text{mM}$  [89, 92]. These magnitudes are already interesting as they can be found during cellular signaling [93]. However, it is typical that calcium concentrations are mostly in the range of 200  $\text{nM}$  to  $\sim 1 \mu\text{M}$  [94]. So, for example, the concentration of calcium in *Xenopus* oocyte is measured to be 1  $\mu\text{M}$  [95], or in cardiac myocyte is found to be 170  $\text{nM}$  [92] or even 1000  $\text{nM}$  in hormonal activation [96].

Thus, our work logically extends these previous studies to a range of ion concentrations that are most commonly found in eukaryotic cells. Therefore, we hope to illuminate to what extent ion-induced aggregation processes of, for example,  $\text{PIP}_2$  can indeed play a role in cellular signaling processes in those circumstances. We also investigate the elasticity properties of the monolayer of  $\text{PIP}_2$ ,  $\text{PI}$  and  $\text{DOPG}$  due to the interaction of bivalent ions. The negative charges on monovalent or polyvalent lipids in the presence of counter ions in the buffer create a double layer that has attracted the attention of many [97-99], and is best described by the Gouy-Chapman Stern theory [65, 100, 101]. This theory states that the surface electrostatic potential is directly proportional to surface charge density. The electrostatic potential is a very important parameter in the study of ion channels and other processes in which cytoplasmic membranes are involved. Based on this theory, many experiments have been done which continue to confirm the theory by determining the surface potential [99]. We want to answer the question, "How do lateral reorganization and surface potential affect the elasticity properties of the bilayer/monolayer?" We found that there is a connection between local potential and isotherm compressibility, but also deduced a term that can be accounted as a term that contributes to surface potential. We believe that this term contributes to the stiffness or deformation of the structure as the surface potential increases or decreases.

Processes that occur at the cell membrane, such as endocytosis and exocytosis, involve changes in membrane elasticity which can be studied from the measurement of the lateral surface pressure of the monolayer when it is equivalent to that of the bilayer.[72, 102]. Studies have shown that these elasticity properties are functions of temperature, salinity, pH and lipid composition (acyl chain and head group) and type [103-105]. Different techniques have been developed [104, 106, 107] to measure the elasticity properties of bilayers. Some techniques present different challenges, such as the extrusion of solvents for the estimation of deformation in a bilayer[104, 106].

### 2.3. Materials and Methods

**Lipids and Reagent:** L- $\alpha$ -phosphatidylinositol (Liver, Bovine) (PI), 1,2-dioleoyl-*sn*-glycero-3-phospho-(1'-myo-inositol-4',5'-bisphosphate) (ammonium salt) (PIP<sub>2</sub>), 1,2-di-Dioleoyl-*sn*-glycero-3-[Phospho-rac-(1-glycerol)] (DOPG) were purchased from Avanti Polar Lipids (Alabaster, Alabama; USA) in a desired concentration of 1mg/ml of Chloroform solution for (DOPG)and chloroform/methanol/water 20:9:1 for (PI(4,5)P<sub>2</sub>) and stored at -20° C without further purification and used within three month periods to avoid oxidation. Calcium Chloride CaCl<sub>2</sub>, Magnesium Chloride MgCl<sub>2</sub>, Sodium Chloride NaCl, Citric Acid, Sodium Citrate and HEPES were purchased from Sigma-Aldrich, (St. Louis, Missouri, USA) in powder form and kept at room temperature.

All buffer solutions, calcium concentrations [Ca<sup>+2</sup>] and magnesium concentrations [Mg<sup>+2</sup>] were prepared in distilled and deionized water from a Milli-Q Apparatus (Millipore) and kept at low temperature (1°C). 10mM of HEPES was used for the monolayer experiment at pH 7.4 and 0.2M Sodium Citrate was used for all the monolayer experiments at low pH (pH 3.5).

The monolayer surface pressure versus area per lipid ( $\pi$ -A) (Figure II-2) measurements were obtained from a computerized KSV Langmuir-Blodgett Minitrough (LB) at a constant compression rate (12 mm/min) after the deposition was completed and 10 minutes elapsed for the

evaporation of chloroform. To avoid contamination of the monolayer, the trough's system was enclosed in a Plexiglas box. A constant temperature was maintained by circulating water through a tube attached to the base of the trough and to a monitoring heat reservoir system. Each experiment was repeated three times and data were processed by using Matlab and Igor-Pro.

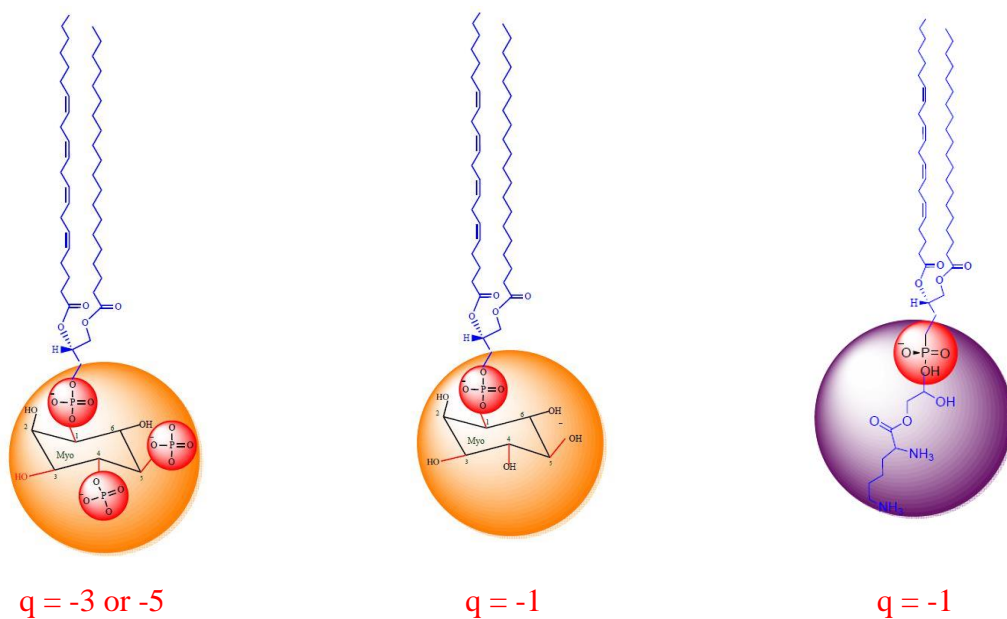


Figure II-1: Highly charged PI(4,5)P<sub>2</sub>, (left), PI (middle) and DOPG (right).

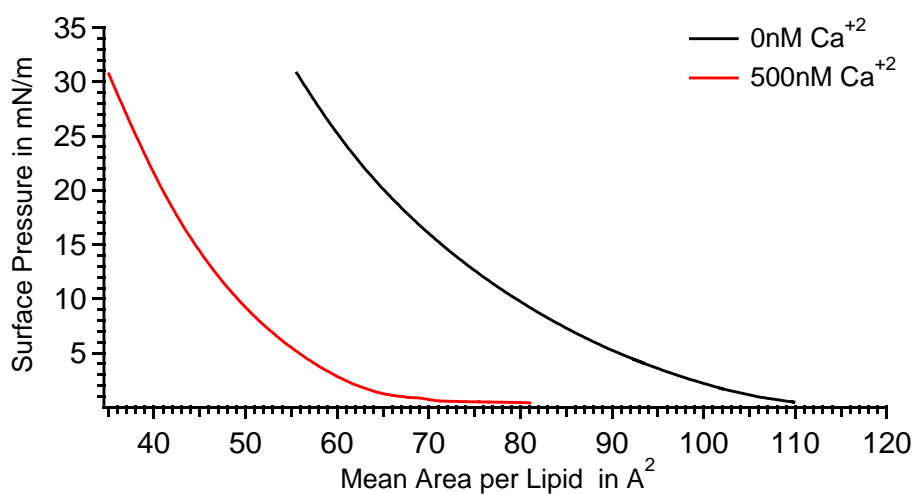


Figure II-2: Isotherm of PIP<sub>2</sub> in the absence of Ca<sup>2+</sup>(black curve) and in the presence of Ca<sup>2+</sup>(red curve).

## 2.4. Data Analysis and Discussion

Most studies on compressibility were conducted between 1970 and 1981 by Evans and his co-workers by using micro pipette aspiration on the red blood cell. They reported a value of  $3.47 \cdot 10^{-3}$  m/mN [108]. Previous work done by Losche [109] on the influence of bivalent ions on the compressibility of dimyristoylglycerophosphate (DMPA) yielded a value of  $\geq 10$  times magnitude compared to recent results, including our results. They also observed a deep decrease in compressibility under the influence of ions [109]. There has been no investigation to our knowledge on the effect of bivalent ions ( $\text{Ca}^{+2}$  and  $\text{Mg}^{+2}$ ) on the compressibility of anionic phospholipids, such as  $\text{PIP}_2$ , DOPG and PI.

The physical properties of lipid bilayers and lipid monolayers are similar for both systems at a lateral surface pressure of 30-35mN/m. Using a monolayer system gives more flexibility [110, 111] to conduct studies that are difficult to do in vitro with a bilayer system. Additionally, we know that monolayers display a surface potential for zwitterionic and anionic lipids [112, 113].

The isotherm plots of most lipids exhibit different phase transitions, gel/liquid or liquid/crystalline, and different domain structures regulated by electrostatic interactions [109]. The dipole moments increase in the liquid/crystalline or in the condensed phase due to an excess of the repulsion force due to an excess of charges [113]. These have an influence on geometries (texture), nucleation, domain shape and size uniformity. It has been shown that ions binding to lipid head groups lower the monolayer surface charge, which in turn leads to a decrease in surface tension [114].

Other results on the lateral isotherm compressibility of POPC show  $C_s^{-1} = 122 \text{ mN/m}$  [115] which is significantly close to our result  $C_s^{-1} = 112 \pm 4 \text{ mN/m}$  in the liquid expanded phase. Studies have shown that the lateral isotherm compressibility of most phospholipids varies from

0.004 m/mN in the liquid phase to 0.002 m/mN in the crystal phase[105]. It has been shown that lateral isotherm compressibility is lesser in liquid-crystal than in the expanded phase, but the effect of bivalent ions on compressibility has not yet been investigated. Figure II-2 shows that bivalent ions have an important effect on lateral isotherm compressibility for charged anionic lipids. As demonstrated by Blank[116], the instantaneous surface pressure is proportional to the mean surface pressure  $\langle \pi \rangle$  and compressibility  $C_A$ , and the penetration of ions or others molecules is directly connected to the magnitude of  $C_A$ ,

$$\pi \cong \langle \pi \rangle \left[ 1 \pm (K_B T C_A / A)^{\frac{1}{2}} \right] \quad (\text{II-1})$$

where  $K_B$  is the Boltzmann constant, T is the absolute temperature and A is the area per lipid.

Lateral isothermal compressibility is determined by the expression below:

$$C_A = \frac{1}{A} \left( \frac{\Delta A}{\Delta \pi} \right)_T \quad (\text{II-2})$$

By

using the formula (II-2) to our isotherm of PIP2, DOPG and PI we were able to compute the compressibilities of PIP2, DOPG and PI at various physiological levels of bivalent ions with an uncertainty of  $\approx 10\%$

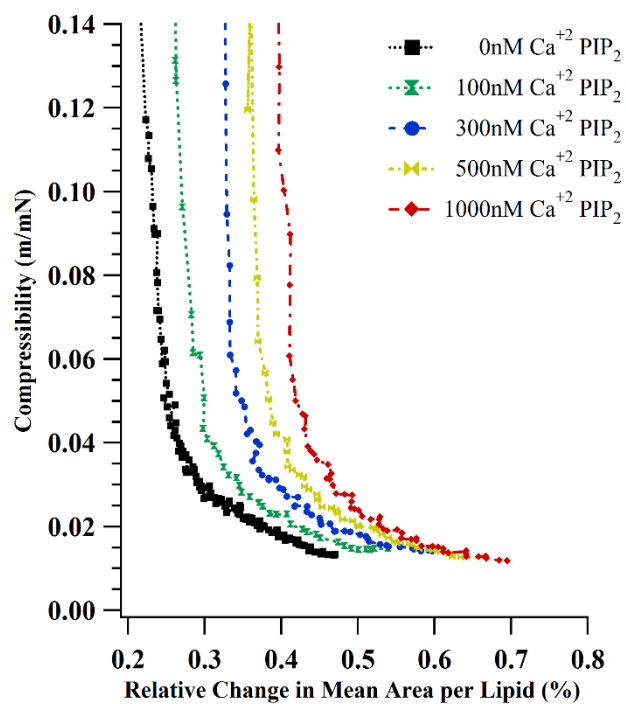


Figure II-3. Modulation of lateral isothermal compressibility of PIP<sub>2</sub> by Ca<sup>2+</sup> ions

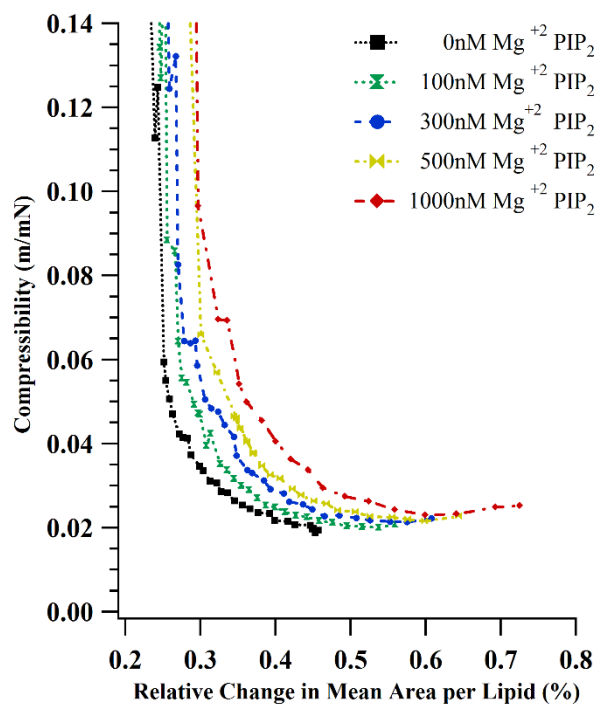


Figure II-4 Modulation of lateral isothermal compressibility of PIP<sub>2</sub> by Mg<sup>2+</sup> ions

$C_A$  is greater at lower surface pressures which means there is a greater fluctuation of lipids than at high surface pressures when there are lesser fluctuations of lipids.  $C_A$  depicts the existence of interactions and structure formations at low surface pressure and the absence of bivalent ions as shown in figures, Figure II-3, Figure II-4, Figure II-7 and Figure II-8. These interactions and structure formations are not observed at other lateral isothermal compressibilities of DOPG, see Figure II-5 and Figure II-6. These observations support the theory that long range interactions for  $PIP_2$  in the presence or absence of  $Ca^{2+}$  and  $Mg^{2+}$  show that bivalent ions have a strong impact on the monolayer structure. DOPG behaves in a different and unusual manner, particularly in the absence of  $Ca^{2+}$ . These behavior are most due to size of the head group of DOPG.

A direct observation of compressibilities as depicted in figures, Figure II-3 through Figure II-8, shows a greater increase in local mean area per lipid, with  $PIP_2$  having the greatest increase, followed by DOPG then PI, which leads to the relation  $PIP_2 > DOPG > PI$ . All of the compressibility results show an undisrupted curve due to isotherms that only exhibited the liquid phase. As we can observe from all the figures, the local relative change in mean area remains constant for a wide range of compressibility values.

The dropping of the surface pressure when  $Ca^{2+}$  goes up suggests the insertion of phospholipase c (PLC) inside the cytoplasmic membrane, as in the case with  $PLC\gamma$  in the fertilization of an egg

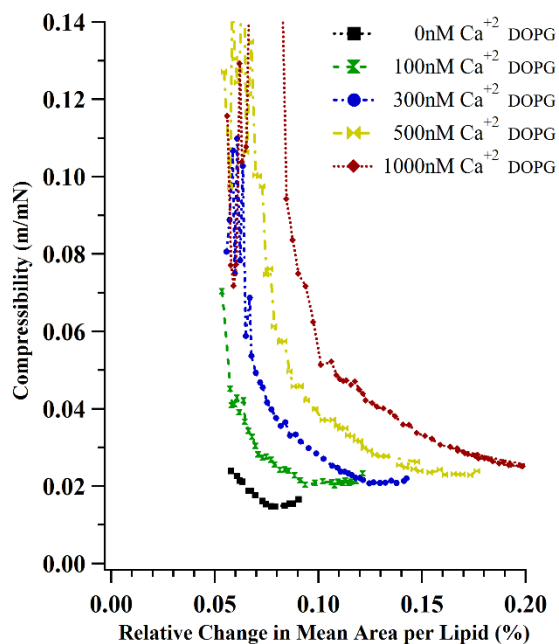


Figure II-5. Modulation of lateral isothermal compressibility of DOPG by  $\text{Ca}^{+2}$  ions

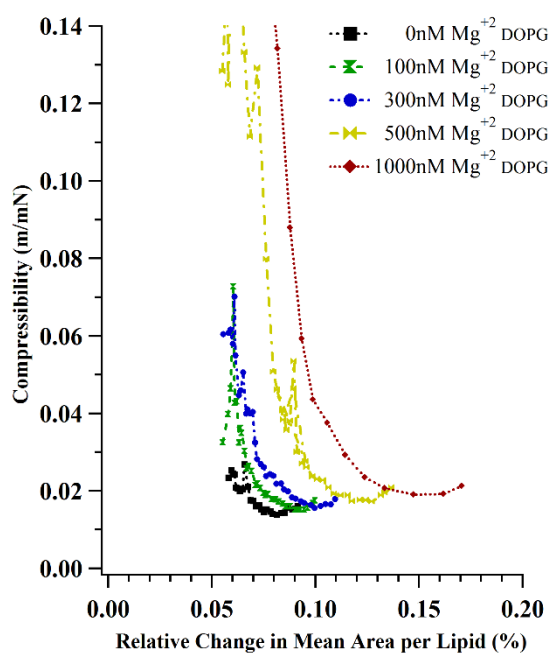


Figure II-6: Modulation of lateral isothermal compressibility of DOPG by  $\text{Mg}^{+2}$  ions



In order to understand the difference in monolayers under the influence of  $\text{Ca}^{2+}$  and  $\text{Mg}^{2+}$ , we need to include the notion of energy barriers [116] which depends on the size of the bivalent ions. In addition, the action of the hydration force on the electrostatic repulsion force at the distance  $< 2\text{nm}$  needs to be included [65]. It has been shown that large molecules pass through the membrane with high values of  $C_A$ . This is also true for membranes with small values of  $C_A$  only when in the presence of  $\text{Ca}^{2+}$  ions. By plugging different values of  $C_A$  (Figure II-3) at a fixed value of the mean surface pressure of the monolayer of  $\text{PIP}_2$  ( $\langle \pi \rangle = 30 \pm 1.2 \text{ mN/m}$ ) into the equation (II-1). We then computed using the equation (II-1) to determine the relative changes in the instantaneous surface pressure of the monolayer, as shown in Table II-1.

$[\text{Ca}^{2+}]$ in nM	$C_A$ (m/mN)	$\left( \frac{\langle \pi \rangle (K_B T C_A / A)^{1/2}}{\pi} \right) / \pi$
0	$0.013254 \pm 0.0002$	28.3%
100	$0.014757 \pm 0.0005$	31.9%
300	$0.014402 \pm 0.0006$	34.0%
500	$0.01266 \pm 0.0003$	33.9%
1000	$0.011554 \pm 0.0005$	33.6%
Table II-1. The impact of $[\text{Ca}^{2+}]$ on the compressibility and on the relative change of surface pressure of $\text{PIP}_2$ at $30\text{mN/m}$		

The change induced by  $\text{Ca}^{2+}$  ions on the surface pressure is significant in magnitude and supports many hypotheses, such as inserting of PLC enzyme into the bilayer and other membrane signaling events when calcium ions interact with cytoplasmic charged lipids. The results shown in the Table II-1 indicates increases in  $\text{PIP}_2$  surface pressure that range from 28% to 34% as the

concentration of  $\text{Ca}^{2+}$  ions increase. This increase shows the importance of surface modification due to electrostatic or lateral interaction in the monolayer.

The aggregation of  $\text{PIP}_2$  is not affected by electrostatic repulsion due to the head group charge but is affected by electrostatic attraction which depends on the presence of bivalent ions [117]. Figure II-3 through Figure II-8 indicate that there is more to the electrostatic interaction; there are more interactions on the monolayer from which the compressibilities have been computed. The lateral compressibility of  $\text{PIP}_2$  suggests more explanation is needed beyond a simple electrostatic interaction with bivalent ions.

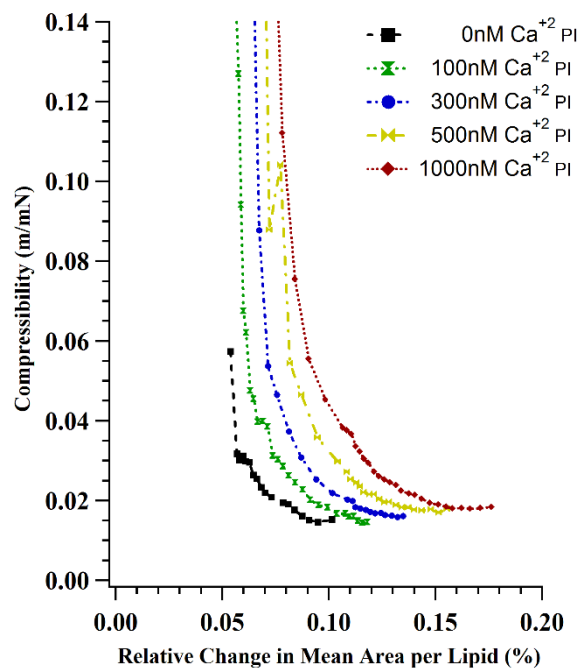


Figure II-7: Modulation of lateral isothermal compressibility of PI by  $\text{Ca}^{+2}$  ions

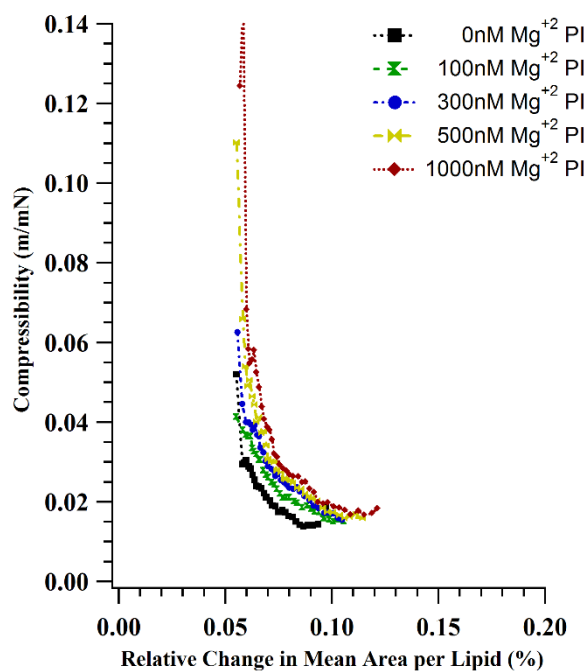


Figure II-8: Modulation of lateral isothermal compressibility of PI by  $\text{Mg}^{+2}$  ions

Other studies that used high concentrations of  $Mg^{2+}$  and  $Ca^{2+}$  ( $\sim 1mM$ ) have suggested that  $Mg^{2+}$  does not induce more aggregation compare to  $Ca^{2+}$  in the monolayer of  $PIP_2$ . This is because  $Mg^{2+}$  does not dehydrate while  $Ca^{2+}$  does dehydrate when interacting with  $PIP_2$  head group [87, 89]. However, I used bivalent ions at physiological levels. The results on compressibility that I found require more explanations, in particular about bivalent ions. The activity of  $Ca^{2+}$  decreases as the molar concentration of  $Ca^{2+}$  increases in a bulk solution in the absence of any salt (NaCl); the value goes further down in the presence of salt [118]. The activity depends on the size of ions. The difference between  $Ca^{2+}$  and  $Mg^{2+}$  is evident, as depicted in Figure II-3 through Figure II-8.

The differences found strongly suggest that the activities and size of these bivalent ions have a strong effect on their adsorbant properties. Compressibilities are also greatly impacted by the geometry and charge(s) of the head group. According to the Stern theory of stoichiometry of association, the interaction between bivalent ions and phospholipids can be 1:1 (ion: phospholipid) or 1:2 (ion with two phospholipids). The latter stoichiometry of association has been proposed by McLaughlin [65, 97]. It has been demonstrated more recently [87, 89] that  $Ca^{2+}$  causes less aggregation of  $PI(3,5)P_2$  than  $PI(4,5)P_2$ , in the monolayer. Another study on magic angle spinning  $^{31}P$ -NMR or  $^1H$ -NMR spectroscopy has revealed a difference in charges between  $PI(3,5)P_2$  and  $PI(4,5)P_2$  on the phosphate groups on the inositol ring.  $PI(4,5)P_2$  has  $-3.99 \pm 10$  C and  $-3.96 \pm 10$  C for  $PI(3,5)P_2$ . The difference can be attributed both to the proximity of the phosphate group and to the oscillation of the proton between the phosphate groups at position 4- and 5- on the inositol ring [119]. In a study on the small unilamellar vesicle, the  $PC/PI(4,5)P_2$  99:1 yielded a value of pKa of 6.5 and 7.7 respectively at the position 4- and 5- on the inositol ring. The pKa of  $PI(4)P$  is 6.1 which is lower than the pKa of  $PI(4,5)P_2$  [2, 119]. Calcium does induce structure even at low surface pressures (high compressibility) compared to  $Mg^{2+}$  where there is negligible interaction

with PIP<sub>2</sub> on the monolayer at a low surface pressure, see Figure II-4. The differences in compressibilities we observed were supported by all previously conducted studies. We also know that biological membranes carry an electrostatic surface potential which is attributed to the charge of the head group of a lipid and to ions in bulk. There are different forms of electrostatic surface potential that have been developed, but the one that is most commonly used is the Gouy-Chapman-Stern (GCS) model.

The Graham equation (II-3), as illustrated below, is based upon the Gouy-Chapman-Stern (GCS) theory which is based upon two theories, the Poisson equation and the Boltzmann equation, but added a third theory, the Langmuir adsorption isotherm theory. Altogether these theories connect the electrostatic surface density( $\sigma$ ) to the surface potential( $\varphi(0)$ ) [120].

$$\sigma = \frac{e/A}{1 + (K_H[H^+] + K_M[M^+]) \exp\left(-\frac{e\varphi(0)}{K_B T}\right) + K_D[D^{2+}] \exp\left(-\frac{2e\varphi(0)}{K_B T}\right)} \quad (\text{II-3})$$

with

$e$  representing the charge of an electron;  $A$ , the mean area per molecule;  $K_B$ , Boltzmann constant;  $T$ , the temperature;  $K_M$ , the binding constant for monovalent ions;  $K_D$ , binding constant of bivalent ions; and  $K_H$  representing the binding constant of a proton ( $K_H = 60M^{-1}$ ).

In instances where there is no salt (NaCl), the term  $K_M[M^+] \exp\left(-\frac{e\varphi(0)}{K_B T}\right)$  can be removed. Therefore, we can rewrite the equation (II-3) as follows:

$$(K_M[M^+] + K_H[H^+]) \exp\left(-\frac{e\varphi(0)}{K_B T}\right) + K_D[D^{2+}] \exp\left(-\frac{2e\varphi(0)}{K_B T}\right) = \frac{e}{\sigma} - 1 \quad (\text{II-4})$$

The concentration of  $[H^+]$  can also be replaced by  $10^{-pH}$

In the case of a system that is completely depleted of  $[H^+]$ , the term,  $K_H[H^+] \exp\left(-\frac{e\varphi(0)}{kT}\right)$  can be neglected so the relation (II-4) becomes:

$$\varphi(0) = -\frac{K_B T}{2e} \ln \left[ \frac{1}{K_D [D^{2+}]} \left( \frac{e}{\sigma} - 1 \right) \right] \quad (\text{II-5})$$

We know that the surface potential is linked with surface pressure by the relation below,

(II-6): The electrostatic free energy per area [111, 121] is given by:

$$\Delta G = -\sigma\varphi + \int_0^\sigma \varphi' d\sigma' = -\int_0^\varphi \sigma' d\varphi' \quad (\text{II-6})$$

with  $\varphi$  representing the surface potential.

With the assumption that the electrostatic interactions are the most predominant[91] and all other interactions can be neglected, we can use Lippmann equation [121, 122] which connects the electrostatic free energy to the interfacial tension, (II-7).

$$\left( \frac{\partial \pi}{\partial \varphi} \right)_{A,T} = \left( \frac{\partial q}{\partial A} \right)_{\varphi,T} = -\sigma \quad (\text{II-7})$$

With  $q$  representing the charge, and  $A$  represents the area. By integrating the relation

(II-7), the average surface tension is given below, (II-8)

$$\Delta G = \Delta \pi = \int_0^\varphi \left( \frac{\partial \pi}{\partial \varphi} \right)_A d\varphi = \int_0^\varphi -\sigma d\varphi \quad (\text{II-8})$$

By

combining the relation (II-8) and (II-1) we deduce (II-9):

$$\varphi \cong \langle \varphi \rangle \left[ 1 \pm (K_B T C_A / A)^{\frac{1}{2}} \right] \quad (\text{II-9})$$

The term  $\langle \varphi \rangle (K_B T C_A / A)^{\frac{1}{2}}$  can be regarded as a corrective term on the electrostatic surface potential and the answer to different values found by different authors in regards to surface potential. For example, another study using the well-known Gouy Chapman Stern (GCS) theory on membranes containing acidic lipids and peptides has presented some failure at high concentrations of the peptide: the result was twice the estimated potential [99]. Another feature of this term is that it includes the change related to the elasticity of the membranes since it depends

on the compressibility. Compressibility strongly depends on the presence of bivalent ions and other parameters.

We know that we can write the surface potential in terms of a Taylor series, (II-10):

$$\varphi(x) = \varphi(x_0) + (x - x_0) \frac{d\varphi(x)}{dx} \quad (\text{II-10})$$

By comparing (II-9) and (II-10), we get  $\varphi(x_0) = \langle \varphi \rangle$  then we found (II-11):

$$C_A = \frac{A}{K_B T \varphi(x_0)^2} \left[ (x - x_0) \frac{d\varphi(x)}{dx} \Big|_{x=x_0} \right]^2 \quad (\text{II-11})$$

We know that  $\varphi(x_0) = 25mV$  at room temperature.

The relation (II-11) shows that the increase in temperature will result in a decrease of compressibility on a charged monolayer or bilayer system. The theoretical model of compressibility that I developed provides deeper insight into a range of surface potentials.

We can rewrite (II-11) as follows:

$$C_A = \frac{A}{K_B T} (x - x_0)^2 C_\varphi \quad (\text{II-12})$$

where  $C_\varphi$  is given by the relation below, (II-13)

$$C_\varphi = \frac{1}{\varphi(x_0)^2} \left[ \frac{d\varphi(x)}{dx} \Big|_{x=x_0} \right]^2 \quad (\text{II-13})$$

So by inserting (II-13) into (II-9), we obtain (II-14):

$$\varphi \cong \langle \varphi \rangle \left[ 1 \pm x C_\varphi^{\frac{1}{2}} \right] \quad (\text{II-14})$$

where  $C_\varphi$  is the surface potential compressibility.

The relation (II-14) show that the corrective term in the potential does not depend on the mean area per lipid, the corrective term in this case depend only on  $C_\varphi$  which has the same unit as  $\kappa^2$ .

The membrane potential  $\varphi(x)$  is given by the GCS theory and is the same as the Zeta potential at  $2\text{\AA}$  from the surface, as shown in relation (II-15) [99].

$$\varphi(x) = 2\ln\left(\frac{1 + \tanh(\varphi(0)/4)e^{-\kappa x}}{1 - \tanh(\varphi(0)/4)e^{-\kappa x}}\right) \quad (\text{II-15})$$

The

Debye length is given by  $1/\kappa$  with  $\kappa = [2K_B T e^2 c / \varepsilon_r \varepsilon_0]^{1/2}$ , with  $\varepsilon_0 = 8.9 \times 10^{-12} \text{ C/Nm}^2$  and with  $\varepsilon_r$  varying from 1 in air to 80 in water. By taking the derivative of (II-15) we obtain (II-16):

$$\varphi(x)' = \frac{d\varphi(x)}{dx} = \frac{4\kappa \tanh(\varphi(0)/4)e^{-\kappa x}}{1 - \tanh^2(\varphi(0)/4)e^{-2\kappa x}} \quad (\text{II-16})$$

We can now insert (II-16) into (II-11) and (II-13) to get (II-17) and (II-18):

$$C_A = \frac{Ax^2}{K_B T \varphi(0)^2} \left( \frac{4\kappa \tanh(\varphi(0)/4)e^{-\kappa x}}{1 - \tanh^2(\varphi(0)/4)e^{-2\kappa x}} \right)^2 \quad (\text{II-17})$$

$$C_\varphi = \frac{1}{\varphi(0)^2} \left( \frac{4\kappa \tanh(\varphi(0)/4)e^{-\kappa x}}{1 - \tanh^2(\varphi(0)/4)e^{-2\kappa x}} \right)^2 \quad (\text{II-18})$$

The

results from our theoretical model on the compressibility are shown in Figure II-9 and Figure II-10 and indicate the same profile as in our experimental results which strongly suggests that there is an agreement between the theoretical framework we developed and the experimental results.



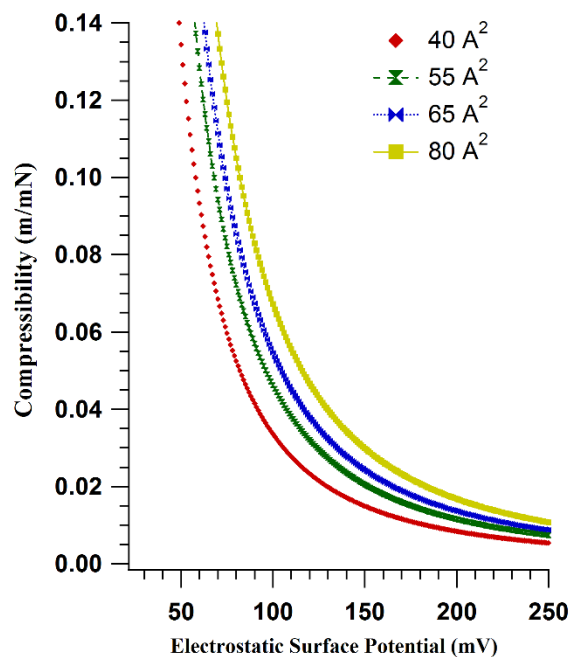


Figure II-9: Theoretical compressibility as a function of electrostatic surface potential for various mean area per molecule

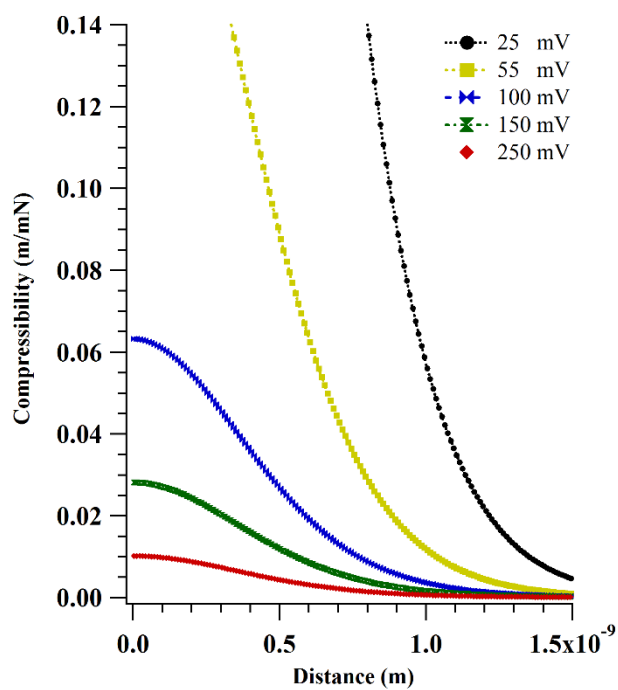


Figure II-10: Theoretical compressibility as function of distance from membrane for various surface potential

As was expected, the compressibility vanished as the distance increased away from the monolayer. Membrane elasticity or mechanical properties are profoundly dependent on the surface electrostatic potential. We also posited and found that highly charged membrane will generate a large surface potential. Based upon our experiments on PIP<sub>2</sub>, we found that this highly charged lipid does induce a large surface potential, which indicates a smaller value of compressibility in the presence of bivalent ions. The theoretical compressibility does support this as observed in Figure II-9 and Figure II-10.

The results of other studies on membrane potential [123] of asymmetrical leaflets composed with PS/PC and PS/PE have produced values of 198mV and 238mV which correspond respectively to 0.0095 m/mN and 0.0068 m/mN at 55 A<sup>2</sup>. The minimum value of compressibility obtained from the formula (II-17) is about 0.0001m/mN at 1475mV(40A) and 1959mV (70A). Beyond these values, the compressibility does not change for a wide range of surface potentials and becomes zero respectively at 2571mV and 3408mV. The theoretical model of compressibility sets a boundary upon the Gouy-Chapman Stern theory.

## 2.5. Conclusion

The experimental results on PI(4,5)P<sub>2</sub> and PI show structural formation in the presence and absence of bivalent ions. While there is a small amount of structure that exists when there are no bivalent ions, when PIP<sub>2</sub> and PI are in the presence of bivalent ions, these structures become more ordered as the concentration of bivalent ions increases. Due to the size of the DOPG's head group, observations of the monolayer suggest a lack of ordered structure in the absence of bivalent ions; but there appears to be an apparent structural formation that occurs as bivalent ions increase, as seen from the results of the compressibility. Our theoretical framework does capture all the parameters that can affect any monolayer/bilayer system, such as temperature, pH, physiological conditions, lipid composition, the area per molecule and the electrostatic potential.

## Chapter III : Calcium Induced Change in Excess Gibbs Energy of Charged Monolayer System

### 3.1 Abstract

The role and importance of phosphatidylinositol-4,5-bisphosphate (PI(4,5)P<sub>2</sub>) in cell membrane signaling and its regulatory role in membrane trafficking are undisputable. Cellular process such as endoplasmic and exoplasmic require PI (4,5)P<sub>2</sub> in their cycle. An important number of actin-protein are activated and bind to PI(4,5)P<sub>2</sub>. In addition, PI(4,5)P<sub>2</sub> bind to more than 350 proteins in vivo[124] in the cell. Moreover, viruses, such as HIV-1, use PI(4,5)P<sub>2</sub> in their budding process. A plausible explanation to many of these processes mediated by PI(4,5)P<sub>2</sub> in the plasma membrane (PM) is the hypothesis that suggest a formation of Pools of PI(4,5)P<sub>2</sub> in the cytoplasm. The mechanism underlying the aggregation of PI(4,5)P<sub>2</sub> into pools is still not understood but different explanations have been proposed in the last few decades. The most convincing hypothesis is due to the electrostatic interaction between PI(4,5)P<sub>2</sub> and Ca<sup>+2</sup>. More recent experiments have shown that Ca<sup>+2</sup> mediates the formation of Pools of PI(4,5)P<sub>2</sub> at high Ca<sup>+2</sup> concentrations. We have investigated the effect of the bivalent ions on excess Gibbs free energy from the monolayer of PI(4,5)P<sub>2</sub> –POPC or pure PI(4,5)P<sub>2</sub> at the physiological level. We found that excess Gibbs free energy does not yield a zero value as predicted by the formula for a pure monolayer. This gives a direct confirmation that bivalent ions induce segregation of PI (4, 5)P<sub>2</sub> in the mixture PI(4,5)P<sub>2</sub>-POPC or pure monolayer of PI(4,5)P<sub>2</sub>. We have shown that the excess Gibbs energy is strongly dependent on temperature and the nature of bivalent ions.

### 3.2 Introduction

Our understanding of Polyphosphoinositides (PPIs) has not yet reached its prime due in part to its multiple roles as a second messenger molecule and on the other hand it due to its binding role to more than 350 proteins in vivo [124]. These special phospholipids have attracted the attention of more and more scientific research due to its multi functionality in numerous cell events. The most predominant phosphorylate Polyphosphoinositides (PPIs) named phosphatidylinositol-4,5-bisphosphate (PI(4,5)P<sub>2</sub>) occupies only 1% of all the PPIs. As a second messenger, PI(4,5)P<sub>2</sub> is the precursor of two messengers: Ins(1,4,5)P<sub>3</sub> leads to the release of Ca<sup>+2</sup> from the ER and produces diacylglycerol (DAG) after its interaction with PLC[14, 28]. The number of biological processes associated with PI(4,5)P<sub>2</sub> as second messenger are numerous. To cite only a few mechanisms that are regulated by PI(4,5)P<sub>2</sub> : fertilization, a process that is triggered by Ins(1,4,5)P<sub>3</sub> and Ca<sup>+2</sup> oscillation which leads to egg activation and embryo development in mammal cell [125, 126]; ion-channel activation, synaptic vesicle trafficking (exocytosis) and recycling are regulated by PI(4,5)P<sub>2</sub>; cytoskeletal attachment, actin-binding proteins [28, 83]. Observations have shown the special presence of pools of PI(4,5)P<sub>2</sub> in cytoplasmic leaflet of membrane[28, 83]. There is a generic question that has been addressed in relation to PPIs special PI(4,5)P<sub>2</sub> -“ How does PI(4,5)P<sub>2</sub> play so many crucial roles in cytoplasmic membranes and other locations, and what are the physicochemical mechanisms attached to this lipids that make the lipid unique among all the phospholipids ?”[28]. The debate about physicochemical mechanism that leads to PI(4,5)P<sub>2</sub> enrich domain in the cytoplasmic membrane [49] is still an open subject. Various experiments provide different answers to underlying interactions that mediate PI(4,5)P<sub>2</sub> clustering of these multi-valent lipids in cytoplasmic leaflet of cell membrane are: PIP<sub>2</sub>-protein interaction

[28]; hydrogen bond mediate PIP<sub>2</sub> clustering; and Cholesterol enrich PIP<sub>2</sub> raft-like domain [49]. Recent monolayer experiments on two different phosphorylate of PI, PI(4,5)P<sub>2</sub> and PI(3,5)P<sub>2</sub> have shown that the charged head group was not the only key player in the condensation effect of these monolayers under bivalent ion interactions but instead the special orientation of these charges are on the inositol ring. A more recent experiment shows a clustering of PIP<sub>2</sub> by divalent cations and a difference in clustering of PI(4,5)P<sub>2</sub> is due to changing enthalpy from the hydration of Ca<sup>+2</sup> or Mg<sup>+2</sup> [127]. Studies have not yet been done that address the energetic side associated with the PI(4,5)P<sub>2</sub> monolayer in relation to electrostatic interactions with bivalent ions. All the literature focuses on either the interaction of peptides with lipids or on the mixture of lipids in different conditions [128].

In investigating the energetic side of the PI(4,5)P<sub>2</sub> monolayer as it relates to the electrostatic interactions with bivalent ions, I experimented on PI(4,5)P<sub>2</sub> and various mixtures of PI(4,5)P<sub>2</sub>-POPC at different temperatures and pH and physiological cations concentration to show that the excess Gibbs free energy is strongly dependent on temperature, pH and cations nature.

### 3.3 Material and Methods

#### *Lipids and Reagent:*

1,2-dioleoyl-*sn*-glycero-3-phospho-(1'-myo-inositol-4',5'-bisphosphate) (ammonium salt) (PIP<sub>2</sub>) and 1-palmitoyl-2-oleoyl-*sn*-glycero-3-phosphocholine (POPC) were purchased from Avanti Polar Lipids (Alabaster, Alabama;USA) in the desired concentration of 1mg/ml in Chloroform solution for (POPC) and chloroform/methanol/water 20:9:1 for (PI(4,5)P<sub>2</sub>). They were both stored at -20° C without further purification and were used within a three months period to avoid oxidation. Calcium Chloride CaCl<sub>2</sub>, Magnesium Chloride MgCl<sub>2</sub>, Sodium Chloride NaCl, Citric Acid, Sodium Citrate and HEPES were purchased from Sigma-Aldrich, (St. Louis, MO, USA) in powder and kept at room temperature.

All buffer solutions, calcium concentrations [Ca<sup>+2</sup>] and magnesium concentrations [Mg<sup>+2</sup>] were prepared in distilled, deionized water from a Milli-Q Apparatus (Millipore) and refrigerated at 1°C. 10mM of HEPES was used for the monolayer experiments at pH 7.4 and 0.2M Sodium Citrate was used for all the monolayer experiments at low pH (pH 3.5).

Lipid mixtures were prepared at three different concentrations ([PI(4,5)P<sub>2</sub>]:[POPC]:10:90,25:75,35:65) and used directly after mixing for all the experiments done at 37 °C. A pure concentration of PIP<sub>2</sub> was used in all other conditions.

The monolayer of surface pressure versus area per lipid ( $\pi - A$ ) was obtained from a computerized KSV Minitrough Langmuir-Blodgett (KSV NIMA Biolin Scientific Tietäjantie 2 FIN-02130 Espoo, Finland) (LB) at Constant Compression (5 mm/min) after the deposition into the trough and the wait of 10 minutes necessary for the evaporation of chloroform. To minimize airflow and stabilize humidity and temperature of the monolayer, the trough's system was enclosed

in a Plexiglass box. A constant temperature was maintained by circulating water through a tube attached to the base of the trough and to a monitoring heat reservoir system. Each experiment was repeated three times and the data were processed by using Matlab and Igor-pro. Figure III-1 shows a five isotherms plot showing the mixture of PI(4,5)P<sub>2</sub> -POPC (25:75) at 37°C and pH 7 for different calcium concentrations.

### 3.4 Data Analysis and Results

An early definition of surface pressure was directly related to the definition of the surface energy of a monolayer of benzene atom. It was found that the surface energy of benzene was significantly affected when a substitution of OH was made to the benzene by a factor of 15% as a result of a tilting of the benzene ring[129]. Another observation made by Irvin Langmuir was related to the unsaturated acyl chain. He observed an increase of approximately 30% for an unsaturated molecule. More recent studies on the energetics aspect related to the interaction of the peptide with biological membrane have shone some light on the free energy associated with the biological membrane [130]. The observations and simulations have shown that there are three different ways that the peptide affects the free energy associated to the membrane. The first way that the peptides affect the free energy comes from the interaction of the peptide to the hydrocarbon core or nonpolar core namely called hydrophobic interaction. The second contribution comes from the interaction with the head group of the phospholipid, the peptide is adsorbed into the head group of the lipid membrane. This category includes charged lipid membranes such as phosphatidylinositol 4 5-bisphosphate (PIP<sub>2</sub>). The third contribution to the free energy comes from the interactions of the peptides with the hydrocarbon core and the head group simultaneously. My investigation focused more on the second type of interaction in the monolayer system. In order to understand the contribution to the free energy, the buffer condition was modulated, by changing



the parameters such as the pH or ionic concentration of  $\text{Ca}^{2+}$  and  $\text{Mg}^{2+}$ . These were made possible with the Langmuir trough.

The surface charge density of a monolayer increases proportionally with the increase of surface pressure as the monovalent ions' concentration increases. The surface pressure drops in the presence of bivalent ions due to the phenomena known due to charge screen effect[120]. The adsorption of these ions onto the lipid membranes is not well-defined by the Poisson-Boltzmann equation. This is partially due to a strong ion-ion interaction and is still an open question[131]

These monovalent and bivalent ions have an important influence on the phase transition by shifting the isotherms [120]. In all the cases of the monolayers of PtdIn, PtdIn (4,5)P<sub>2</sub> and POPC , there were no phase transitions observed, not in the absence of bivalent ions or in the presence of bivalent ions. Their isotherms are characterized by one phase, called the fluid phase.

The surface charged density of eukaryotic cell membrane is approximately  $0.025 \text{ C.m}^{-2}$  which corresponds to an electrostatic free energy of  $1\text{kJ mol}^{-1}$  from the contribution of electrostatic interaction. But in an artificial membrane, the surface charged density can be greater than  $0.25 \text{ C.m}^{-2}$  which in theory results in a value that is less or equal to  $10\text{kJ mol}^{-1}$  [78].

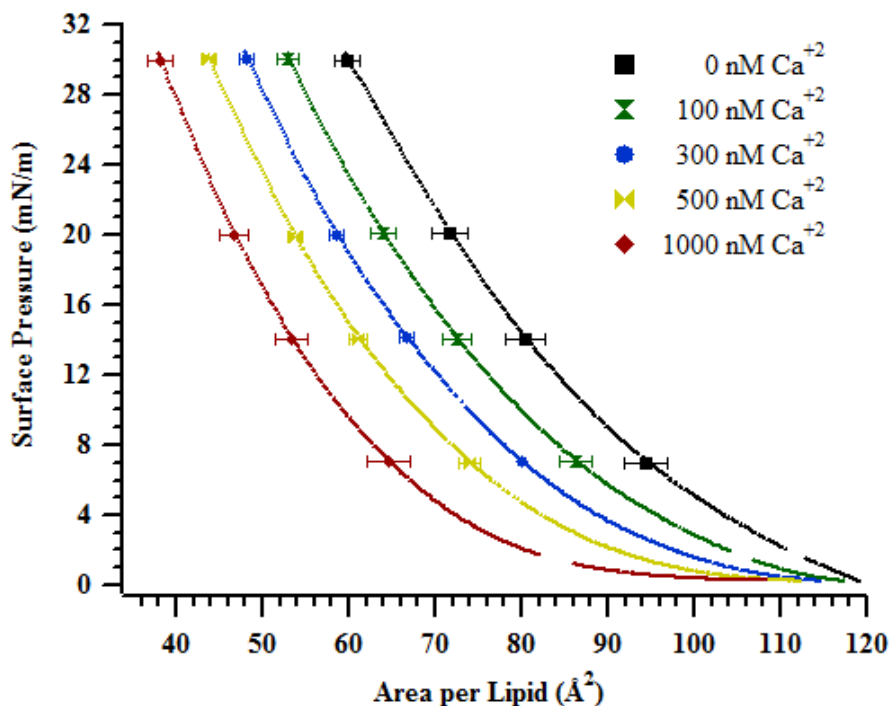


Figure III-1: Isotherm of the mixture of PI(4,5)P<sub>2</sub> -POPC (25:75) at 37C and pH 7.4

From a thermodynamic point of view, the same formulation can be used for the surface pressure to calculate the Gibbs free energy of a monolayer as shown below. For variations that happen at the plane of a lipid monolayer, the Gibbs free energy is given by the following equation [132] [128, 133]

$$dG^{ex} = -S^{ex}dT + \sum \mu_i dn_i^{ex} + \pi dA \quad (\text{III-1})$$

Where  $G^{ex}$  is the excess Gibbs free energy,  $S^{ex}$  is the entropy,  $T$  is the temperature,  $\pi$  is the surface pressure,  $A$  is the area per lipids,  $\mu_i$  is the chemical potential and  $n_i^{ex}$  is the number of particles,.

In an isothermal system with a constant  $n_i^{ex}$ , the expression (III-1) becomes

$$dG^{ex} = Ad\pi \quad (\text{III-2})$$

with  $A$  given according to [134, 135] as in the following equation (III-3),

$$A = (A_{12} - X_1A_1 - X_2A_2) \quad (\text{III-3})$$

with  $A_{12}$  as the mean area of the mixture monolayer of PI(4,5)P<sub>2</sub>-POPC,  $X_i$  and  $A_i$  which represents, respectively, the molar fraction and area per lipid for each individual monolayer of lipid  $i$ .

In the case of a two-lipid mixture, the excess Gibbs free energy must be given by substituting the relation (III-3) into the relation shown at (III-2) and integrating the relation (III-2) as shown below:

$$\Delta G^{ex} = \int_0^\pi (A_{12} - X_1A_1 - X_2A_2) d\pi \quad (\text{III-4})$$

$\Delta G^{ex}$  can be determined from the isotherm  $\pi - A$  shown in the Figure III-1

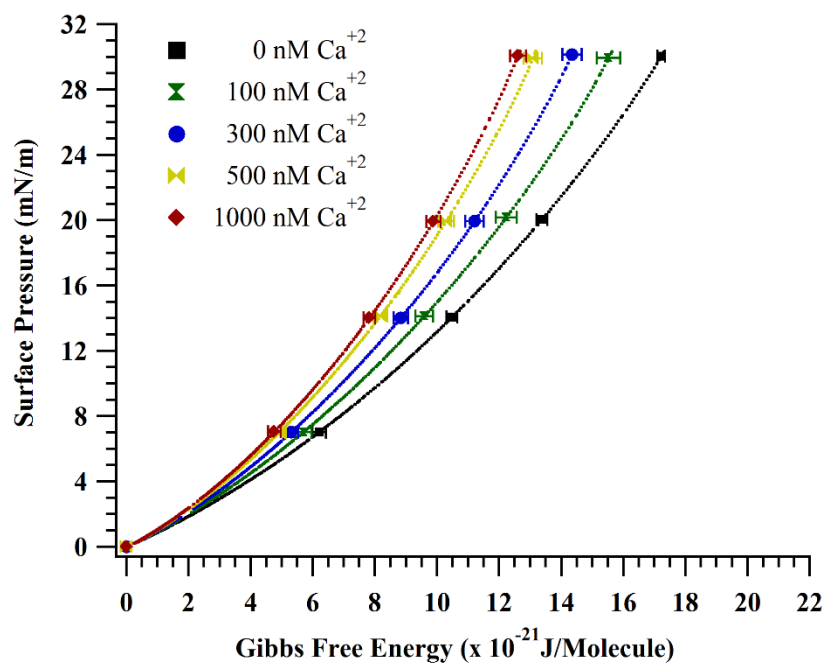
The excess free energy reveals the nature of the interaction between the lipids in the mixture. If  $\Delta G^{ex} > 0$ , there is a repulsive interaction between the lipids. If  $\Delta G^{ex} < 0$ , there is an attractive interaction. In analyzing my data, I used the relation (III-4) to examine the action of bivalent ions in the mixture of PI(4,5)P<sub>2</sub>-POPC instead of looking at the interaction between PI(4,5)P<sub>2</sub> and POPC. The relation (III-4) can be modified by examining the interaction of the mixture with the bivalent ions as shown in the equation below:

$$\Delta G^{ex} = \int_0^\pi (A_{12} - X_1A_1 - X_2A_2) d\pi = \pi(A_{+B^{+2}} - A_{-B^{+2}}) \quad (\text{III-5}) \quad \text{With}$$

$B^{+2}$

representing the bivalent ions ( $\text{Ca}^{2+}$  or  $\text{Mg}^{2+}$ ). From the relation (III-5), the Gibbs free energy can be defined by both the presence of bivalent ions:  $\Delta G^+ = \pi A_{+B}^{2+}$  and the absence of bivalent ions  $\Delta G^- = \pi A_{-B}^{+2}$ . The figures, Figure III-2 and Figure III-3, show how the bivalent ions regulate the Gibbs free energy of the mixture of  $\text{PIP}_2$ -POPC and the pure monolayer of POPC.

a. 10% PI(4,5)P<sub>2</sub> and 90% POPC



b 25% PI(4,5)P<sub>2</sub> and 75% POPC

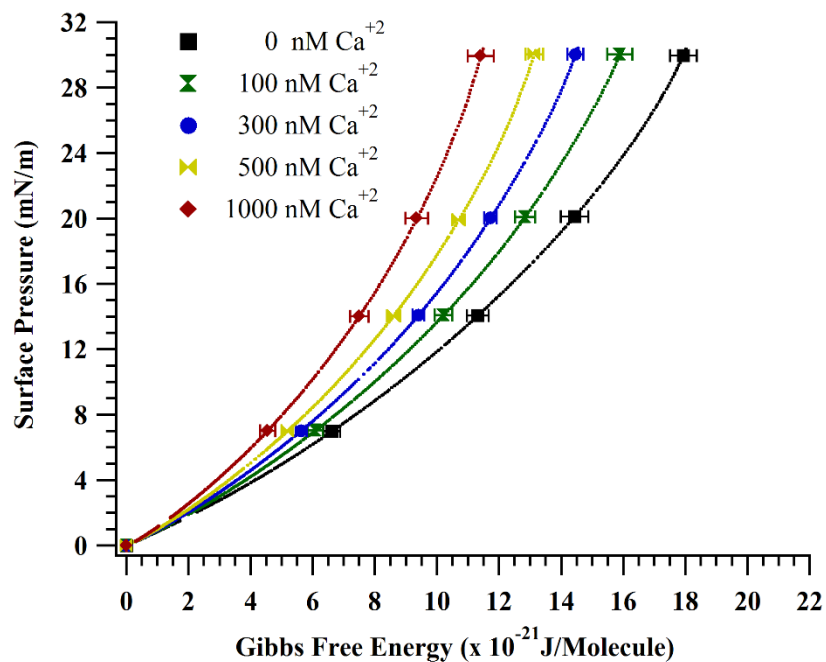
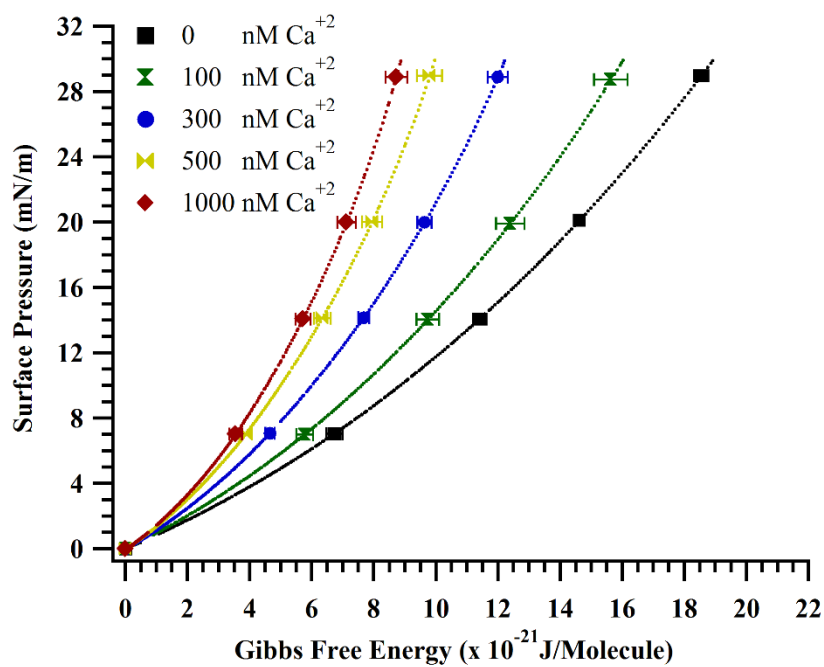


Figure III-2: Graph (a) shows surface pressure versus Gibbs free energy in the mixture of 10% PI (4, 5) P<sub>2</sub> and 90% POPC. Graph (b) shows the surface pressure versus Gibbs free energy in the mixture of 25% PI (4, 5) P<sub>2</sub> and 75% POPC. Both are regulated by Ca<sup>2+</sup> concentration at 37 °C and pH 7.4.

a. 35% PI(4,5)P<sub>2</sub> and 65% POPC



b. Pure POPC

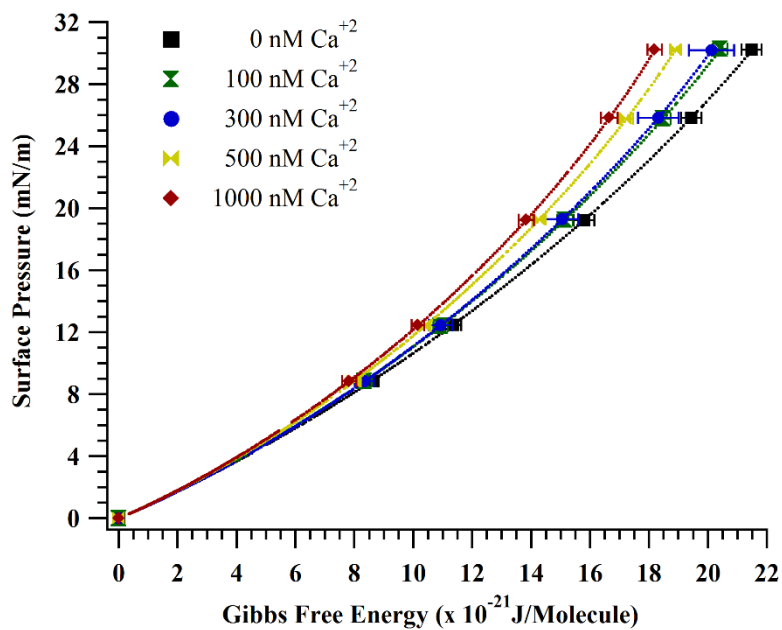


Figure III-3: Graph (a) shows surface pressure versus Gibbs free energy in the mixture of 35% PI (4, 5) P<sub>2</sub> and 65% POPC. Graph (b) shows the surface pressure versus Gibbs free energy of pure POPC. Both are regulated by  $\text{Ca}^{2+}$  concentration at 37 °C and pH 7.4

The ideal mixing of Gibbs energy is given by the relation:

$$\Delta G^{ideal} = RT(X_i \ln X_i) = RT(X_{PIP_2} \ln X_{PIP_2} + X_{POPC} \ln X_{POPC}) \quad (\text{III-6})$$

where R represents the ideal gas constant and T the temperature in (Kelvin), and the Gibbs energy of mixture is given by:

$$\Delta G^{mix} = \Delta G^{ideal} + \Delta G^{ex} \quad (\text{III-7})$$

We can also determine the activity coefficient  $\gamma_i$  and the interaction parameter  $\omega$  from the framework developed by Kodama [136] and Bordini [133].

$$\ln \gamma_i = \left( \frac{\omega}{RT} \right) (1 - X_i)^2 \quad (\text{III-8})$$

$$\omega = \left( \frac{\Delta G^{ex}}{X_{PIP_2} X_{POPC}} \right) \quad (\text{III-9})$$

Table III-1 Interaction Parameter  $\omega$  ( $\cdot K_B T$ /molecule)

$[Ca^{+2}]$	(PIP <sub>2</sub> -POPC)10:90	(PIP <sub>2</sub> -POPC)25:75	(PIP <sub>2</sub> -POPC)35:65
100	-4.33±0.3	-2.69±0.5	-3.04±0.2
300	-7.60±0.4	-4.53±0.3	-7.09±0.6
500	-10.95±0.3	-6.11±0.4	-9.35±0.5
1000	-12.37±0.2	-8.44±0.5	-10.56±0.4

We need to see that the interaction parameter  $\omega$  in this case is not only reflecting the interaction between PI (4,5)P<sub>2</sub> and POPC, it is also showing a strong interaction between PI(4,5)P<sub>2</sub> and Ca<sup>+2</sup> in the complex system of PI(4,5)P<sub>2</sub>-POPC- Ca<sup>+2</sup>. The Figure III-2(b) shows Ca<sup>2+</sup> has less impact on the Gibbs free energy of POPC. As shown on Table II-1,  $\omega$  increases as  $X_{PIP_2}$  decreases, which allows an increased interaction between PI (4,5)P<sub>2</sub>-Ca<sup>+2</sup> which then results in increasing the  $\Delta G^{ex}$ . The more negative the  $\Delta G^{ex}$  becomes, the more interaction occurs between PI(4,5)P<sub>2</sub> and Ca<sup>+2</sup>. The graphs shown in Figure III-4 and Figure III-5 reveals an interdependence between the Ca<sup>+2</sup> concentration and the PI(4,5)P<sub>2</sub> concentration in the magnitude of  $\Delta G^{ex}$ . It was found that any increase in Ca<sup>+2</sup> significantly affects  $\Delta G^{ex}$ , but when there is also an increase in PI(4,5)P<sub>2</sub> (decrease of POPC), there is an even greater increase in  $\Delta G^{ex}$ . There was no dramatic change in  $\Delta G^{ex}$  at 100nM of Ca<sup>+2</sup> which is the resting calcium level. The excess Gibbs free energy associated with different pools of PI(4,5)P<sub>2</sub> is not affected by the Ca<sup>+2</sup> in the cytosolic of a resting cell. Another very important parameter that greatly impacts the excess Gibbs free energy is the temperature. Observations show that  $\Delta G^{ex}$  has significant dependence on temperature. An increase in temperature causes an increase in thermal fluctuation in the monolayer which allows more interaction between PI(4,5)P<sub>2</sub> in the presence of Ca<sup>+2</sup> ions as shown in Figure III-4. It is also pH dependent as shown in Figure III-5 .

The trend observed in Figure III-4 is not linear for the differing concentration levels of Ca<sup>+2</sup> but each of them is quite similar and tends to increase above 500nM Ca<sup>+2</sup>. The one exception is found in the monolayer of 10:90 PI(4,5)P<sub>2</sub>-POPC which suggests saturation started to occur.



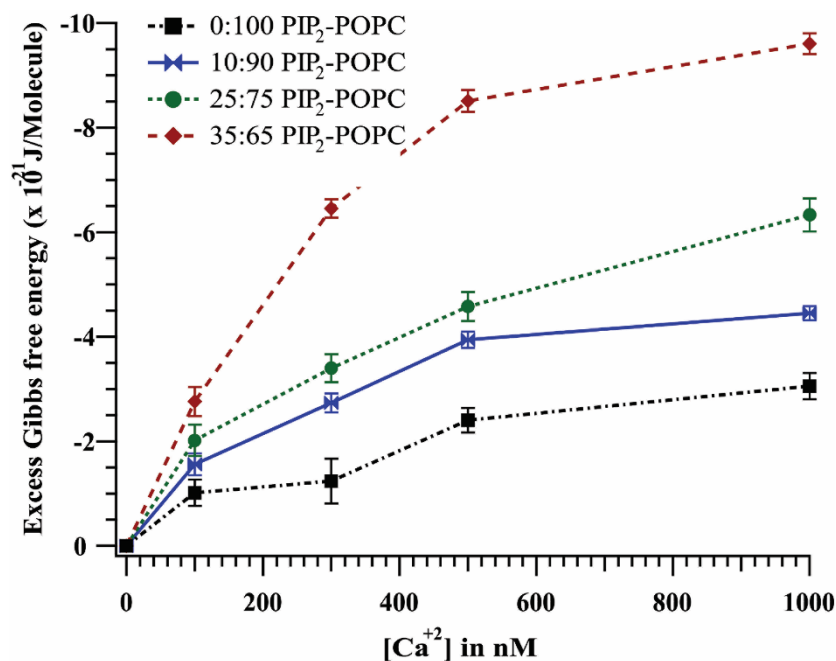


Figure III-4: Excess Gibbs free energy ( $\Delta G^{ex}$ ) from the mixture of PI(4,5)P<sub>2</sub> and POPC at 37 °C, pH 7.4 and for different Ca<sup>2+</sup> at a surface pressure of 28mN/m.

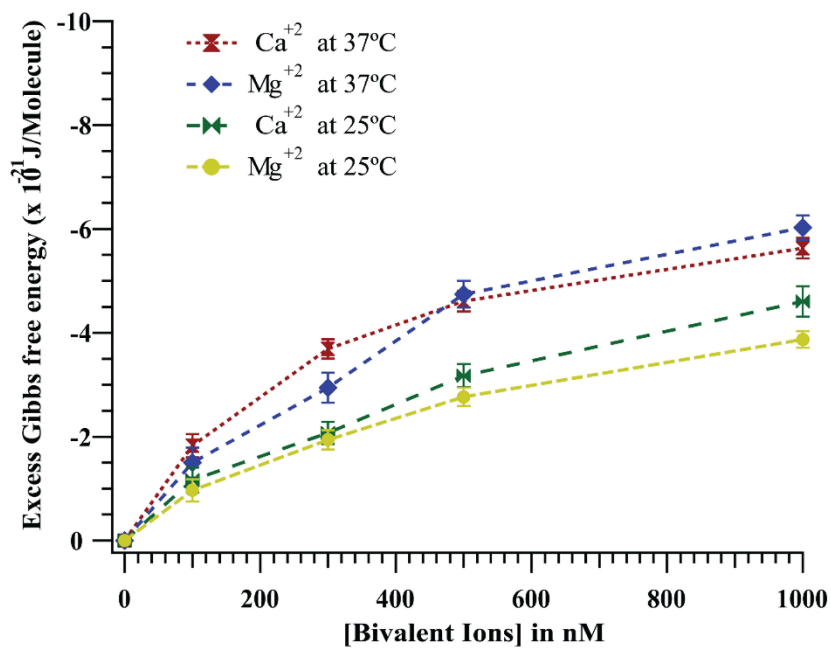


Figure III-5. Excess Gibbs free energy ( $\Delta G^{ex}$ ) from PI(4,5)P<sub>2</sub> at 37 C and 25 °C pH 3.5 and for different bivalent ion concentrations at a surface pressure of 28mN/m.

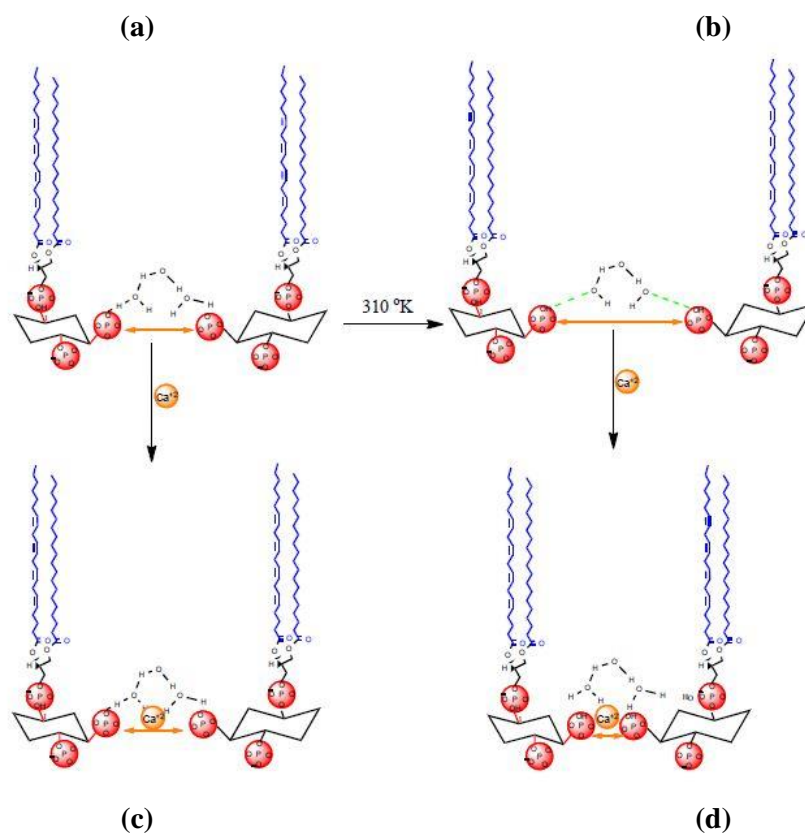


Figure III-6: Schematic of the monolayer of PI(4,5)P<sub>2</sub> in various conditions  
**(a)** Hydrogen bond or hydration forces mediate interactions in the monolayer of PI(4,5)P<sub>2</sub>, at pH7.4 and room temperature; **(b)** Increase of temperature which breaks the hydrogen bond interaction and increases spacing in the monolayer of PI(4,5)P<sub>2</sub>, at pH7.4; **(c)** Electrostatic interaction and hydrogen bond mediates the interaction of PI(4,5)P<sub>2</sub> molecules at the room temperature; **(d)** Electrostatic interaction increases significantly at 37C(310°K) in PI(4,5)P<sub>2</sub> monolayer.

The strength of electrostatic interaction in cell membranes depends on the charges of the phospholipids and Bjerrum length ( $l_B=7.1 \text{ \AA}$ ). For the monovalent lipid, the energy associated with electrostatic interaction is slightly greater than thermal energy  $k_B T$  ( $\sim 7.1 \text{ \AA}$ ) [87]. In these conditions, the monovalent lipids are compared to a point charge that generates an orthogonal field in the cytosolic membrane.

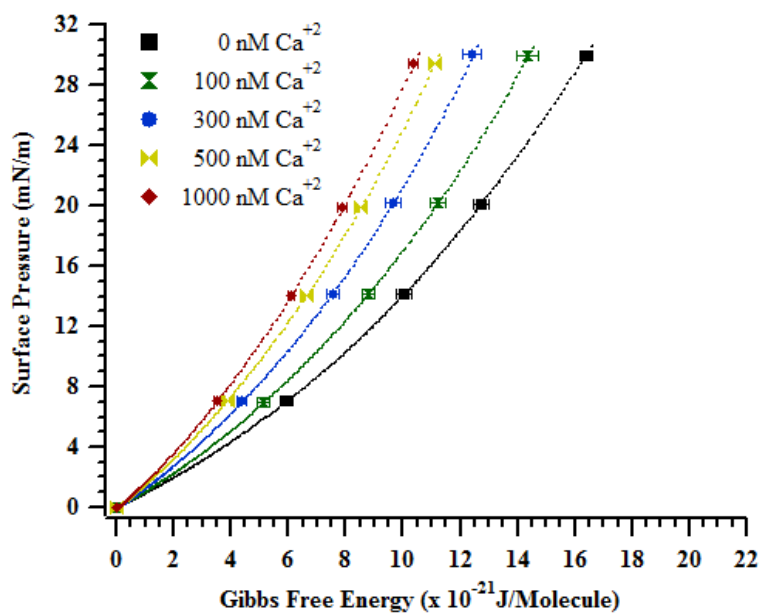


Figure III-7. Modulation of surface pressure versus Gibbs free energy of PI(4,5) P<sub>2</sub> by Ca<sup>+2</sup> at 25°C and pH 7.4

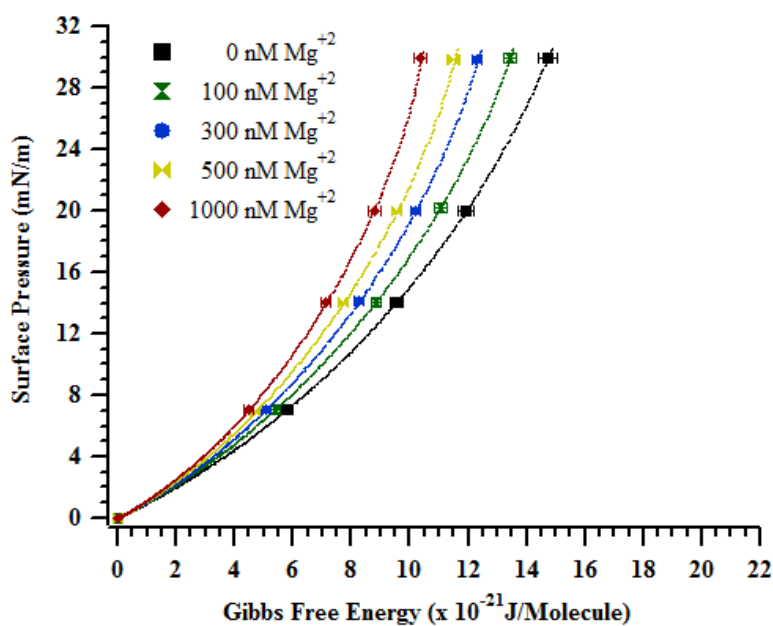


Figure III-8: Modulation of surface pressure versus Gibbs free energy of PI(4,5) P<sub>2</sub> by Mg<sup>+2</sup> at 25°C and pH 7.4

In the case of multivalent lipids, such as PI(4,5)P<sub>2</sub>, the distance between adjacent lipids becomes less than Bjerrum length ( $l_B$ ). This has a tremendous impact on the electrostatic interaction on the plane of a cytoplasmic membrane. The result on the excess Gibbs free energy indicates that multivalent lipids such as PI(4,5)P<sub>2</sub> cause an increase when there is increase of thermal energy in the membrane. The excess Gibbs free energy due to the electrostatic interactions and the thermal energy that depleted any hydrogen bond from the mixture of the monolayer of PI(4,5)P<sub>2</sub>-POPC above 100nM[Ca<sup>+2</sup>] varies between 0.5 K<sub>B</sub>T to 5 K<sub>B</sub>T as shown in Figure III-6. These values are above the Bjerrum length and the Figure III-6 depicts the working combination of thermal energy with electrostatic interaction between adjacent lipids. I observed that before any changes were made in the monolayer of PI(4,5)P<sub>2</sub>-POPC, the Bjerrum length and hydrogen bonds regulate the interaction in the monolayer system, PIP<sub>2</sub>-POPC. As the temperature increases in the monolayer, the repulsion force dominates due to a depletion of hydrogen bonds and the charge on PIP<sub>2</sub>. These phenomena have been recently observed in the monolayer experiments of zwitterionic lipids, DOTAP and DPPC[133], where the surface tension increases with the increase of temperature leading to a positive  $\Delta G^{ex} > 0$ . Another work done on the monolayer of PI(4,5)P<sub>2</sub>-Ca<sup>+2</sup> ([Ca<sup>+2</sup>]  $\gg 1\mu M$ ) has also show that the electrostatic interaction plays a dominant role in the clustering of PI(4,5)P<sub>2</sub> at room temperature and pH 7.4 [89].

The difference observed in the surface pressure versus Gibbs free energy as depicted in Figure III-7 and Figure III-8 is primarily due by the nature of the bivalent ions. Calcium ions have more of an effect on the monolayer of PI(4,5)P<sub>2</sub> than magnesium ions at room temperature and pH 7.4. This can be explained by taking in account the size of bivalent ions. The smaller the bivalent ions, the more readily its adsorption into the monolayer

But the observations shown in Figure III-9 and Figure III-10 the surface pressure versus Gibbs free energy on the monolayer of PIP<sub>2</sub> at a low pH3.5 and high temperature (37°C) show the opposite. Magnesium ions have more effect than calcium ions. This can be explained by taking into consideration the abundance of H<sup>+</sup> that shields the PIP<sub>2</sub>. Also, the increase in temperature allows the adsorption of Mg<sup>+2</sup> more than Ca<sup>+2</sup> in the monolayer.

However, the observations shown in Figure III-11 and Figure III-12 of the surface pressure versus Gibbs free energy on the monolayer of PIP<sub>2</sub> at a low pH3.5 and room temperature indicate that magnesium ions and calcium ions have similar effect on the monolayer of PIP<sub>2</sub>. Not much difference was observed between these two bivalent ions.

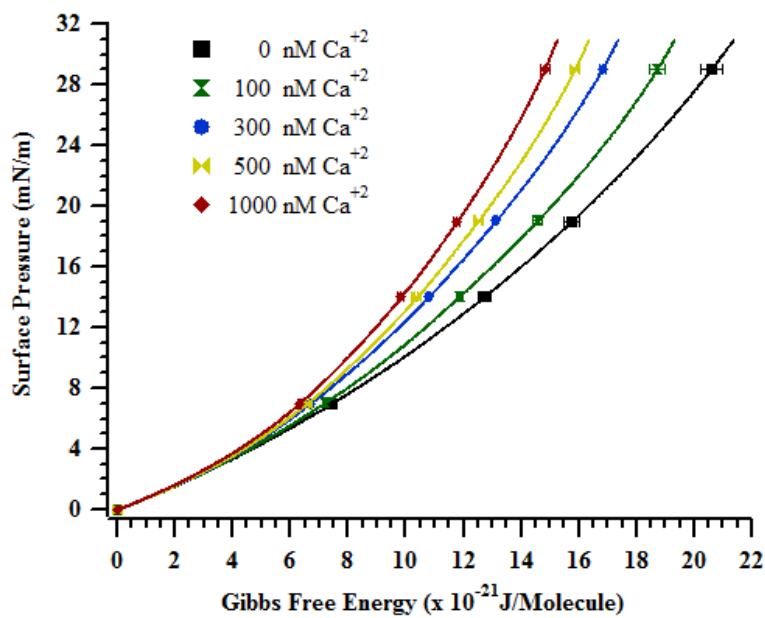


Figure III-9. Modulation of surface pressure versus Gibbs free energy of PI(4,5) P<sub>2</sub> by  $\text{Ca}^{+2}$  at 37 °C and pH 3.5

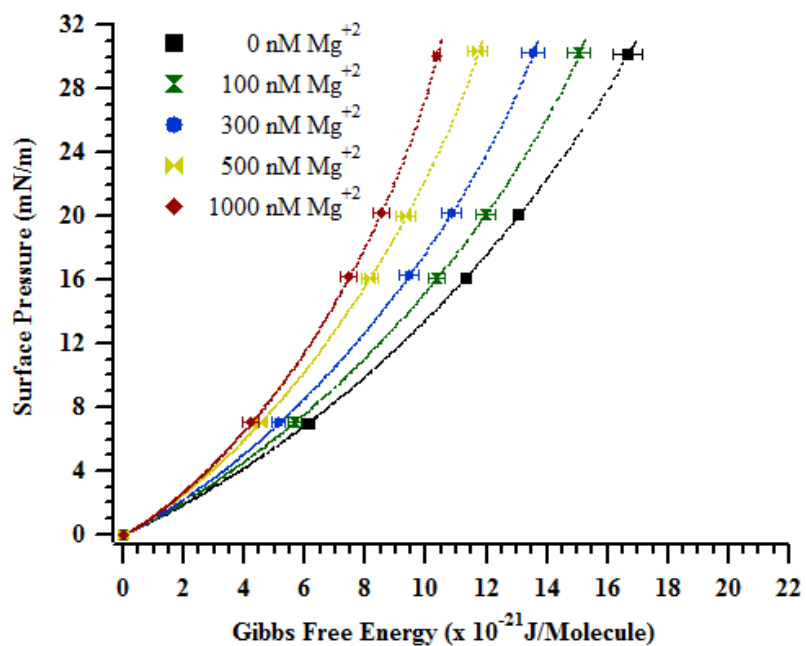


Figure III-10. Modulation of surface pressure versus Gibbs free energy of PI(4,5) P<sub>2</sub> by  $\text{Mg}^{+2}$  37 °C at pH 3.5

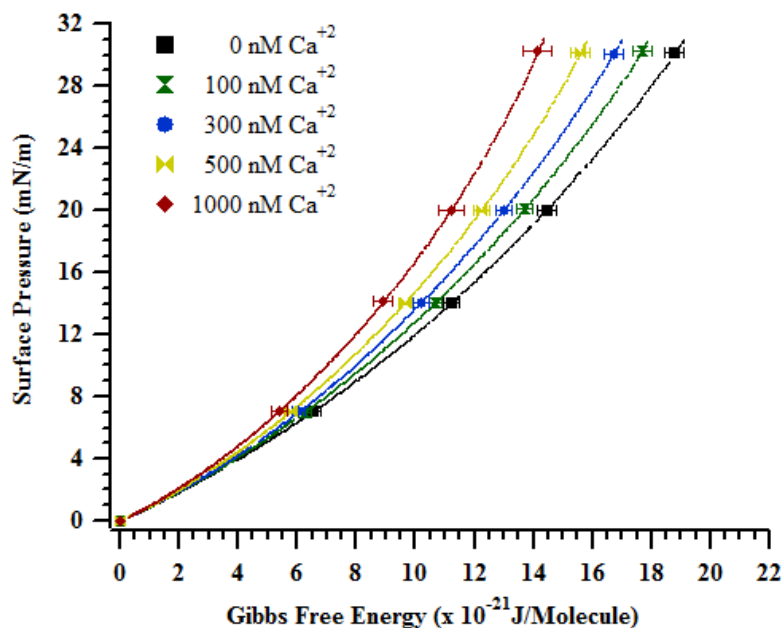


Figure III-11. Modulation of surface pressure versus Gibbs free energy of PI(4,5) P<sub>2</sub> by  $\text{Ca}^{+2}$  25 °C at pH 3.5

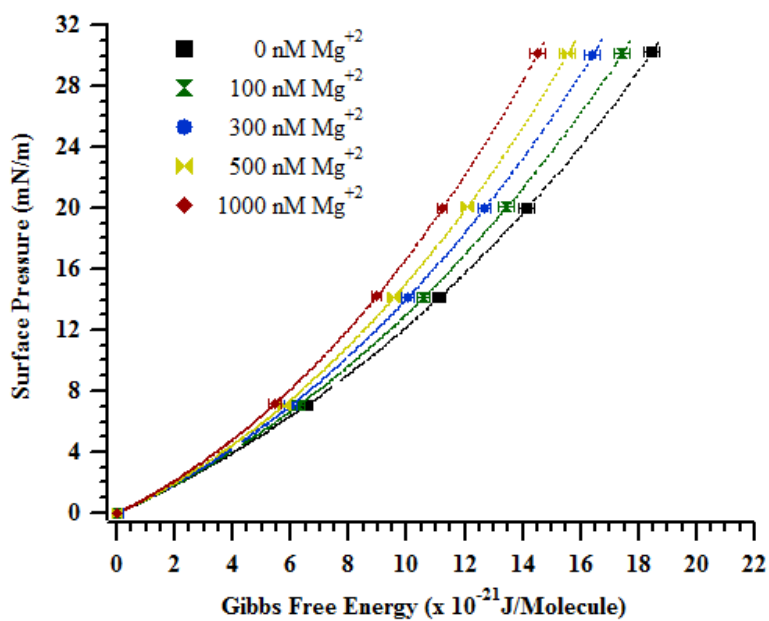


Figure III-12. Modulation of surface pressure versus Gibbs free energy of PI(4,5) P<sub>2</sub> by  $\text{Mg}^{+2}$  25 °C at pH 3.5

### **3.5 Conclusion**

The results presented here on the modulation of surface pressure and excess Gibbs free energy support our hypothesis. Bivalent ions induce the aggregation of PIP<sub>2</sub> molecules at the monolayer due to electrostatic interaction. We also see that these aggregations depend on temperature, pH and the kind of bivalent ions at various physiological levels.



## Chapter IV : NOVEL TECHNIQUE FOR CALCIUM OSCILLATION

### 4.1 Abstract

The intracellular  $\text{Ca}^{2+}$  ion signaling is a universal messenger that regulates a huge number of cellular processes such as muscle contractions, neurotransmitter releases, apoptosis and fertilization. In addition,  $\text{Ca}^{2+}$  signaling forms spatiotemporal microdomains [92]. More signaling events can be combined to form a large signaling wave or an increase of the intracellular  $\text{Ca}^{2+}$  concentration that invades the whole cell. This phenomenon is known as calcium induced calcium release (CICR) and can be stimulated by the coupling process of PLC- $\text{PIP}_2$ - $\text{Ca}^{2+}$  or by calcium a spark through a stimulus [94, 137]. A long lasting concentration of  $\text{Ca}^{2+}$  can lead to a catastrophic failure in regulating of the process mentioned above, including the process of memory consolidation and memory erasure that occur during sleep in Alzheimer disease [138]. For example an irreversible damage of cardiac and cerebral ischaemia is in general a direct result of a persisting large concentration of  $\text{Ca}^{2+}$  ions[139]. Biological cells have developed a sophisticated mechanism to keep calcium concentrations at low levels between 20nM to 100nM. The influence of CICR on cytoplasmic  $\text{PIP}_2$ -membrane lateral reorganization has not been investigated. We attempted to develop a technique that combines different calcium dyes to mimic the intracellular calcium induce calcium release (CICR). Our first data show a possibility of developing such technique relying on the emission and absorption spectral of florescence dyes.

## 4.2 Introduction

The calcium ion,  $\text{Ca}^{2+}$  is a messenger that has been intensively studied in relation to a wide range of cellular processes or events [140]. A phenomenon known as Calcium Induced Calcium Release (CICR) was first observed in muscle cells [93, 141] and then in many other cell types [32, 93, 94, 142-145] for an incredible huge amount of cell process and the brain is a sea of this particular behavior of  $\text{Ca}^{2+}$  ions or signaling in its coupling mechanism with Inositol1,4,5trisphosphate( $\text{IP}_3$ ) [32, 93, 94, 146] .

The cytoplasm of eukaryotic cells is a highly active and heterogenic media where different cell events happen in different regions.  $\text{Ca}^{+2}$  ions happen to be involved in almost all the cell processes that occur inside or at the plasma membrane. When the cell is at rest, the concentration of  $\text{Ca}^{+2}$  lies between 20 and 100 nM [92, 140]. When excited the intracellular calcium can increase up to many micro molar depending on the cell type[92]. There are two ways the cytosol is supplied by  $\text{Ca}^{+2}$ . The first way by which the cytosol is supplied is by the release of calcium from a finite storage such as the endoplasmic reticulum (ER) or sarcoplasmic reticulum (SR) through the calcium receptors (InsP3Rs/RYR). The second means of supply is from an infinite, external source, and  $\text{Ca}^{+2}$  enters into the cytosol through channels. There are three types of channels, voltage operated channels (VOC), receptor-operated channels (ROC) and store-operated channels (SOC).

Therefore  $\text{Ca}^{+2}$  signaling regulates numerous cell functions such as muscle contraction, neurotransmitter release, apoptosis and fertilization. In addition,  $\text{Ca}^{+2}$  signaling forms spatiotemporal microdomains [92] and additional signaling events can combine to form a large signaling wave or an increase of the intracellular  $\text{Ca}^{+2}$  concentration.

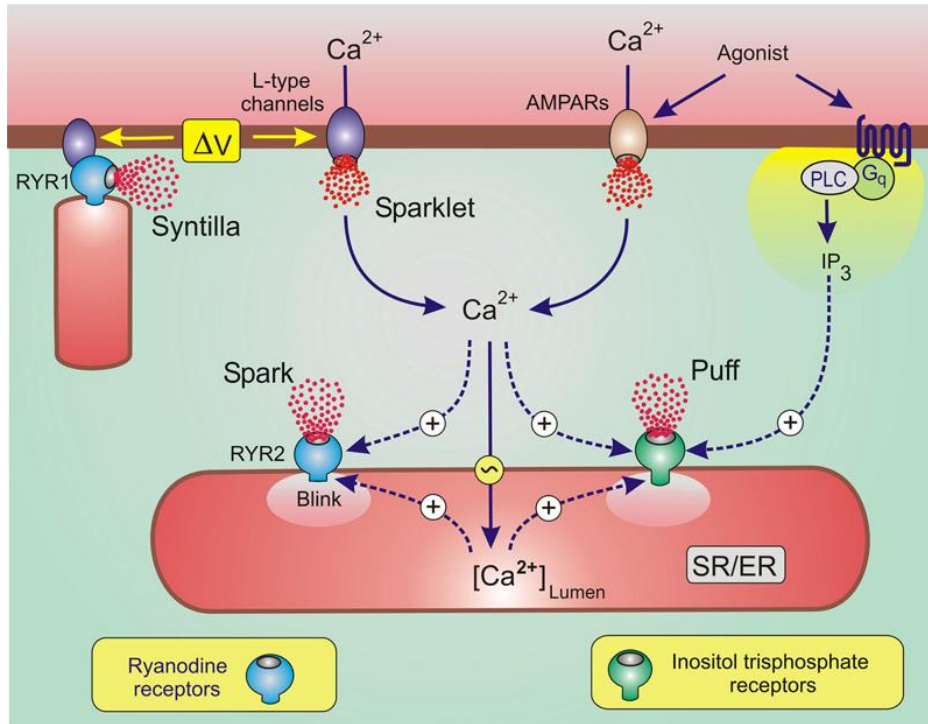


Figure IV-1: Calcium microdomain. A global signal of calcium ions result in the summation of different microdomains. Calcium released from SR/ER(spark/puff) and calcium entering through channels (sparklet) [147]

The microdomains are also defined as elementary calcium events that constitute the basic construct of calcium signaling. Depending on the origin of these microdomains different names are associated with each different microdomain. (Syntilla, Sparklet, puff, spark, Blink) [147] as shown in Figure IV-1. Two important elementary signaling events are released from the ER and SR. The ER and SR are not only the factory of lipids and proteins, but it also provide large calcium storage.

The endoplasmic reticulum and sarcoplasmic reticulum receptors each have three isoforms that form a total molecular mass of 2.4 millions daltons and 1.2 millions daltons respectively and each share an equal amount between their isoforms. Moreover these receptors are ten times more

effective than the voltage gate  $\text{Ca}^{+2}$  and  $\text{Na}^{+}$  with a conductance of 100 pS: ten times more than that of a  $\text{Ca}^{+2}$  channel[148].

**Puffs** are calcium releases from inositol1,4,5-trisphosphate receptors ( $\text{InsP}_3\text{Rs}$ ) as shown in Figure IV-1 upon interaction with the intracellular messenger  $\text{IP}_3$  [149]. In fact, puffs and sparks are the basic building blocks that contribute to the formation of a large calcium signaling wave as shown in Figure IV-2 or a global  $\text{Ca}^{+2}$  wave as in Figure IV-3. But less is known about the mechanism that reassembles these elementary calcium signaling events inside the cytosol. Puffs have been observed in the astrocyte ending of synapses and in HeLa cells after being stimulated by histamine. Puffs are characterized by the magnitude of the signal event during the release ( $\geq 50\text{nM}$ ) and time interval (360ms). Release events that reach a maximum of  $\leq 40\text{nM}$  during the time interval of 130ms are called blips [149]. In addition, puffs and sparks can combine together to form a large microdomain. In neocortical glutamatergic presynaptic  $\text{Ca}^{+2}$  release this phenomenon is known as calcium induced calcium release (CICR) which is the amplification of  $\text{Ca}^{+2}$  concentration in the cytosol due to the sensitivity of ryanodine RYRs and  $\text{InsP}_3\text{Rs}$  receptors [150]. A dysfunction of these receptors can lead to many pathologies or diseases such as cardiac death [151]

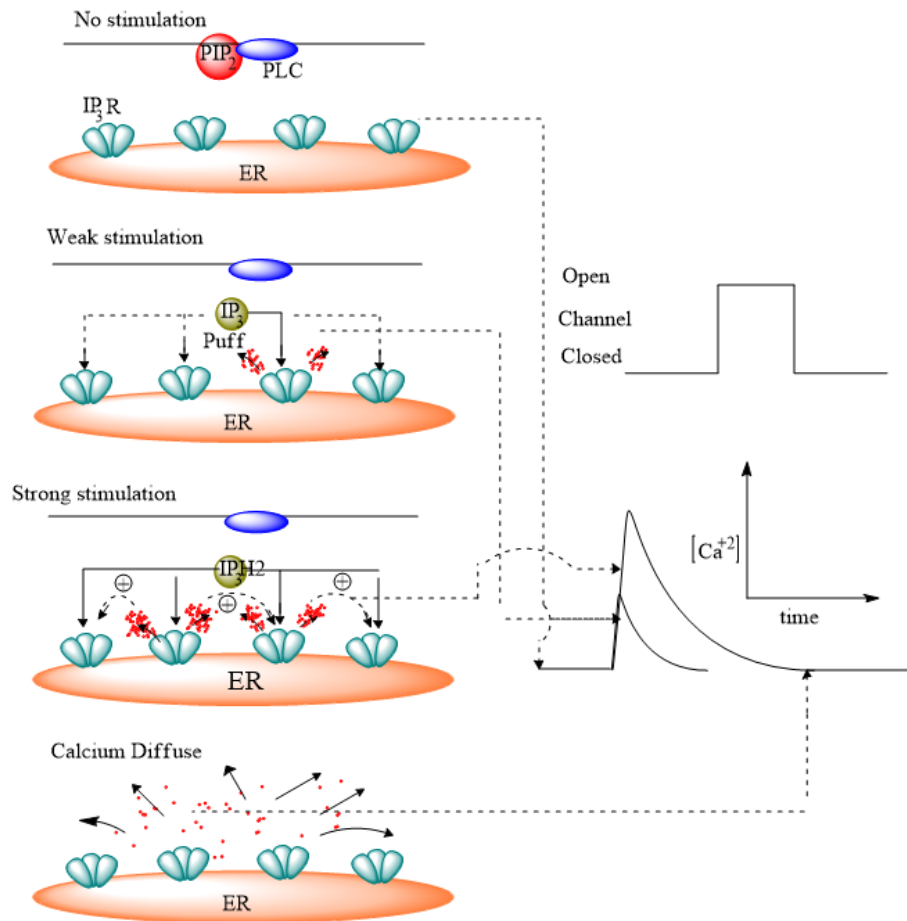


Figure IV-2: Calcium puffs in Xenopus Oocyte : Transient opening of inositol 1,4 ,5-trisphosphate (InsP<sub>3</sub>) receptors and elementary events of Ca<sup>+2</sup> signaling (red dots) from the endoplasmic reticulum (ER). A strong signaling of Ca<sup>+2</sup> is released from few IP<sub>3</sub> receptors [92, 140].

The release of calcium inside the cytosol depends on the biphasic properties of calcium: the release of Ca<sup>+2</sup> from InsP<sub>3</sub>R, and the induced release of Ca<sup>+2</sup> due by the sensitivity of the receptor to Ca<sup>+2</sup>. Ca<sup>+2</sup> cannot trigger the receptor to release more Ca<sup>+2</sup> without first being released by InsP<sub>3</sub>R as InsP<sub>3</sub> binds to InsP<sub>3</sub>R as shown in Figure IV-2c. The Ca<sup>+2</sup> release from RyR is similar. In Xenopus oocytes, Ca<sup>+2</sup> puffs are localized first due to their weak diffusibility within the cytosol, and IP<sub>3</sub>R sites are separated by 30 $\mu$ m<sup>2</sup>. But when more IP<sub>3</sub>R channels are open, there is an increase

in  $\text{Ca}^{+2}$  in the cytosol and this  $\text{Ca}^{+2}$  plays the role of a messenger to enhance the release of more  $\text{Ca}^{+2}$  that results in high frequency waves of  $\text{Ca}^{+2}$  as seen in Figure IV-2.

**Sparks** are calcium released from ryanodine receptors (RyRs) located at SR/ER. Spark was first observed in the cardiac cells of idle rats [142] during the mechanism that lead to the excitation-contraction. The spontaneous increase of calcium release from the SR of heart cells into the cytosol was observed with a laser scanning confocal microscope and calcium indicator fluo-3. The elementary calcium sparks were observed in the cardiac cells of idle rats around  $0.2\mu\text{M}$ , the macro spark observed has a maximum of  $533\text{nM}$  and the propagating wave appeared at  $900\text{nM}$ . The latter value has been restricted by the limitations of the optical system used and the diameter of the microdomain is around  $2\mu\text{m}$ . The calcium sparks are responsible for the calcium cascade that induces the coupling event of excitation-contraction. This cascade increases calcium concentration in the cytosol. This particular type of calcium increase, called Calcium induced Calcium release (CICR), is found in many types of muscle cells and cells that have internal storage [142]. Calcium sparks are involved in many cellular events, in cell presynaptic terminals [152] and in smooth muscle cell spark activated calcium dependent potassium(BK) channels[153] during relaxation. In contrast with calcium Puffs, calcium sparks are triggered by voltage-operated channels (VOC) whereas Calcium puffs are released from  $\text{IP}_3$  receptors after their interaction with  $\text{IP}_3$ .

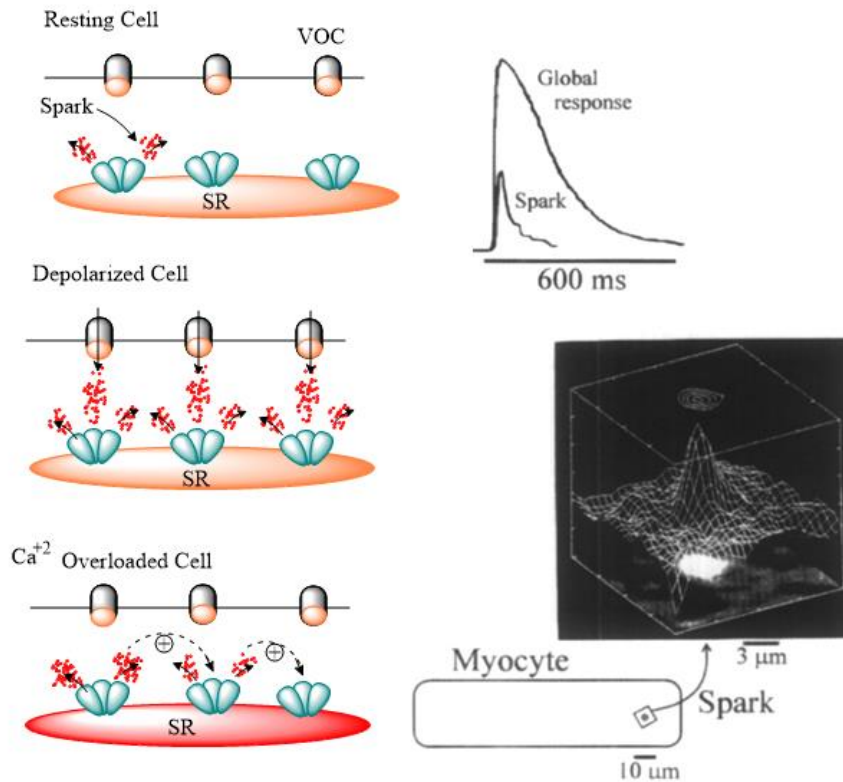


Figure IV-3: Calcium Sparks and the Global response of  $\text{Ca}^{2+}$  in Myocyte. [92]

The cell stochastically recruits VOC during membrane depolarization induced by the release of sparks and their localization is directly linked to the special location of calcium. Spark has a short duration compared to a depolarization that induces a global response as observed in cardiac myocytes (Figure IV-3)

The intracellular  $\text{Ca}^{2+}$  ions are modulated by the phenomenon known as homeostasis which consists of keeping the intracellular  $\text{Ca}^{2+}$  ions at the lower level after the cell has accomplished a specific function. The first step to understanding the mechanism of homeostasis is to look at the two main sources of cytoplasmic  $\text{Ca}^{2+}$  ions entries. The plasma membrane contains three different calcium gates such as VOCs, receptor-operated channels(ROCs) and store-operated channels (SOCs) [140]. The calcium entry is denoted by  $\text{Ca}_o^{2+}$ . The second source of cytoplasmic  $\text{Ca}^{2+}$  ions

is the calcium release from ER or SR through their calcium receptors InsP<sub>3</sub>R and RYR. The calcium release is denoted by  $Ca_s^{2+}$  ( Figure IV-4)

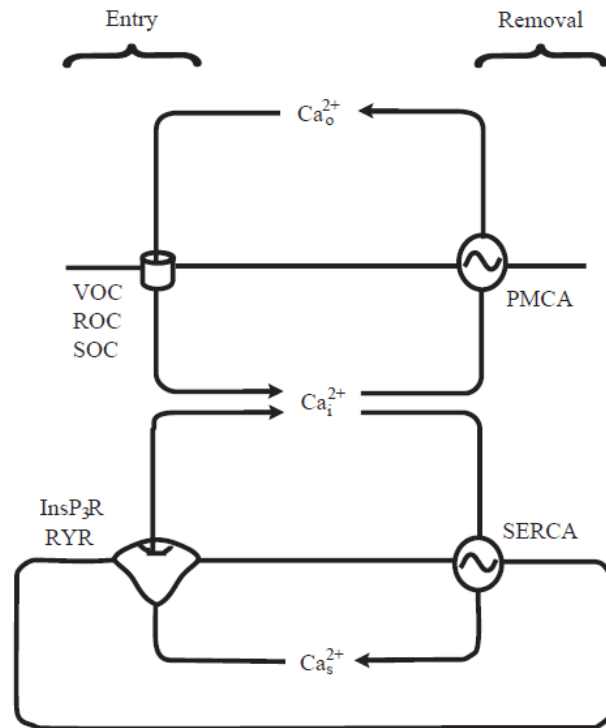


Figure IV-4 Calcium homeostasis mechanism[140]

The biphasic aspect of intracellular  $Ca^{2+}$  plays the role of switching on and off, or positive feedback and negative feedback. The positive feedback is achieved by calcium induced calcium release (CICR) as explained above . After the concentration of  $Ca_i^{2+}$  ( $Ca_o^{2+} + Ca_s^{2+}$ ) reaches a desired level through CICR, the positive feedback is switched to negative feedback by  $Ca^{2+}$  inhibiting the channel [154, 155]. Homeostasis is achieved by pumping calcium either by a set of plasma membrane  $Ca^{2+}$  -ATPase (PMCA) or by sarco (endo)plasmic reticulum  $Ca^{2+}$  -ATPase (SERCA) to maintain the cytoplasmic  $Ca^{2+}$  at its resting level.



## 4.2 Reagents and Procedures

Calcium Chloride  $\text{CaCl}_2$ , Magnesium Chloride  $\text{MgCl}_2$ , Sodium Chloride  $\text{NaCl}$ , Diazo (salt form, with an excitation at 330nm) and MOPS were purchased from Sigma-Aldrich, (St. Louis, MO, USA) in powder and kept at room temperature. Calcium ion concentrations were adjusted by mixing a low calcium buffer solution (110 mM  $\text{KCl}$ , 20 mM MOPS, 20 mM  $\text{NaCl}$  and 10 mM  $\text{K}_2\text{H}_2\text{EGTA}$ ) and a high calcium solution (110 mM  $\text{KCl}$ , 20 mM MOPS, 20 mM  $\text{NaCl}$ , and 10 mM  $\text{K}_2\text{CaEGTA}$ ) in the appropriate proportions [156]. All aqueous solutions were prepared using organic-free doubled-deionized (DI) water of high specific resistivity (approx. 18.0  $\text{m}\Omega/\text{cm}$ ).

Asante Calcium Red (ACR) was purchased in salt form from TEFLabs, Inc9415 Capitol View Drive Austin, TX 78747 and 10 $\mu\text{M}$  was prepared stored. ACR was used in non-ratiometric mode with an excitation wave length of 540nm and an emission wave length of 650 nm and  $k_d = 400\text{nM}$ .

## 4.2 Preliminary Results

The primary goal in this section is to be able to investigate the dynamics of membrane reorganization as calcium concentrations change over time. Figure IV-5 shows a schematic of calcium oscillation in membranes containing fluorescence labels of PIP<sub>2</sub>. As described earlier, the intracellular calcium wave is one of the most ubiquitous signaling events that accompanies or orchestrates a large scale cellular responses, e.g. T-cell activation, cell motility or neuronal signaling [157, 158].

Calcium induced calcium release (CICR) in the cytoplasm has a profile that looks like a sinusoidal wave. Previous studies have demonstrated that Ca<sup>2+</sup> strongly interacts with anionic lipids and has a profound effect on the spatial organization and dynamic properties of the charged lipid species [159]. Phosphatidylinositol 4,5-bisphosphate (PIP<sub>2</sub>) is an example of a negatively charged lipid that also plays an important role in cellular signaling.

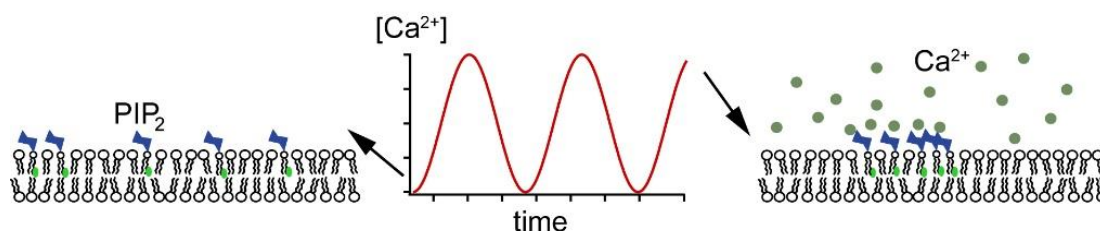


Figure IV-5: Calcium oscillation induced changes in membrane organization. In the absence of Ca<sup>2+</sup>, PIP<sub>2</sub> is homogeneously distributed throughout the lipid bilayer (left). At heightened calcium levels, domains of high PIP<sub>2</sub> concentration will form (right)

r

The combination of Asante Calcium Red dye and the scavenger (DIAZO) dye shows the possibility of making a system that can mimic the oscillation behavior of the intracellular calcium, as seen in Figure IV-6, Figure IV-7 and Figure IV-8.

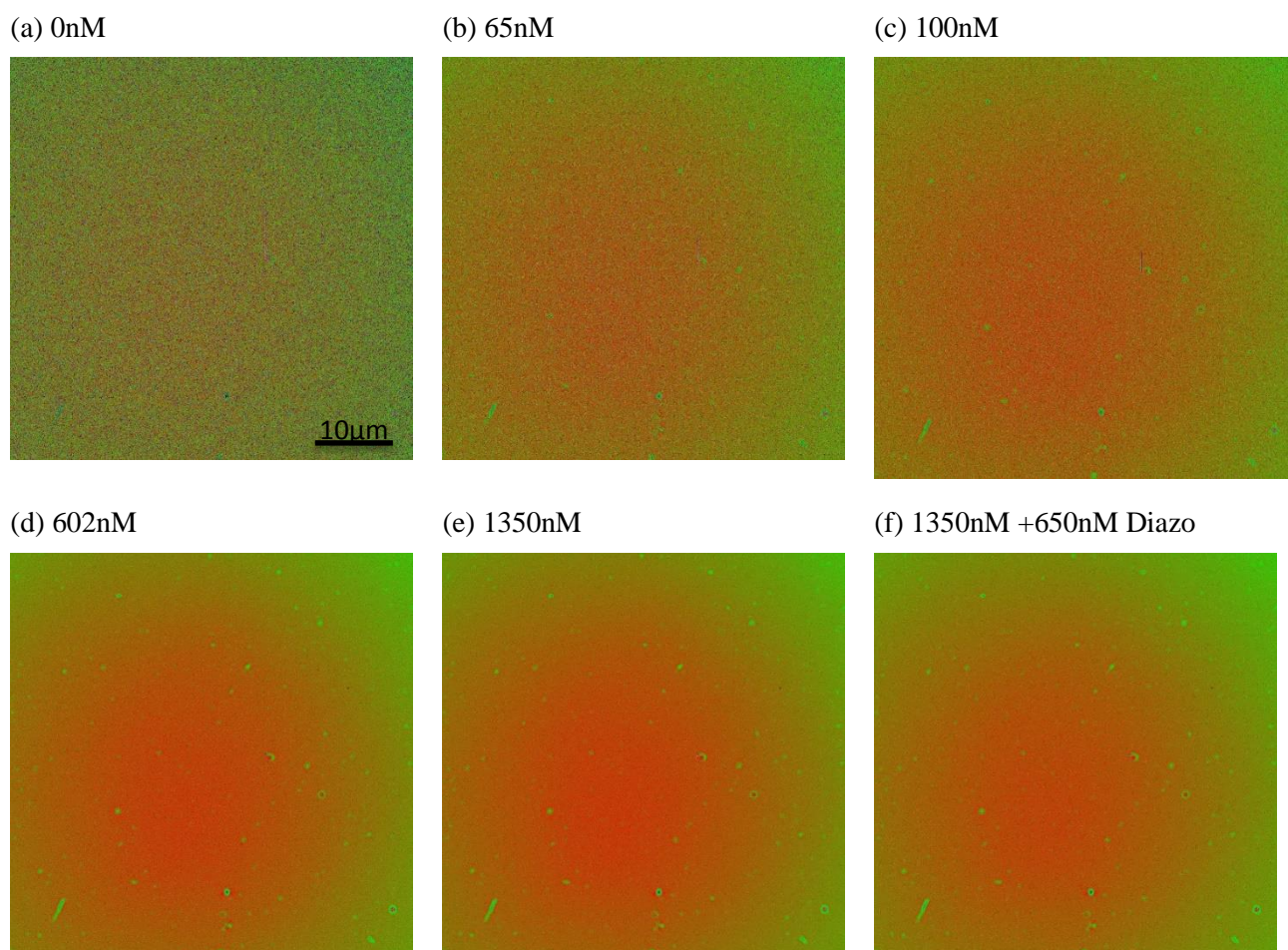


Figure IV-6: Fluorescent images of Asante Calcium Red for different calcium concentrations (as shown from (a) to (f) and with the added effect of the scavenger (Diazo) on the  $[Ca^{+2}]$  (f).

Figure IV-6 shows the fluorescent image of ACR at different calcium concentrations. With the addition of 650nM Diazo the intensity is reduced by nearly half. Figure IV-7 shows the mean intensity of all various calcium concentrations at a wavelength of 500 nm. However, in Figure IV-8 we see a plot of the mean intensity of ACR as a function of various calcium concentrations.

We also see in Figure IV-8 that the scavenger reduces the concentration of calcium to approximately 700nM.

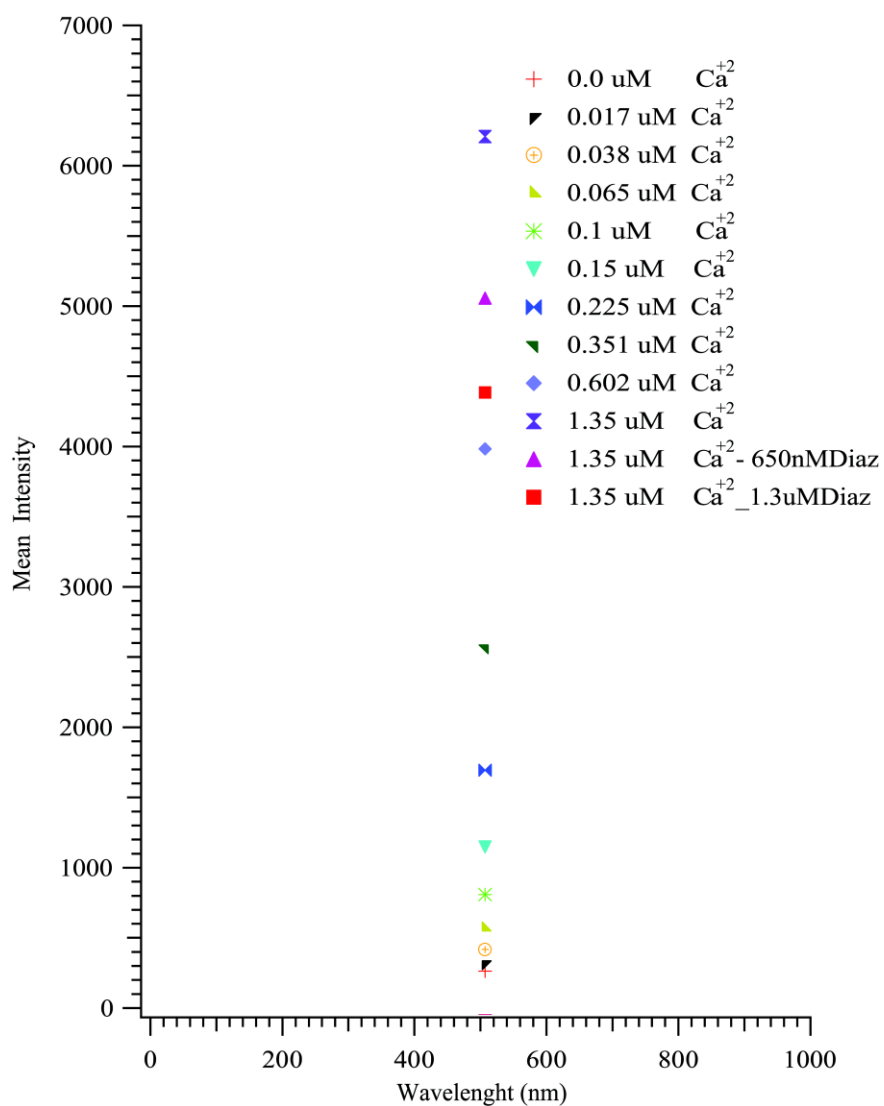


Figure IV-7: Fluorescent Intensity of Asante Calcium Red for different calcium concentrations. All emissions for various of  $[Ca^{+2}]$  occur at 500nm, even after adding the scavenger (Diazo).

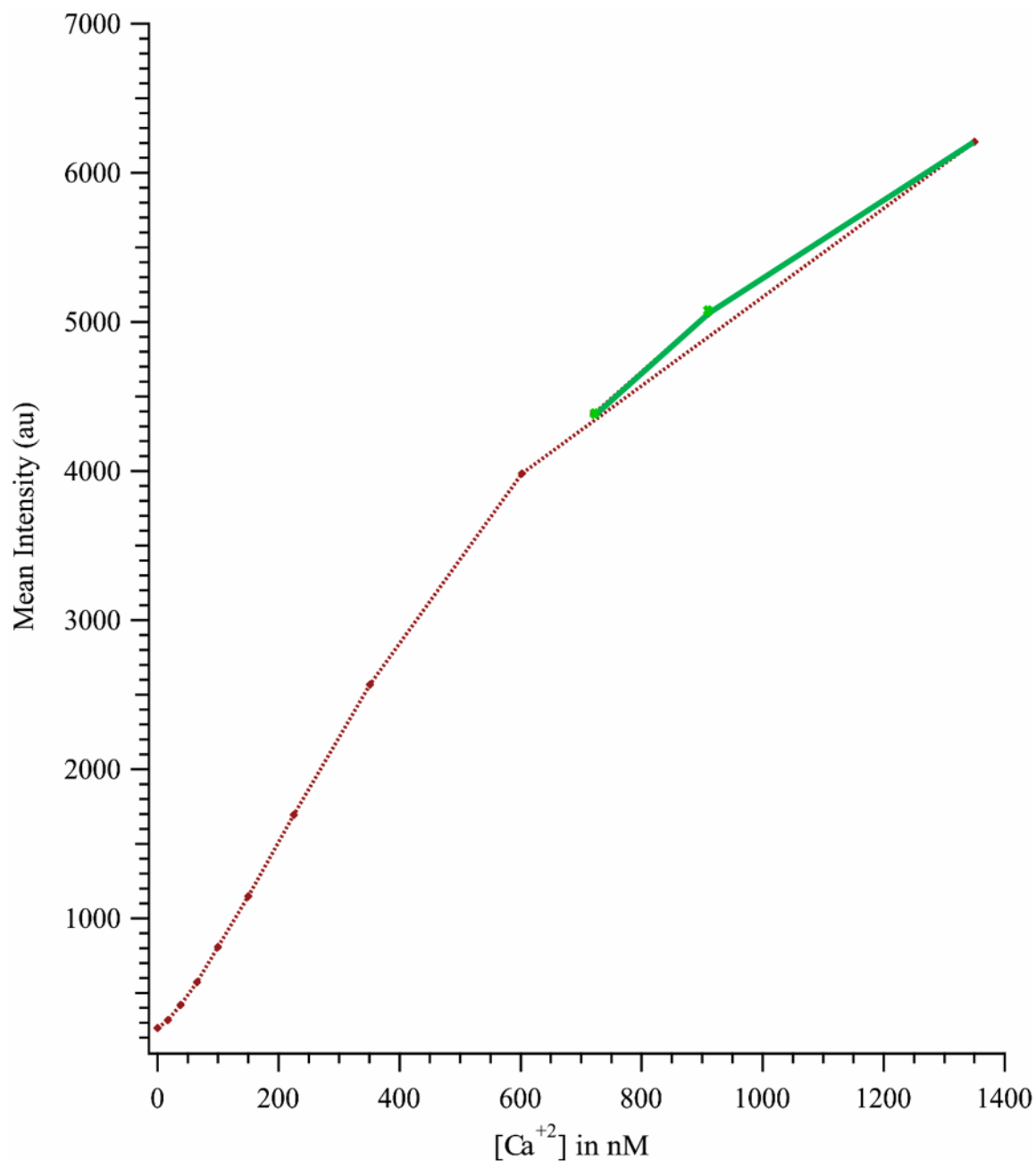


Figure IV-8: Fluorescent images of Asante Calcium Red for different calcium concentrations. We first see an increase in the mean intensity as calcium concentrations increase (red), then we observe the impact of the scavenger (DIAZO) as it was added to the system which reduced the calcium concentration by nearly in half (green).

## Chapter V: General Conclusion

Our findings have shown that the physiological levels of bivalent ions induce cluster formations of anionic lipids, particularly phosphatidylinositol 3,4-bisphosphate (PI(4,5)P<sub>2</sub>). We also found from the compressibility computed from the isotherms that these clusters depend on the nature of bivalent ions and pH. Moreover, the condensation in the monolayer significantly depends on the charge and the kind of phospholipids. We have observed from the compressibility of phosphatidylglycerol (DOPG) that the head group does not show any long range interaction at low surface pressure in the absence of bivalent ions. In contrast, we do find compressibility of PIP<sub>2</sub> and phosphatidylinositol (PtdIns or PI) even at low surface pressure which indicates the action of a long range interaction mediated by a dual interaction of hydration forces and electrostatic interactions. I also developed a theoretical framework of the compressibility, which was supported by the results of the experiment. In addition, our theoretical framework of compressibility predicts a decrease in the compressibility as the temperature increases. It also depends on the electrostatic surface potential and the Debye length. Our investigation on Gibbs free energy and excess Gibbs free energy has shown and revealed the nature of the interaction in the monolayer systems of PIP<sub>2</sub>-POPC and PIP<sub>2</sub> as they are modulated by the physiological level of Ca<sup>+2</sup> ions. This confirms the aggregation of PIP<sub>2</sub> observed from the compressibility results. The attraction in the monolayer increases significantly as the temperature increases, which suggests that the hydration force breaks down as the temperature increases; this observation has been supported by other research. This impact of temperature allows an important increase in the electrostatic interaction between PIP<sub>2</sub> molecules under bivalent ions' modulations at various physiological levels. These findings are supported by the observations seen in the Gibbs free energy and the excess Gibbs free energy of the PIP<sub>2</sub> monolayer at 25°C and in the mixture of PIP<sub>2</sub>-POPC at 37°C.

This attempt at developing a technique that mimics a calcium wave in the cytoplasm indicates that there is a real possibility of making such a system with Calcium Asante Red, the calcium scavenger, Diazo, and calcium release nitrophenyl-EGTA (NP-EGTA) dyes. As seen from our preliminary results, a careful combination of different dyes that have different excitation and emission spectra can lead to a system that can be turned on and off.

### **Future Research**

Most monolayer experiments on polyphosphoinositides (PPIs) are usually done with PI(4,5)P<sub>2</sub> which is one of the seven phosphorylates of PtdIns. It is important to conduct similar experiments using either PI(3,5)P<sub>2</sub>, PI(3,4)P<sub>2</sub> or PI(1,4,5)P<sub>3</sub> to see how the geometry of the phosphates group on the myo-ring affects the compressibility and the excess Gibbs free energy of a mono or bilayer system. Moreover the experiment conducted here used few and highly controlled parameters, so further investigation is needed by including more parameters, such as PLC or other proteins that bind to PIP<sub>2</sub>. For example, PPIs interacts with more than 350 proteins. PIP<sub>2</sub> is also a well-known precursor to two important second messengers, IP<sub>3</sub> and DAG, after PIP<sub>2</sub> is hydrolyzed by PLC. A further step would be to look at the behavior of the PIP<sub>2</sub>-PLC system as they are modulated by calcium ions. Another route would be to improve the system so that it can mimic the oscillation of calcium in the cytoplasm and use it in a bilayer system of PIP<sub>2</sub>-PLC.

## Reference

1. Sprong, H., P. van der Sluijs, and G. van Meer, *How proteins move lipids and lipids move proteins (vol 2, pg 504, 2001)*. Nature Reviews Molecular Cell Biology, 2001. **2**(9): p. 698-698.
2. McLaughlin, S., et al., *PIP2 AND proteins: Interactions, organization, and information flow*. Annual Review of Biophysics and Biomolecular Structure, 2002. **31**: p. 151-175.
3. Simons, K. and M.J. Gerl, *Revitalizing membrane rafts: new tools and insights*. Nature Reviews Molecular Cell Biology, 2010. **11**(10): p. 688-699.
4. Waheed, A.A. and E.O. Freed, *Lipids and membrane microdomains in HIV-1 replication*. Virus Research, 2009. **143**(2): p. 162-176.
5. Scheiffele, P., et al., *Influenza viruses select ordered lipid domains during budding from the plasma membrane*. Journal of Biological Chemistry, 1999. **274**(4): p. 2038-2044.
6. Landfear, S.M., *Transporters for Drug Delivery and as Drug Targets in Parasitic Protozoa*. Clinical Pharmacology & Therapeutics, 2010. **87**(1): p. 122-125.
7. Stambolic, V., *CANCER Precise control of localized signals*. Nature, 2015. **522**(7554): p. 38-40.
8. Hollander, M.C., G.M. Blumenthal, and P.A. Dennis, *PTEN loss in the continuum of common cancers, rare syndromes and mouse models*. Nature Reviews Cancer, 2011. **11**(4): p. 289-301.
9. Baumgartner, H. and R.P. Bagozzi, *Specification, Estimation, and Testing of Moment Structure Models Based on Latent Variates Involving Interactions among the Exogenous Constructs*. Sociological Methods & Research, 1995. **24**(2): p. 187-213.
10. Holthuis, J.C.M. and A.K. Menon, *Lipid landscapes and pipelines in membrane homeostasis*. Nature, 2014. **510**(7503): p. 48-57.
11. Lai, Y.H., et al., *Contribution of thermal energy to initial ion production in matrix-assisted laser desorption/ionization observed with 2,4,6-trihydroxyacetophenone*. Rapid Communications in Mass Spectrometry, 2014. **28**(15): p. 1716-1722.
12. Mason, W.T., et al., *Control of Secretion in Anterior-Pituitary Cells - Linking Ion Channels, Messengers and Exocytosis*. Journal of Experimental Biology, 1988. **139**: p. 287-316.
13. Bretschke, M., *Asymmetrical Lipid Bilayer Structure for Biological-Membranes*. Nature-New Biology, 1972. **236**(61): p. 11-&.
14. Di Paolo, G. and P. De Camilli, *Phosphoinositides in cell regulation and membrane dynamics*. Nature, 2006. **443**(7112): p. 651-657.
15. Smoligovets, A.A., et al., *Characterization of dynamic actin associations with T-cell receptor microclusters in primary T cells*. Journal of Cell Science, 2012. **125**(3): p. 735-742.
16. Bottomley, M.J., P. Lo Surdo, and P.C. Driscoll, *Endocytosis: How dynamin sets vesicles PHree!* Current Biology, 1999. **9**(8): p. R301-R304.
17. Aoyagi, K., et al., *The activation of exocytotic sites by the formation of phosphatidylinositol 4,5-bisphosphate microdomains at syntaxin clusters*. Journal of Biological Chemistry, 2005. **280**(17): p. 17346-17352.



18. Wenk, M.R. and P. De Camilli, *Protein-lipid interactions and phosphoinositide metabolism in membrane traffic: Insights from vesicle recycling in nerve terminals*. Proceedings of the National Academy of Sciences of the United States of America, 2004. **101**(22): p. 8262-8269.
19. Forstner, M.B., et al., *Attractive membrane domains control lateral diffusion*. Physical Review E, 2008. **77**(5).
20. Lingwood, D. and K. Simons, *Lipid Rafts As a Membrane-Organizing Principle*. Science, 2010. **327**(5961): p. 46-50.
21. Alberts, B., *Essential cell biology : an introduction to the molecular biology of the cell*. 1998, New York: Garland Pub.
22. Alberts, B., *Essential cell biology*. 3rd ed. 2010, New York, N.Y. ; London: Garland Science.
23. Huang, B., M. Bates, and X.W. Zhuang, *Super-Resolution Fluorescence Microscopy*. Annual Review of Biochemistry, 2009. **78**: p. 993-1016.
24. Huang, B., H. Babcock, and X.W. Zhuang, *Breaking the Diffraction Barrier: Super-Resolution Imaging of Cells*. Cell, 2010. **143**(7): p. 1047-1058.
25. Shevchenko, A. and K. Simons, *Lipidomics: coming to grips with lipid diversity*. Nature Reviews Molecular Cell Biology, 2010. **11**(8): p. 593-598.
26. Jacobson, K., O.G. Mouritsen, and R.G.W. Anderson, *Lipid rafts: at a crossroad between cell biology and physics*. Nature Cell Biology, 2007. **9**(1): p. 7-14.
27. Czech, M.P., *PIP2 and PIP3: Complex roles at the cell surface*. Cell, 2000. **100**(6): p. 603-606.
28. McLaughlin, S. and D. Murray, *Plasma membrane phosphoinositide organization by protein electrostatics*. Nature, 2005. **438**(7068): p. 605-611.
29. Hinchliffe, K.A., A. Ciruela, and R.F. Irvine, *PIPkins, their substrates and their products: new functions for old enzymes*. Biochimica Et Biophysica Acta-Molecular and Cell Biology of Lipids, 1998. **1436**(1-2): p. 87-104.
30. Billcliff, P.G. and M. Lowe, *Inositol lipid phosphatases in membrane trafficking and human disease*. Biochemical Journal, 2014. **461**: p. 159-175.
31. Raucher, D., et al., *Phosphatidylinositol 4,5-bisphosphate functions as a second messenger that regulates cytoskeleton-plasma membrane adhesion*. Cell, 2000. **100**(2): p. 221-228.
32. Berridge, M.J., *Inositol trisphosphate and calcium signalling mechanisms*. Biochimica Et Biophysica Acta-Molecular Cell Research, 2009. **1793**(6): p. 933-940.
33. Bollinger, C.R., V. Teichgraber, and E. Gulbins, *Ceramide-enriched membrane domains*. Biochimica Et Biophysica Acta-Molecular Cell Research, 2005. **1746**(3): p. 284-294.
34. Barenholz, Y. and T.E. Thompson, *Sphingomyelins in Bilayers and Biological-Membranes*. Biochimica Et Biophysica Acta, 1980. **604**(2): p. 129-158.
35. Simons, K. and E. Ikonen, *Functional rafts in cell membranes*. Nature, 1997. **387**(6633): p. 569-572.
36. Holthuis, J.C.M. and T.P. Levine, *Lipid traffic: Floppy drives and a superhighway*. Nature Reviews Molecular Cell Biology, 2005. **6**(3): p. 209-220.

37. Murase, K., et al., *Ultrafine membrane compartments for molecular diffusion as revealed by single molecule techniques*. Biophysical Journal, 2004. **86**(6): p. 4075-4093.
38. Abbe, E. and E. Telatar, *Polar Codes for the m-User Multiple Access Channel*. IEEE Transactions on Information Theory, 2012. **58**(8): p. 5437-5448.
39. Brown, D., *Structure and function of membrane rafts*. International Journal of Medical Microbiology, 2002. **291**(6-7): p. 433-437.
40. Zafarani-Moattar, M.T. and S. Dehghanian, *Intermolecular interactions in mixtures of poly (ethylene glycol) with methoxybenzene and ethoxybenzene: Volumetric and viscometric studies*. Journal of Chemical Thermodynamics, 2014. **71**: p. 221-230.
41. tutorvista, *Plasma Membrane*. 2015
42. Ramstedt, B. and J.P. Slotte, *Membrane properties of sphingomyelins*. Febs Letters, 2002. **531**(1): p. 33-37.
43. Brown, D.A. and E. London, *Structure and function of sphingolipid- and cholesterol-rich membrane rafts*. Journal of Biological Chemistry, 2000. **275**(23): p. 17221-17224.
44. Balla, T., *Phosphoinositides: Tiny Lipids with Giant Impact on Cell Regulation*. Physiological Reviews, 2013. **93**(3): p. 1019-1137.
45. Agranoff, B.W., *Textbook Errors - Cyclitol Confusion*. Trends in Biochemical Sciences, 1978. **3**(12): p. N283-N285.
46. Falkenburger, B.H., J.B. Jensen, and B. Hille, *Kinetics of M-1 muscarinic receptor and G protein signaling to phospholipase C in living cells*. Journal of General Physiology, 2010. **135**(2): p. 81-97.
47. Bell, R.M., L.M. Ballas, and R.A. Coleman, *Lipid Topogenesis*. Journal of Lipid Research, 1981. **22**(3): p. 391-403.
48. Kiessling, V., J.M. Crane, and L.K. Tamm, *Transbilayer effects of raft-like lipid domains in asymmetric planar bilayers measured by single molecule tracking (vol 91, pg 3313, 2006)*. Biophysical Journal, 2007. **92**(2): p. 698-698.
49. Wang, C., L.L. Qiao, and Z.L. Mao, *Simulation of Far-Field Superresolution Fluorescence Imaging with Two-Color One-Photon Excitation of Reversible Photoactivatable Protein*. Chinese Physics Letters, 2011. **28**(5).
50. Yadav, K., Y. Dwivedi, and N. Jaggi, *Effect of annealing temperature on the structural and optical properties of ZnSe nanoparticles*. Journal of Materials Science-Materials in Electronics, 2015. **26**(4): p. 2198-2204.
51. Simons, K. and G. Van Meer, *Lipid Sorting in Epithelial-Cells*. Biochemistry, 1988. **27**(17): p. 6197-6202.
52. Brown, D.A. and J.K. Rose, *Sorting of Gpi-Anchored Proteins to Glycolipid-Enriched Membrane Subdomains during Transport to the Apical Cell-Surface*. Cell, 1992. **68**(3): p. 533-544.
53. Suomalainen, M., *Lipid rafts and assembly of enveloped viruses*. Traffic, 2002. **3**(10): p. 705-709.
54. Campbell, S.M., S.M. Crowe, and J. Mak, *Lipid rafts and HIV-1: from viral entry to assembly of progeny virions*. Journal of Clinical Virology, 2001. **22**(3): p. 217-227.

55. Falkenburger, B.H., et al., *Phosphoinositides: lipid regulators of membrane proteins*. Journal of Physiology-London, 2010. **588**(17): p. 3179-3185.
56. Huang, C.L., S.Y. Feng, and D.W. Hilgemann, *Direct activation of inward rectifier potassium channels by PIP2 and its stabilization by G beta gamma*. Nature, 1998. **391**(6669): p. 803-806.
57. Lassing, I. and U. Lindberg, *Specific Interaction between Phosphatidylinositol 4,5-Bisphosphate and Profilactin*. Nature, 1985. **314**(6010): p. 472-474.
58. Yin, H.L. and P.A. Janmey, *Phosphoinositide regulation of the actin cytoskeleton*. Annual Review of Physiology, 2003. **65**: p. 761-789.
59. Sechi, A.S. and J. Wehland, *The actin cytoskeleton and plasma membrane connection: PtdIns(4,5)P-2 influences cytoskeletal protein activity at the plasma membrane*. Journal of Cell Science, 2000. **113**(21): p. 3685-3695.
60. Wang, Y., et al., *Regulation of EGFR nanocluster formation by ionic protein-lipid interaction*. Cell Research, 2014. **24**(8): p. 959-976.
61. Strunker, T., et al., *The CatSper channel mediates progesterone-induced Ca<sup>2+</sup> influx in human sperm*. Nature, 2011. **471**(7338): p. 382-+.
62. Grassme, H., J. Riethmuller, and E. Gulbins, *Biological aspects of ceramide-enriched membrane domains*. Progress in Lipid Research, 2007. **46**(3-4): p. 161-170.
63. Chan, R., et al., *Retroviruses Human Immunodeficiency Virus and Murine Leukemia Virus Are Enriched in Phosphoinositides*. Journal of Virology, 2008. **82**(22): p. 11228-11238.
64. Foster, W.J. and P.A. Janmey, *The distribution of polyphosphoinositides in lipid films*. Biophysical Chemistry, 2001. **91**(3): p. 211-218.
65. Mclaughlin, S., *The Electrostatic Properties of Membranes*. Annual Review of Biophysics and Biophysical Chemistry, 1989. **18**: p. 113-136.
66. Wang, Y., et al., *Controllable Synthesis and Photocatalytic Properties of C-doped BiVO<sub>4</sub> with Self-Heterostructure Under Different Light Sources*. Nano, 2015. **10**(1).
67. Rand, R.P., *Interacting Phospholipid-Bilayers - Measured Forces and Induced Structural-Changes*. Annual Review of Biophysics and Bioengineering, 1981. **10**: p. 277-314.
68. Sirbuly, D.J., et al., *Nanomechanical force transducers for biomolecular and intracellular measurements: is there room to shrink and why do it?* Reports on Progress in Physics, 2015. **78**(2).
69. Tsuchiya, T., et al., *In Situ and Nonvolatile Photoluminescence Tuning and Nanodomain Writing Demonstrated by All-Solid-State Devices Based on Graphene Oxide*. Acs Nano, 2015. **9**(2): p. 2102-2110.
70. Perry, E.S., W.R. Miller, and S. Lindsay, *Looking at tardigrades in a new light: using epifluorescence to interpret structure*. Journal of Microscopy, 2015. **257**(2): p. 117-122.
71. Dalawai, S.P., A.B. Gadkari, and P.N. Vasambekar, *Electrical switching in cadmium ferrite with different rare-earth ions (Sm<sup>3+</sup>, Y<sup>3+</sup>, and La<sup>3+</sup>)*. Rare Metals, 2015. **34**(2): p. 133-136.

72. Brockman, H., *Lipid monolayers: why use half a membrane to characterize protein-membrane interactions?* Current Opinion in Structural Biology, 1999. **9**(4): p. 438-443.
73. Langmuir, I., *The constitution and fundamental properties of solids and liquids. II. Liquids.* Journal of the American Chemical Society, 1917. **39**: p. 1848-1906.
74. Agnes P Girard-Egrot, L.J.B., *Langmuir-Blodgett Technique for Synthesis of Biomimetic Lipid Membranes.* Springer, 2007: p. pp 23-74.
75. Castellana, E.T. and P.S. Cremer, *Solid supported lipid bilayers: From biophysical studies to sensor design.* Surface Science Reports, 2006. **61**(10): p. 429-444.
76. Holden, M.A., et al., *Creating fluid and air-stable solid supported lipid bilayers.* Journal of the American Chemical Society, 2004. **126**(21): p. 6512-6513.
77. Wesolowska, O., et al., *Giant unilamellar vesicles - a perfect tool to visualize phase separation and lipid rafts in model systems.* Acta Biochimica Polonica, 2009. **56**(1): p. 33-39.
78. Cevc, G., *Membrane Electrostatics.* Biochimica Et Biophysica Acta, 1990. **1031**(3): p. 311-382.
79. Lee, H.G., M.K. Choi, and S.C. Lee, *Grain-oriented segmentation of images of porous structures using ray casting and curvature energy minimization.* Journal of Microscopy, 2015. **257**(2): p. 92-103.
80. Oldham, K.B., *A Gouy-Chapman-Stern model of the double layer at a (metal)/(ionic liquid) interface.* Journal of Electroanalytical Chemistry, 2008. **613**(2): p. 131-138.
81. Peterson, I.R., *Langmuir-Blodgett-Films.* Journal of Physics D-Applied Physics, 1990. **23**(4): p. 379-395.
82. Jost, M., et al., *Phosphatidylinositol-4,5-bisphosphate is required for endocytic coated vesicle formation.* Current Biology, 1998. **8**(25): p. 1399-1402.
83. Huang, C.L., *Complex roles of PIP2 in the regulation of ion channels and transporters.* American Journal of Physiology-Renal Physiology, 2007. **293**(6): p. F1761-F1765.
84. Zhang, X., et al., *Depolarization Increases Phosphatidylinositol (PI) 4,5-Bisphosphate Level and KCNQ Currents through PI 4-Kinase Mechanisms.* Journal of Biological Chemistry, 2010. **285**(13): p. 9402-9409.
85. Saarikangas, J., H.X. Zhao, and P. Lappalainen, *Regulation of the Actin Cytoskeleton-Plasma Membrane Interplay by Phosphoinositides.* Physiological Reviews, 2010. **90**(1): p. 259-289.
86. Chen, X.J., et al., *Membrane Depolarization Increases Membrane PtdIns(4,5)P-2 Levels through Mechanisms Involving PKC beta II and PI4 Kinase.* Journal of Biological Chemistry, 2011. **286**(46): p. 39760-39767.
87. Levental, I., P.A. Janmey, and A. Cebers, *Electrostatic contribution to the surface pressure of charged monolayers containing polyphosphoinositides.* Biophysical Journal, 2008. **95**(3): p. 1199-1205.
88. Levental, I., A. Cebers, and P.A. Janmey, *Combined electrostatics and hydrogen bonding determine intermolecular interactions between polyphosphoinositides.* Journal of the American Chemical Society, 2008. **130**(28): p. 9025-9030.

89. Levental, I., et al., *Calcium-Dependent Lateral Organization in Phosphatidylinositol 4,5-Bisphosphate (PIP<sub>2</sub>)- and Cholesterol-Containing Monolayers*. *Biochemistry*, 2009. **48**(34): p. 8241-8248.
90. Wang, Y.H., D.R. Slochower, and P.A. Janmey, *Counterion-mediated cluster formation by polyphosphoinositides*. *Chemistry and Physics of Lipids*, 2014. **182**: p. 38-51.
91. Toner, M., et al., *Adsorption of Cations to Phosphatidylinositol 4,5-Bisphosphate*. *Biochemistry*, 1988. **27**(19): p. 7435-7443.
92. Bootman, M.D. and M.J. Berridge, *The Elemental Principles of Calcium Signaling*. *Cell*, 1995. **83**(5): p. 675-678.
93. Berridge, M.J. and R.F. Irvine, *INOSITOL TRISPHOSPHATE, A NOVEL 2ND MESSENGER IN CELLULAR SIGNAL TRANSDUCTION*. *Nature*, 1984. **312**(5992): p. 315-321.
94. Berridge, M.J., *Calcium Oscillations*. *Journal of Biological Chemistry*, 1990. **265**(17): p. 9583-9586.
95. Berridge, M.J., P.H. Cobbold, and K.S.R. Cuthbertson, *Spatial and Temporal Aspects of Cell Signaling*. *Philosophical Transactions of the Royal Society of London Series B-Biological Sciences*, 1988. **320**(1199): p. 325-343.
96. Bootman, M.D., et al., *Calcium signalling - an overview*. *Seminars in Cell & Developmental Biology*, 2001. **12**(1): p. 3-10.
97. McLaughlin, G. Szabo, and G. Eisenman, *DIVALENT IONS AND SURFACE POTENTIAL OF CHARGED PHOSPHOLIPID MEMBRANES*. *Journal of General Physiology*, 1971. **58**(6): p. 667-&.
98. Mathias, R.T., et al., *The Electrostatic Potential Due to a Single Fixed Charge at a Membrane-Solution Interface*. *Biophysical Journal*, 1988. **53**(2): p. A128-A128.
99. Murray, D., et al., *Electrostatic properties of membranes containing acidic lipids and adsorbed basic peptides: Theory and experiment*. *Biophysical Journal*, 1999. **77**(6): p. 3176-3188.
100. Cafiso, D., et al., *Measuring Electrostatic Potentials Adjacent to Membranes*. *Methods in Enzymology*, 1989. **171**: p. 342-364.
101. Mcdaniel, R. and S. Mclaughlin, *The Interaction of Calcium with Gangliosides in Bilayer-Membranes*. *Biochimica Et Biophysica Acta*, 1985. **819**(2): p. 153-160.
102. Welzel, P.B., I. Weis, and G. Schwarz, *Sources of error in Langmuir trough measurements Wilhelmy plate effects and surface curvature*. *Colloids and Surfaces a-Physicochemical and Engineering Aspects*, 1998. **144**(1-3): p. 229-234.
103. Rawicz, W., et al., *Effect of chain length and unsaturation on elasticity of lipid bilayers*. *Biophysical Journal*, 2000. **79**(1): p. 328-339.
104. Koenig, B.W., H.H. Strey, and K. Gawrisch, *Membrane lateral compressibility determined by NMR and X-ray diffraction: Effect of acyl chain polyunsaturation*. *Biophysical Journal*, 1997. **73**(4): p. 1954-1966.
105. Phillips, M.C., D.E. Graham, and H. Hauser, *Lateral Compressibility and Penetration into Phospholipid Monolayers and Bilayer Membranes*. *Nature*, 1975. **254**(5496): p. 154-156.
106. Evans, E.A., R. Waugh, and L. Melnik, *Elastic Area Compressibility Modulus of Red-Cell Membrane*. *Biophysical Journal*, 1976. **16**(6): p. 585-595.

107. Lis, L.J., et al., *Measurement of the Lateral Compressibility of Several Phospholipid-Bilayers*. *Biophysical Journal*, 1982. **37**(3): p. 667-672.
108. Nagle, J.F. and H.L. Scott, *Lateral Compressibility of Lipid Monolayers and Bilayers Theory of Membrane-Permeability*. *Biochimica Et Biophysica Acta*, 1978. **513**(2): p. 236-243.
109. Losche, M. and H. Mohwald, *Electrostatic Interactions in Phospholipid-Membranes .2. Influence of Divalent Ions on Monolayer Structure*. *Journal of Colloid and Interface Science*, 1989. **131**(1): p. 56-67.
110. Le, M.T., et al., *Hg- and Cd-induced modulation of lipid packing and monolayer fluidity in biomimetic erythrocyte model systems*. *Chemistry and Physics of Lipids*, 2013. **170**: p. 46-54.
111. Marsh, D., *Lateral pressure in membranes*. *Biochimica Et Biophysica Acta-Reviews on Biomembranes*, 1996. **1286**(3): p. 183-223.
112. Hauser, H., D. Oldani, and M.C. Phillips, *Mechanism of Ion Escape from Phosphatidylcholine and Phosphatidylserine Single Bilayer Vesicles*. *Biochemistry*, 1973. **12**(22): p. 4507-4517.
113. Fischer, A., et al., *On the Nature of the Lipid Monolayer Phase-Transition*. *Journal De Physique Lettres*, 1984. **45**(16): p. L785-L791.
114. Ohshima, H. and S. Ohki, *Effects of Divalent-Cations on the Surface-Tension of a Lipid Monolayer Coated Air Water Interface*. *Journal of Colloid and Interface Science*, 1985. **103**(1): p. 85-94.
115. Brockman, R.E.B.a.H.L., *Using Monomolecular Films to Characterize Lipid Lateral Interactions*. NIH, 2008: p. 41-58.
116. Blank, M., *Monolayer Permeability and Properties of Natural Membranes*. *Journal of Physical Chemistry*, 1962. **66**(10): p. 1911-&.
117. Flanagan, L.A., et al., *The structure of divalent cation-induced aggregates of PIP2 and their alteration by gelsolin and tau*. *Biophysical Journal*, 1997. **73**(3): p. 1440-7.
118. Butler, J.N., *The thermodynamic activity of calcium ion in sodium chloride-calcium chloride electrolytes*. *Biophys J*, 1968. **8**(12): p. 1426-33.
119. Kooijman, E.E., et al., *Ionization Properties of Phosphatidylinositol Polyphosphates in Mixed Model Membranes*. *Biochemistry*, 2009. **48**(40): p. 9360-9371.
120. Losche, M., et al., *Formation of Langmuir-Blodgett-Films Via Electrostatic Control of the Lipid Water Interface*. *Thin Solid Films*, 1985. **133**(1-4): p. 51-64.
121. Verwey, E.J.W., *Theory of the Stability of Lyophobic Colloids*. *Philips Research Reports*, 1945. **1**(1): p. 33-49.
122. Mugele, F. and J.C. Baret, *Electrowetting: From basics to applications*. *Journal of Physics-Condensed Matter*, 2005. **17**(28): p. R705-R774.
123. Gurtovenko, A.A. and I. Vattulainen, *Membrane potential and electrostatics of phospholipid bilayers with asymmetric transmembrane distribution of anionic lipids*. *Journal of Physical Chemistry B*, 2008. **112**(15): p. 4629-4634.
124. Baddeley, D., M. Cannell, and C. Soeller, *Three-dimensional sub-100 nm super-resolution imaging of biological samples using a phase ramp in the objective pupil*. *Nano Research*, 2011. **4**(6): p. 589-598.

125. Honigmann, A., et al., *STED microscopy detects and quantifies liquid phase separation in lipid membranes using a new far-red emitting fluorescent phosphoglycerolipid analogue*. Faraday Discussions, 2013. **161**: p. 77-89.
126. Ronzitti, E., B. Harke, and A. Diaspro, *Frequency dependent detection in a STED microscope using modulated excitation light*. Optics Express, 2013. **21**(1): p. 210-219.
127. Iketaki, Y., *Three-Dimensional Super-Resolution Microscope Using Two-Color Annular Phase Plate*. Applied Physics Express, 2010. **3**(8).
128. Bordi, F., et al., *Charged lipid monolayers at the air-solution interface: coupling to polyelectrolytes*. Colloids and Surfaces B-Biointerfaces, 2003. **29**(2-3): p. 149-157.
129. Aguayo, S., et al., *Single-bacterium nanomechanics in biomedicine: unravelling the dynamics of bacterial cells*. Nanotechnology, 2015. **26**(6).
130. Kessel, A. and N. Ben-Tal, *Free energy determinants of peptide association with lipid bilayers*. Peptide-Lipid Interactions, 2002. **52**: p. 205-+.
131. Bertero, M., et al., *Image deblurring with Poisson data: from cells to galaxies*. Inverse Problems, 2009. **25**(12).
132. Unger, W.G. and K.A. Evans, *Analysis of Neurogenic Contractile Responses of the Isolated Iris Sphincter Muscle by Electrical-Field Stimulation*. Ophthalmic Research, 1987. **19**(1): p. 14-14.
133. Bordi, F., et al., *Influence of temperature on microdomain organization of mixed cationic-zwitterionic lipidic monolayers at the air-water interface*. Colloids and Surfaces B-Biointerfaces, 2008. **61**(2): p. 304-310.
134. Jendrasiak, G.L. and R.L. Smith, *The interaction of water with the phospholipid head group and its relationship to the lipid electrical conductivity*. Chemistry and Physics of Lipids, 2004. **131**(2): p. 183-195.
135. Chou, T.H. and C.H. Chang, *Thermodynamic characteristics of mixed DPPC/DHDP monolayers on water and phosphate buffer subphases*. Langmuir, 2000. **16**(7): p. 3385-3390.
136. Kodama, M., et al., *A monolayer study on three binary mixed systems of dipalmitoyl phosphatidyl choline with cholesterol, cholestanol and stigmasterol*. Colloids and Surfaces B-Biointerfaces, 2004. **33**(3-4): p. 211-226.
137. Berridge, M.J., *Inositol Lipids and Calcium Signaling*. European Journal of Pharmacology, 1990. **183**(1): p. 84-85.
138. Berridge, M.J., *Calcium regulation of neural rhythms, memory and Alzheimer's disease*. Journal of Physiology-London, 2014. **592**(2): p. 281-293.
139. Phelps, P.C., et al., *Studies on the Mechanism of Sulofenur and Ly295501 Toxicity - Effect on the Regulation of Cytosolic Calcium in Relation to Cytotoxicity in Normal and Tumorigenic Rat-Kidney Cell-Lines*. Cancer Letters, 1995. **97**(1): p. 7-15.
140. Berridge, M.J., *Elementary and global aspects of calcium signalling*. Journal of Experimental Biology, 1997. **200**(2): p. 315-319.
141. Endo, M., *Calcium Release from Sarcoplasmic-Reticulum*. Physiological Reviews, 1977. **57**(1): p. 71-108.

142. Cheng, H., W.J. Lederer, and M.B. Cannell, *Calcium Sparks - Elementary Events Underlying Excitation-Contraction Coupling in Heart-Muscle*. Science, 1993. **262**(5134): p. 740-744.
143. Berridge, M.J., *Phosphatidylinositol Hydrolysis and Calcium Signaling*. Advances in Cyclic Nucleotide Research, 1981. **14**: p. 289-299.
144. Berridge, M.J., *Oncogenes, Inositol Lipids and Cellular Proliferation*. Bio-Technology, 1984. **2**(6): p. 541-546.
145. Berridge, M.J., *Inositol Trisphosphate and Calcium Mobilization*. Journal of Cardiovascular Pharmacology, 1986. **8**: p. S85-S90.
146. Finch, E.A. and G.J. Augustine, *Local calcium signalling by inositol-1,4, 5-trisphosphate in Purkinje cell dendrites*. Nature, 1998. **396**(6713): p. 753-756.
147. Berridge, M.J., *Calcium microdomains: Organization and function*. Cell Calcium, 2006. **40**(5-6): p. 405-412.
148. Marks, A.R., *Cardiac intracellular calcium release channels - Role in heart failure*. Circulation Research, 2000. **87**(1): p. 8-11.
149. Bootman, M.D., M.J. Berridge, and P. Lipp, *Cooking with calcium: The recipes for composing global signals from elementary events*. Cell, 1997. **91**(3): p. 367-373.
150. Simkus, C.R.L. and C. Stricker, *The contribution of intracellular calcium stores to mEPSCs recorded in layer II neurones of rat barrel cortex*. Journal of Physiology-London, 2002. **545**(2): p. 521-535.
151. Lehnart, S.E., et al., *Stabilization of cardiac ryanodine receptor prevents intracellular calcium leak and arrhythmias*. Proceedings of the National Academy of Sciences of the United States of America, 2006. **103**(20): p. 7906-7910.
152. Conti, R., Y.P. Tan, and I. Llano, *Action potential-evoked and ryanodine-sensitive spontaneous Ca<sup>2+</sup> transients at the presynaptic terminal of a developing CNS inhibitory synapse*. Journal of Neuroscience, 2004. **24**(31): p. 6946-6957.
153. Brenner, R., et al., *Vasoregulation by the beta 1 subunit of the calcium-activated potassium channel*. Nature, 2000. **407**(6806): p. 870-876.
154. Bezprozvanny, L. and R.W. Tsien, *Voltage-Dependent Blockade of Diverse Types of Voltage-Gated Ca<sup>2+</sup> Channels Expressed in Xenopus Oocytes by the Ca<sup>2+</sup> Channel Antagonist Mibefradil (Ro-40-5967)*. Molecular Pharmacology, 1995. **48**(3): p. 540-549.
155. Bezprozvanny, I., R.H. Scheller, and R.W. Tsien, *Functional Impact of Syntaxin on Gating of N-Type and Q-Type Calcium Channels*. Nature, 1995. **378**(6557): p. 623-626.
156. Mcguigan, J.A.S., D. Luthi, and A. Buri, *Calcium Buffer Solutions and How to Make Them - a Do It Yourself Guide*. Canadian Journal of Physiology and Pharmacology, 1991. **69**(11): p. 1733-1749.
157. Clapham, D.E., *Calcium Signaling*. Cell, 1995. **80**(2): p. 259-268.
158. Berridge, M.J., *Neuronal calcium signaling*. Neuron, 1998. **21**(1): p. 13-26.
159. Ross, M., et al., *Visualization of chemical and physical properties of calcium-induced domains in DPPC/DPPS Langmuir-Blodgett layers*. Langmuir, 2001. **17**(8): p. 2437-2445.



*Adolphe Kazadi Badiambile***Vita****RESEARCH/JOB INTERESTS**


---

Cell Culture, Biotechnology, Nanofabrication, Nanophotonics, Physics of Cancer, Nanotechnology, Neuronal or Cardiovascular Diseases, Data Analysis, Teaching Physics or Relate Sciences.

**EXPERTISE AND RESEARCH SKILLS**


---

I have Accumulated Experience over a Period of Five Years and half in the Field of Biomimetic Model and Teaching Science Physics. Has Demonstrated Expertise in the Field of Experimental Soft Condensed Matter and Biophysics, Optical Microscopy and Imaging Science. A very Good Creative Problem and Solving Skills.

**PROFESSIONAL OVERVIEW**


---

Self-Motivated and Excellent at Multiple tasks and Very Fast Learner, and Good in Development of Mathematics Model and Capable of Learning Any Software at Lightning Speed, An Excellent Adaptable and Very Committed to the Tasks at Hand.

**EMPLOYMENT**


---

Graduate Teaching and Research Assistant	2008-
Department of Physics, Syracuse University, Syracuse, NY 13244	2015

Responsible of setting up the equipment, designing the experiment, ordering chemical product, preparing sample and running the experiment, collecting data, processing data, presenting, discussing and interpreting data .

Cell culture: changing cell medium and splitting cell.

Faculty Member	2006-
Department of Physics, University of Kinshasa, Kinshasa, DRC	2007

**EDUCATION**


---

PhD Physics	2010-2015
Department of Physics, Syracuse University, Syracuse, NY 13244	
Modulation of Charged Biomimetic Membranes by Bivalent Ions" Thesis advisor: Martin B Forstner	
M.Sc. in Physics	2008-2010
Department of Physics, Syracuse University, Syracuse, NY 13244	
PGD in Mathematical Sciences	2007-2008
African Institute for Mathematical Sciences (AIMS), University of Cape Town, SA.	

Synthetic Aperture Radar Processing " Supervised by: Prof. Michael Inggs	
B.Ed. in Physics	2000-2005
Department of Physics ,University of Kinshasa, Dem Rep of Congo	
Coursera : Understanding the Brain	2015-2015

#### PENDING MANUSCRIPTS

---

- Adolphe K.B, Martin.B.F "Modulation of Phosphoinositide Monolayer Compressibilities by Physio-logical Levels of Ca<sup>2+</sup>"
- Adolphe K.B, Martin.B.F " Bivalent ions induce change in Gibbs Free Energy of Phosphoinositides

#### COMPUTER SKILLS

---

- Igor Pro, Origin, Mathematica...: Very good,
- Lumerical FDTD: Very good, I worked in team and used Lumerical FDTD to study Surface Plasmon Resonance and its Application to Biosensing
- C/C++: Very good, work in many projects and wrote a code to solve a linear system AX=B capable of handling a huge matrix of data
- Python/VPython: Very good, spend more than 1000 hours and wrote a codes to solve physics problem by using Fine Element Analysis. Wrote code for the formation of image by using FFT
- LabVIEW: Very good, spend more than 120 hours and studies different electronics system.
- Mat lab: Very good, spend more than 1000 hours, processing and analyzing data.

#### TEACHING

---

@ University of Syracuse, Physics Dept.:

- 2 Summer 15: : PHY 101, \General Physics Laboratory I
- 3 Spring 15: PHY344/462 Experimental Physics I and II
- 4 Fall 13: AST101 Our Corner of the Universe
- 5 Spring 09: PHY 221, \General Physics Laboratory I"
- 6 Fall 08: AST101 Our Corner of the Universe

#### SELECTED CONFERENCES AND POSTERS PRESENTATIONS

---

1. Biophysical Society 59th Annual Meeting, 02/15, "Modulation of Phosphoinositide Monolayer Com-pressibilities by Physiological Levels of Ca<sup>2+</sup>" by Adolphe K.B, Martin.B.F,Baltimore,MD,2014

2. Stevenson Biomaterials, IGERT, 11/14 "Modulation of Phosphoinositide Monolayer Compressibilities by Physiological Levels of Ca<sup>2+</sup>" by Adolphe K.B, Martin.B.F ,Syracuse, NY 2014
3. Biophysical Society 57th Annual Meeting, 02/13, "Calcium Dependent Aggregation of Phosphoinositides " by Adolphe K.B, Martin.B.F,Philadelphia,PA,2013
4. American Physical Society March Meeting , "Calcium Dependent Aggregation of Phosphoinositides  
" by Adolphe K.B, Martin.B.F, Boston, MA 2012
5. 12th New York Complex Matter Workshop, Poster, 8/12 "Calcium Dependent Aggregation of Phosphoinositides "by Adolphe K.B, Martin.B.F, Syracuse Biomaterial/Physics Department, Syracuse, NY 2012
6. Biophysical Society 55th Annual Meeting, "Calcium Dependent Aggregation of Phosphoinositides  
by Adolphe K.B, Martin.B.F,Baltimore,MD,2011